



SMAI-JCM

SMAI JOURNAL OF COMPUTATIONAL MATHEMATICS

Analysis of curvature
approximations via covariant curl
and incompatibility for Regge
metrics

JAY GOPALAKRISHNAN, MICHAEL NEUNTEUFEL,
JOACHIM SCHÖBERL & MAX WARDETZKY

Volume 9 (2023), p. 151-195.

<https://doi.org/10.5802/smai-jcm.98>

© The authors, 2023.



*The SMAI Journal of Computational Mathematics is a member
of the Centre Mersenne for Open Scientific Publishing
<http://www.centre-mersenne.org/>*

Submissions at <https://smai-jcm.centre-mersenne.org/ojs/submission>

e-ISSN: 2426-8399



Analysis of curvature approximations via covariant curl and incompatibility for Regge metrics

JAY GOPALAKRISHNAN ¹
MICHAEL NEUNTEUFEL ²
JOACHIM SCHÖBERL ³
MAX WARDETZKY ⁴

¹ Portland State University, PO Box 751, Portland OR 97207, USA

E-mail address: gjay@pdx.edu

² Institute for Analysis and Scientific Computing, TU Wien, Wiedner Hauptstr. 8-10, 1040 Wien, Austria

E-mail address: michael.neunteufel@tuwien.ac.at

³ Institute for Analysis and Scientific Computing, TU Wien, Wiedner Hauptstr. 8-10, 1040 Wien, Austria

E-mail address: joachim.schoeberl@tuwien.ac.at

⁴ Institute of Numerical and Applied Mathematics, University of Göttingen, Lotzestr. 16-18, 37083 Göttingen, Germany

E-mail address: wardetzky@math.uni-goettingen.de.

Abstract. The metric tensor of a Riemannian manifold can be approximated using Regge finite elements and such approximations can be used to compute approximations to the Gauss curvature and the Levi-Civita connection of the manifold. It is shown that certain Regge approximations yield curvature and connection approximations that converge at a higher rate than previously known. The analysis is based on covariant (distributional) curl and incompatibility operators which can be applied to piecewise smooth matrix fields whose tangential-tangential component is continuous across element interfaces. Using the properties of the canonical interpolant of the Regge space, we obtain superconvergence of approximations of these covariant operators. Numerical experiments further illustrate the results from the error analysis.

2020 Mathematics Subject Classification. 65N30, 53A70, 83C27.

Keywords. Gauss curvature, Regge calculus, finite element method, differential geometry.

1. Introduction

This paper is concerned with the finite element approximation of the Gauss curvature K of a two-dimensional Riemannian manifold. As shown by Gauss's Theorema Egregium, K is an intrinsic quantity of the manifold. It can be computed solely using the metric tensor of the manifold. Therefore, when a finite element approximation of the metric tensor is given, it is natural to ask if an approximation to K can be computed. The answer was given in the affirmative by the recent work of [27], assuming that the metric is approximated using Regge finite elements, and further improved by [10]. The convergence theorems of this paper are heavily based on these works. We prove that the resulting curvature and connection approximations converge at a higher rate than previously known for the approximation given by the canonical Regge interpolant. Our method of analysis is different and new. In particular, we show how covariant curl and incompatibility can be approximated using appropriate finite element spaces, given a nonsmooth Regge metric. These operators arise in a myriad of other applications, so

Jay Gopalakrishnan was supported by NSF grant DMS-1912779.

Michael Neunteufel and Joachim Schöberl were supported by the Austrian Science Fund (FWF) project F65.

<https://doi.org/10.5802/smai-jcm.98>

© The authors, 2023

our intermediate results regarding them are of independent interest. Notions of curvature while gluing together piecewise smooth metrics has been a preoccupation in varied fields far away from computing, as early as [29] to recent years [45], so we note at the outset that we approach the topic with numerical computation in mind.

The Regge finite element takes its name from Regge calculus, originally developed for solving Einstein field equations in general relativity. It discretizes the metric tensor through edge-length specifications, allowing the curvature to be approximated by means of angle deficits [40]. Regge calculus was established in theoretical and numerical physics and routinely finds applications in relativity and quantum mechanics. In [9, 41, 51] a comprehensive overview of the development of Regge calculus over the last fifty years can be found. Just as Whitney forms [50] can be interpreted as finite elements, it was observed that Regge's approach of prescribing quantities on edges is equivalent to defining a piecewise constant metric tensor whose tangential-tangential components are continuous across element interfaces [44, Section II.A.]. The first rigorous proof of convergence of Regge's angle deficits to the scalar curvature, for a sequence of appropriate triangulations in the sense of measures, was accomplished in [15]. Later, it was also shown [18] that for a given metric in the lowest order Regge finite element space, the curvature of a sequence of mollified metrics converges to the angle deficit in the sense of measures. Methods based on angle deficits for approximating the Gauss curvature on triangulations consisting of piecewise flat triangles are well-established in discrete differential geometry and computer graphics. On specific triangulations satisfying certain conditions, convergence in the L^∞ -norm up to quadratic order was proven, but for a general irregular grid there is no reason to expect convergence [12, 52, 53]. In [35], Regge's concept of angle deficits has been extended to quadrilateral meshes. Notable among the results applicable for higher dimensional manifolds is the proof of convergence for approximated Ricci curvatures of isometrically embedded hypersurfaces $\subset \mathbb{R}^{n+1}$ presented in [24], and used later for Ricci flows [25].

Another natural perspective to place the modern developments on the Regge finite element is within the emergence of *finite element exterior calculus* (FEEC) [5, 6]. The utility of discrete spaces of constant metric tensors with continuous tangential-tangential components was noted in [44]. Later, finite element structures for Regge calculus were developed in [16, 17] and the resulting elements became popular in FEEC under the name Regge finite elements [34]. Regge elements approximating metric and strain tensors were extended to arbitrary polynomial order on triangles, tetrahedra, and higher dimensional simplices in [34], and for quadrilaterals, hexahedra, and prisms in [36]. The utility of Regge elements when discretizing parts of the Kröner complex, or the elasticity complex, was considered in [7, 17, 28]. Properties of Regge elements were exploited to construct a method avoiding membrane locking for general triangular shell elements [37].

In this backdrop, the recent work of [27] provides an interesting application of Regge elements by developing a high-order Gauss curvature approximation formula based on higher degree Regge elements. (It was applied to Ricci and Ricci–DeTurck flow [26].) The key is an integral formulation of the angle deficit, extendable to higher orders. Using it, rigorous proofs of convergence at specific rates were proved in [27]. Even more recently, in [10], this approach has been reformulated in terms of a nonlinear distributional curvature and connection 1-form (Levi-Civita connection), using the element-wise Gauss curvature, jump of geodesic curvature at edges, and angle deficits at vertices as sources of curvature [45, 46]. The authors show that L^2 -convergence of the approximated curvature can be obtained if Regge elements using polynomials of degree at least two are used to approximate the metric. This is in line with the rule of thumb that a second order differential operator approximated using polynomials of degree k leads to convergence rates of order $k - 2$. Nonetheless, convergence rates better than this rule of thumb have often been observed in compatible discretizations in FEEC. One of our goals in this paper is to establish such an improved rate for the curvature and connection approximations, as well as for the intermediate covariant operators arising in our analysis, such as the curl and incompatibility.

In a later section, we extend the ideas in [10, 27] by exploiting certain orthogonality properties for the error in the canonical interpolation by Regge finite elements to obtain one extra order of convergence for the curvature approximation. This extra order is comparable to super-convergence properties of mixed methods [11, 21] and has been observed for the Hellan–Herrmann–Johnson method for the biharmonic plate and shell equation [8, 48]. The heart of the matter are FEEC-type identities that show that the error in canonical interpolations superconverges. A typical example is the order k Raviart–Thomas interpolant $\Pi_k q$ of a smooth flux q whose error $\operatorname{div}(q - \Pi_k q)$ is orthogonal to piecewise polynomials of degree k . One can extend this property for the Euclidean incompatibility operator “inc” applied to the error in the degree k Regge interpolant $\sigma - \mathcal{I}_k^R \sigma$ to conclude that $\operatorname{inc}(\sigma - \mathcal{I}_k^R \sigma)$ is orthogonal to the Lagrange space of degree $k + 1$ (in the sense of equation (6.11) proved later). On general manifolds however, instead of this perfect orthogonality, we can only show that the error superconverges (see Theorem 6.3). While perfect orthogonality properties have been known for various canonical interpolants, including the Regge interpolant, the key new ingredient we bring into play is such an orthogonality property for the distributional Christoffel symbols of first kind, namely the “Christoffel orthogonality property” of Lemma 6.10.

Another difference in our analysis, in comparison to [10, 27], is the use of the intrinsic (or covariant) incompatibility operator (which we define using the covariant curl on the manifold). It is now well known that linearizing the curvature operator around the Euclidean metric gives a first order term involving the incompatibility operator [17] and we exploit this relationship in the analysis of the curvature approximation. On Euclidean manifolds, the incompatibility operator is well known to be the natural differential operator for Regge elements in any dimension. By showing that the curvature approximation can be analyzed via the incompatibility operator, we hope to generate new ideas for computing and analyzing approximations of the intrinsic curvature tensor of higher dimensional manifolds. The incompatibility operator also arises in modeling elastic materials with dislocations [1, 2], another potential area of application. The key insight on which we base our definition of these covariant operators for Regge metrics is revealed by the essential role played by a glued smooth structure (described in §4.2). Since coordinates in this glued smooth structure are generally inaccessible for computations, we detail how to compute these operators in the coordinates in which the Regge metric is given as input.

This paper can be read linearly, but we have structured it so a numerical analyst can also directly start with the error analysis in Section 6—where the main convergence theorems appear in §6.1—referring back to the previous sections as needed. (Only coordinate-based formulas are used in §6; their derivations from intrinsic geometry are in the previous sections.) The next section (§2) establishes notation and introduces geometric preliminaries and finite element spaces. Section 3 defines the curvature approximation formula and details coordinate formulas we use for numerical computations. In §4, covariant differential operators on piecewise smooth metric tensors are derived, concentrating on the covariant curl and incompatibility operator, and how they arise from linearization of curvature. Section 5 is devoted to the approximation of the connection 1-form. Section 6 is devoted to the numerical analysis of the errors in the method. The analysis is performed by first proving optimal convergence rates for the distributional covariant curl and inc, and then for the approximations of the Gauss curvature and connection 1-form. Numerical examples illustrating the theoretical results are presented in §7.

2. Notation and preliminaries

This section provides definitions that we use throughout. We give intrinsic definitions of quantities on a manifold, but in view of our computational goals, we also make extensive use of coordinate expressions. We use the Einstein summation convention, by which a term where the same integer index appears

twice, as both an upper and a lower subscript, is tacitly assumed to be summed over the values of that index in $\{1, 2\}$. Summation convention does not apply when a repeated index is not an integer (such as when a subscript or a superscript represents a vector field or other non-integer quantities).

2.1. Spaces on the manifold.

Let M denote a two-dimensional oriented manifold with or without boundary. Endowed with a smooth metric \bar{g} , let (M, \bar{g}) be a Riemannian manifold. Let the unique Levi-Civita connection generated by \bar{g} be denoted by $\bar{\nabla}$. Let $\mathfrak{X}(M)$, $\Lambda^k(M)$, and $\mathcal{T}_l^k(M)$ denote, respectively, the sets of smooth vector fields on M , k -form fields on M , and (k, l) -tensor fields on M . The value of a tensor $\rho \in \mathcal{T}_l^k(M)$ acting on k vectors $X_i \in \mathfrak{X}(M)$ and l covectors $\mu_j \in \Lambda^1(M)$ is denoted by $\rho(\mu_1, \dots, \mu_l, X_1, \dots, X_k)$. Note that $\Lambda^1(M) = \mathcal{T}_0^1(M)$ and $\mathfrak{X}(M) = \mathcal{T}_1^0(M)$. Note also that it is standard to extend the Levi-Civita connection $\bar{\nabla}$ from vector fields to tensor fields (see e.g., [32, Lemma 4.6]) so that the Leibniz rule holds.

For coordinate computations, we use a chart to move locally to a Euclidean domain with coordinates x^1, x^2 . Let the accompanying coordinate frame and coframe be denoted by ∂_i and dx^i . We assume these coordinates preserve orientation, so the orientation of M is given by the ordering (∂_1, ∂_2) . Let $\mathcal{S}(M) = \{\sigma \in \mathcal{T}_0^2(M) : \sigma(X, Y) = \sigma(Y, X) \text{ for } X, Y \in \mathfrak{X}(M)\}$ and $\mathcal{S}^+(M) = \{\sigma \in \mathcal{S}(M) : \sigma(X, X) > 0 \text{ for } 0 \neq X \in \mathfrak{X}(M)\}$. They represent the subspace of symmetric tensors in $\mathcal{T}_0^2(M)$, whose elements σ can be expressed in coordinates as $\sigma = \sigma_{ij} dx^i \otimes dx^j$ with smoothly varying coefficients σ_{ij} satisfying $\sigma_{ij} = \sigma_{ji}$ and are additionally positive definite, respectively.

We will use standard operations on 2-manifold spaces such as the Hodge star $\star : \Lambda^k(M) \rightarrow \Lambda^{2-k}(M)$, the exterior derivative $d : \Lambda^k(M) \rightarrow \Lambda^{k+1}(M)$, the tangent to cotangent isomorphism $\flat : \mathfrak{X}(M) \rightarrow \Lambda^1(M)$, and the reverse operation $\sharp : \Lambda^1(M) \rightarrow \mathfrak{X}(M)$. Their definitions can be found in standard texts [32, 38, 47].

2.2. Curvature.

The exact metric \bar{g} is an element of $\mathcal{S}^+(M)$. We define the *Riemann curvature tensor* $\bar{R} \in \mathcal{T}_0^4(M)$ of the manifold following [32],

$$\bar{R}(X, Y, Z, W) = \bar{g}(\bar{\nabla}_X \bar{\nabla}_Y Z - \bar{\nabla}_Y \bar{\nabla}_X Z - \bar{\nabla}_{[X, Y]} Z, W), \quad X, Y, Z, W \in \mathfrak{X}(M). \quad (2.1)$$

If X and Y are linearly independent, the *Gauss curvature* of M can be expressed by

$$K(\bar{g}) = \frac{\bar{R}(X, Y, Y, X)}{\bar{g}(X, X)\bar{g}(Y, Y) - \bar{g}(X, Y)^2}, \quad (2.2)$$

whose value is well known to be independent of the choice of the basis (see, e.g., [32, p. 144] or [14, Ch. 4, Proposition 3.1]).

We will also need the *geodesic curvature* along a curve Γ in the manifold (M, \bar{g}) . To recall its standard definition (see [47, p. 140] or [32]), we let $0 < s < a$ be the \bar{g} -arclength parameter so that Γ is described by $\mu(s)$ for some smooth $\mu : [0, a] \rightarrow M$ and its \bar{g} -unit tangent vector is $T(s) = d\mu/ds$. Let $N(s)$ be such that $(T(s), N(s))$ is a \bar{g} -orthonormal set of two vectors in the tangent space whose orientation is the same as that of M , i.e., $dx^1 \wedge dx^2(T(s), N(s)) > 0$. Then

$$\kappa(\bar{g}) = \bar{g}(\bar{\nabla}_{T(s)} T(s), N(s)) \quad (2.3)$$

gives the geodesic curvature at the point $\mu(s)$ of Γ .

2.3. Approximate metric.

We are interested in approximating $K(\bar{g})$ when the metric is given only approximately. We assume that M has been subdivided into a geometrically conforming triangulation \mathcal{T} . The edges of \mathcal{T} may be curved, but do not necessarily consist of geodesics.

On each element $T \in \mathcal{T}$, we are given an approximation $g|_T \in \mathcal{S}(T)$ of $\bar{g}|_T$. When the approximation is sufficiently good, g will also be positive definite since \bar{g} is. Then each $T \in \mathcal{T}$ can be considered to be a Riemannian manifold $(T, g|_T)$ with $g|_T$ as its metric. Since $g|_T$ is smooth within each element T (not across ∂T), we use the unique Levi-Civita connection ∇ generated by $g|_T$ to compute covariant derivatives within T . (Constraints on g across element boundaries are clarified below in (2.12)). We drop the accent $\bar{\cdot}$ in any previous definition to indicate that it pertains to the manifold $(T, g|_T)$ instead of (M, \bar{g}) , e.g., R refers to the Riemann curvature tensor computed using g and ∇ in place of \bar{g} and $\bar{\nabla}$ in (2.1).

A point $p \in T$ can be viewed either as a point in the manifold M or as a point in the manifold T . Irrespective of the two viewpoints, the meanings of coordinate frame ∂_i , coframe dx^i , and the tangent space $T_p M$ at p are unchanged. In coordinates,

$$g_{ij} = g(\partial_i, \partial_j), \quad g^{ij} = g^{-1}(dx^i, dx^j) \quad (2.4)$$

may be viewed as entries of symmetric positive definite matrices. *Christoffel symbols of the first kind* (Γ_{ijk}) and the *second kind* (Γ_{ij}^k) are defined by

$$\Gamma_{ijk} = g(\nabla_{\partial_i} \partial_j, \partial_k), \quad \nabla_{\partial_i} \partial_j = \Gamma_{ij}^k \partial_k. \quad (2.5a)$$

They can alternately be expressed, using (2.4), as

$$\Gamma_{ijl} = \frac{1}{2}(\partial_i g_{jl} + \partial_j g_{li} - \partial_l g_{ij}), \quad \Gamma_{ij}^k = g^{kl} \Gamma_{ijl}. \quad (2.5b)$$

Later, we will also use $\Gamma_{ijl}(\sigma)$ to denote $\frac{1}{2}(\partial_i \sigma_{jl} + \partial_j \sigma_{li} - \partial_l \sigma_{ij})$ for other tensors σ in $\mathcal{T}_0^2(M)$.

2.4. Tangents and normals on element boundaries.

Throughout this paper, we use τ to denote a tangent vector (not g -normalized; cf. (3.15) later) along an element boundary ∂T for any $T \in \mathcal{T}$. The orientation of τ is aligned with the boundary orientation of ∂T (inherited from the orientation of T , which is the same as the orientation of M). For any $p \in \partial T$, define $\tilde{\nu} \in T_p M$ by

$$g(\tilde{\nu}, X) = (dx^1 \wedge dx^2)(\tau, X), \quad \text{for all } X \in T_p M. \quad (2.6)$$

It is easy to see from (2.6) that the ordered basis $(\tau, \tilde{\nu})$ has the same orientation as (∂_1, ∂_2) since $(dx^1 \wedge dx^2)(\tau, \tilde{\nu}) > 0$, and moreover,

$$g(\tilde{\nu}, \tau) = 0, \quad \text{and} \quad g(\tilde{\nu}, \tilde{\nu}) \det(g) = g(\tau, \tau). \quad (2.7)$$

In particular, defining

$$\hat{\nu} = \frac{\tilde{\nu}}{\sqrt{g_{\tilde{\nu}} \tilde{\nu}}}, \quad \hat{\tau} = \frac{\tau}{\sqrt{g_{\tau} \tau}}, \quad (2.8)$$

we obtain a g -orthonormal basis $(\hat{\tau}, \hat{\nu})$ of normal and tangent vectors along every element boundary ∂T , whose orientation matches the manifold's orientation. E.g., if M is the unit disc in \mathbb{R}^2 with the Euclidean metric $g = \delta$ and the standard orientation, then $\hat{\tau}$ is oriented counterclockwise and $\hat{\nu}$ points inward. As $\hat{\tau}^\flat \wedge \hat{\nu}^\flat$ is the volume form, the definition of the Hodge star implies $\alpha \wedge (\star \beta) = g(\alpha, \beta) \text{vol}_{M,g}$ for all $\alpha \in \wedge^1(M)$, that $\star(\hat{\tau}^\flat) = \hat{\nu}^\flat$, $\star(\hat{\nu}^\flat) = -\hat{\tau}^\flat$, and thus for any $\omega \in \wedge^1(M)$ by expanding $\omega = \omega(\hat{\tau})\hat{\tau}^\flat + \omega(\hat{\nu})\hat{\nu}^\flat$, we have

$$(\star\omega)(\hat{\nu}) = \omega(\hat{\tau}), \quad (\star\omega)(\hat{\tau}) = -\omega(\hat{\nu}). \quad (2.9)$$

In (2.8) and throughout, we use σ_{uv} to denote $\sigma(u, v)$ for any vectors $u, v \in T_p M$ and $\sigma \in \mathcal{S}(M)$. Note that g_{uv} is not to be confused with the g_{ij} introduced in (2.4) where the indices are integers (which trigger the summation convention) rather than vectors.

To write $\tilde{\nu}$ in coordinates, it is useful to introduce the alternating symbol ε^{ij} whose value is 1, -1 , or 0 according to whether (i, j) is an even permutation, odd permutation, or not a permutation of $(1, 2)$, respectively. The value of the symbols ε_{ij} , ε_i^j , and ε^i_j equal ε^{ij} . It is easy to see that (2.6) implies

$$\tilde{\nu}^k = -g^{kj}\varepsilon_{ji}\tau^i. \quad (2.10)$$

2.5. Finite element spaces.

Let $C^\infty(\mathcal{T})$ denote the space of *piecewise smooth* functions on \mathcal{T} , by which we mean functions that are infinitely smooth within each mesh element and continuous up to (including) the boundary of each mesh element T . A notation in §2.1 with \mathcal{T} in place of M indicates the piecewise smooth analogue, e.g.,

$$\mathfrak{X}(\mathcal{T}) = \{X = X^i \partial_i : X^i \in C^\infty(\mathcal{T})\}, \quad \mathcal{S}(\mathcal{T}) = \{\sigma_{ij} dx^i \otimes dx^j : \sigma_{ij} = \sigma_{ji} \in C^\infty(\mathcal{T})\},$$

etc. Note that a $\sigma \in \mathcal{S}(\mathcal{T})$ need not be continuous across the element interfaces. (Although $\Lambda^0(\mathcal{T})$ and $C^\infty(\mathcal{T})$ are the same as sets, we typically use the latter for coefficients like X^i .) Let $E = \partial T_+ \cap \partial T_-$ denote an interior mesh edge (possibly curved) shared between elements $T_\pm \in \mathcal{T}$. Let $T_p E$ denote the one-dimensional tangent space of the curve E at any one of its points p . (Note that the tangent space at p from either element T_\pm coincides with $T_p M$ and $T_p E \subset T_p M$.) We say that a $\sigma \in \mathcal{S}(\mathcal{T})$ has “tangential-tangential continuity” or that σ is *tt-continuous* if

$$\sigma|_{T_+}(X, X) = \sigma|_{T_-}(X, X), \quad \text{for all } X \in T_p E, \quad (2.11)$$

at all $p \in E$, and for every interior mesh edge E . Here and throughout, to simplify notation, we do not explicitly indicate the point p at which the tensor σ is evaluated. Let

$$\mathcal{R}(\mathcal{T}) = \{\sigma \in \mathcal{S}(\mathcal{T}) : \sigma \text{ is tt-continuous}\}, \quad (2.12a)$$

$$\mathcal{R}^+(\mathcal{T}) = \{\sigma \in \mathcal{R}(\mathcal{T}) : \sigma(X, X) > 0 \text{ for all } X \in T_p M\}. \quad (2.12b)$$

The approximate metric g is assumed to be in $\mathcal{R}^+(\mathcal{T})$. For the numerical analysis later, we will additionally assume that it is in \mathcal{R}_h^k defined below.

In finite element computations, we use a reference element \hat{T} , the unit triangle, and the space $\mathcal{P}^k(\hat{T})$ of polynomials of degree at most k on \hat{T} . Let \tilde{T} denote a Euclidean triangle with possibly curved edges that is diffeomorphic to \hat{T} via $\hat{\Phi} : \hat{T} \rightarrow \tilde{T}$. For finite element computations on manifolds, we need charts so that each whole element $T \in \mathcal{T}$ of the manifold is covered by a single chart giving the coordinates x^i on T . The chart identifies the parameter domain of T as the (possibly curved) Euclidean triangle \tilde{T} diffeomorphic to T . Let $\Phi : T \rightarrow \tilde{T}$ denote the diffeomorphism. Then $\Phi_T = \hat{\Phi}^{-1} \circ \Phi : T \rightarrow \hat{T}$ maps diffeomorphically to the reference element where $\mathcal{P}^k(\hat{T})$ is defined. We use its pullback Φ_T^* below, which is simply the composition with Φ_T for scalar functions.

Define the *Regge finite element space* of degree k on the manifold M by

$$\mathcal{R}_h^k = \{\sigma \in \mathcal{R}(\mathcal{T}) : \text{for all } T \in \mathcal{T}, \sigma|_T = \sigma_{ij} dx^i \otimes dx^j \text{ with } \sigma_{ij} \circ \Phi_T \in \mathcal{P}^k(\hat{T})\}. \quad (2.13)$$

The subscript h indicates a mesh size parameter, e.g., on meshes whose elements are close to straight-edged triangles, one may set $h = \max_{T \in \mathcal{T}} \text{diam}(T)$. Let

$$\mathcal{V}(\mathcal{T}) = \{u \in \Lambda^0(\mathcal{T}) : u \text{ is continuous on } M\},$$

$$\mathring{\mathcal{V}}_\Gamma(\mathcal{T}) = \{u \in \mathcal{V}(\mathcal{T}) : u|_\Gamma = 0\},$$

where Γ denotes a subset of the boundary ∂M of positive boundary measure.

The *Lagrange finite element space* on M and its subspaces with essential boundary conditions are defined by

$$\begin{aligned}\mathcal{V}_h^k &= \{u \in \mathcal{V}(\mathcal{T}) : \text{for all } T \in \mathcal{T}, u|_T \circ \Phi_T \in \mathcal{P}^k(\hat{T})\}, \\ \mathring{\mathcal{V}}_{h,\Gamma}^k &= \{u \in \mathcal{V}_h^k : u|_\Gamma = 0\} \quad \text{and} \quad \mathring{\mathcal{V}}_h^k = \mathring{\mathcal{V}}_{h,\partial M}^k.\end{aligned}\tag{2.14}$$

The previous definitions in this subsection were independent of the metric. We will now introduce a metric-dependent space of normal-continuous vector fields. First, we introduce the following notation surrounding an interior mesh edge E shared by two adjacent elements in \mathcal{T} ,

$$E = \partial T_- \cap \partial T_+, \quad T_\pm \in \mathcal{T}.\tag{2.15a}$$

In this context, the g -orthonormal tangent and normal vectors introduced above along ∂T_\pm are denoted by $\hat{\tau}_\pm$ and $\hat{\nu}_\pm$, respectively. For a collection of scalar functions, $\{f_{\partial T}(\hat{\nu}) : T \in \mathcal{T}\}$, each depending linearly on the normal $\hat{\nu}$ at an element boundary, we define the jump on E by

$$[f(\hat{\nu})] = f_{\partial T_+}(\hat{\nu}_+) - f_{\partial T_-}(\hat{\nu}_-).\tag{2.15b}$$

The jump function $[f(\hat{\nu})]$ is single-valued on the union of all interior mesh edges, excluding the mesh vertices. The jump of an element boundary function dependent on $\hat{\tau}$ (in place of $\hat{\nu}$) is defined similarly.

We say that a piecewise smooth vector field $W \in \mathfrak{X}(\mathcal{T})$ has “ g -normal continuity” across element interfaces if $[g(W, \hat{\nu})] = 0$. Define

$$\begin{aligned}\mathcal{W}_g(\mathcal{T}) &= \{W \in \mathfrak{X}(\mathcal{T}) : [g(W, \hat{\nu})] = 0\}, \\ \mathring{\mathcal{W}}_{g,\Gamma}(\mathcal{T}) &= \{W \in \mathcal{W}_g(\mathcal{T}) : g(W|_\Gamma, \hat{\nu}) = 0\}, \quad \mathring{\mathcal{W}}_g(\mathcal{T}) = \mathring{\mathcal{W}}_{g,\partial M}(\mathcal{T}).\end{aligned}\tag{2.16}$$

Also define their polynomial subspaces

$$\begin{aligned}\mathcal{W}_{g,h}^k &= \{W \in \mathcal{W}_g(\mathcal{T}) : \text{for all } T \in \mathcal{T}, W|_T = \Phi_T^* \hat{W} \text{ for some } \hat{W} \in \mathcal{P}^k(\hat{T}, \mathbb{R}^2)\}, \\ \mathring{\mathcal{W}}_{g,h,\Gamma}^k &= \{W \in \mathcal{W}_{g,h}^k : g(W|_\Gamma, \hat{\nu}) = 0\}, \quad \mathring{\mathcal{W}}_{g,h}^k = \mathring{\mathcal{W}}_{g,h,\partial M}^k.\end{aligned}$$

2.6. Integrals over the manifold’s triangulation.

On every element $T \in \mathcal{T}$, in order to integrate a scalar function $f \in \Lambda^0(T)$, adopting the notation of [33], we tacitly use the unique Riemannian volume form $\text{vol}_{T,g}$ to convert it to a 2-form and then pullback to integrate over the Euclidean parameter domain \hat{T} , i.e.,

$$\int_{(T,g)} f \equiv \int_T f \text{vol}_{T,g} = \int_{\hat{T}} (\Phi^{-1})^*(f \text{vol}_{T,g}) = \int_{\hat{T}} f \circ \Phi^{-1} \frac{\sqrt{\det g}}{\det(D\Phi)} \text{da},\tag{2.17}$$

where $\det(D\Phi)$ denotes the Jacobian determinant of Φ , we have used the standard extension of pullback to forms, and we have appended an area measure notation “da” to emphasize that the right most integral is a standard Lebesgue integral over the Euclidean domain \hat{T} . For $v, w \in \Lambda^0(\mathcal{T})$, set

$$\int_{\mathcal{T}} w = \sum_{T \in \mathcal{T}} \int_{(T,g)} w, \quad (v, w)_{\mathcal{T}} = \sum_{T \in \mathcal{T}} \int_{(T,g)} v w,$$

with the understanding that the right hand sides above must be evaluated using (2.17). In order to integrate along the boundary curve ∂T , we use the one-dimensional analogue of the formula in (2.17) to compute on the Euclidean domain $\partial \hat{T} = \Phi(\partial T)$, namely

$$\int_{(\partial T,g)} f = \int_{\partial \hat{T}} (\Phi^{-1})^*(f \text{vol}_{\partial T,g}) = \int_{\partial \hat{T}} f \circ \Phi^{-1} \sqrt{g_{tt}} \text{dl},\tag{2.18}$$

where t is a tangent vector along $\partial\tilde{T}$ of unit Euclidean length—and to emphasize that the last integral is a standard Euclidean integral, we have appended the length measure “dl”. We use

$$\int_{\partial\mathcal{T}} w = \sum_{T \in \mathcal{T}} \int_{(\partial T, g)} w$$

to simplify notation for sum of integrals over element boundaries.

3. Curvature approximation

In this section we give the curvature approximation formula and discuss a few nontrivial computational details on curved elements. In order to approximate the Gauss curvature $K(\bar{g})$, one may consider computing $K(g|_T)$ on each element $T \in \mathcal{T}$ using the given approximation g of the exact metric \bar{g} . However, this alone cannot generally be a good approximation to $K(\bar{g})$ because discontinuities of g across elements generate additional sources of curvature on the edges and vertices of the mesh. Below we provide a curvature approximation incorporating these extra sources. Since it coincides with the formula given in a recent work [10] for a specific case, we opt for a brief description, expanding only on aspects complementary to that work.

3.1. A finite element curvature approximation

Given a metric $g \in \mathcal{R}^+(\mathcal{T})$ approximating \bar{g} we identify three sources of curvature, modeled after similar terms in the Gauss–Bonnet formula, and define them as the following linear functionals acting on $\varphi \in \mathcal{V}(\mathcal{T})$:

$$\begin{aligned} \langle K_g^T, \varphi \rangle_{\mathcal{V}(\mathcal{T})} &= \int_{(T, g)} K(g) \varphi, & \langle K_{E,g}^T, \varphi \rangle_{\mathcal{V}(\mathcal{T})} &= \int_{(E, g)} \kappa(g) \varphi, \\ \langle K_{V,g}, \varphi \rangle_{\mathcal{V}(\mathcal{T})} &= \left(2\pi - \sum_{T \in \mathcal{T}_V} \triangle_V^T g \right) \varphi(V), \end{aligned} \tag{3.1}$$

where \mathcal{T}_V denotes the set of all elements of \mathcal{T} which have V as a vertex. Here $K(g)$ and $\kappa(g)$ are defined by (2.2) and (2.3) after replacing \bar{g} by g , and $\triangle_V^T(\cdot)$ denotes the interior angle at a vertex V of T determined using the metric in its argument (computable using (3.5) below). Note that for vertices V and edges E on the boundary ∂M , neither $K_{V,g}$ nor $K_{E,g}^T$ vanishes in general, but they will be weakly matched with boundary data below. Throughout, we use $\langle f, \varphi \rangle_H$ to denote duality pairing on a vector space H that gives the action of a linear functional $f \in H'$ acting on a $\varphi \in H$. Also, \mathcal{V} and \mathcal{E} denote the set of mesh vertices and edges, respectively (so in (3.1), $V \in \mathcal{V}$ and $E \in \mathcal{E}$). Define $K_g \in \mathcal{V}(\mathcal{T})'$ by

$$K_g = \sum_{T \in \mathcal{T}} \left(K_g^T + \sum_{E \in \mathcal{E}_T} K_{E,g}^T \right) + \sum_{V \in \mathcal{V}} K_{V,g}. \tag{3.2}$$

Here \mathcal{E}_T denotes the set of three edges of ∂T .

In addition to g , suppose that we are also given boundary curvature data in essential (Dirichlet) or natural (Neumann) forms for manifolds with boundary. The former type of data arises when we know that M is a submanifold of a larger manifold whose Gauss curvature is known outside of M . To accommodate such information only on a part of the boundary of M , we split ∂M into two non-overlapping parts Γ_D and Γ_N . One of these can be empty. In case none of them is empty, both must have positive length. On Γ_D , we assume that we are given $K^D = K(\bar{g})|_{\Gamma_D}$ and that K^D is in the trace of the Lagrange finite element space \mathcal{V}_h^k . E.g., when a manifold is flat around Γ_D (i.e., $K(\bar{g})$ vanishes in a neighborhood of Γ_D), we may set homogeneous Dirichlet data $K^D = 0$ on Γ_D . The other type of boundary data, in the form of a natural (or Neumann) boundary condition, is motivated

by the Gauss–Bonnet theorem, and provides geodesic curvature data at the boundary. These natural Neumann-type boundary data is given in the form of a data functional $\kappa^N \in \mathcal{V}(\mathcal{T})'$,

$$\langle \kappa^N, \varphi \rangle_{\mathcal{V}(\mathcal{T})} = \int_{(\Gamma_N, \bar{g})} \kappa(\bar{g}) \varphi + \sum_{V \in \mathcal{V}^N} \tilde{\alpha}_V^N(\bar{g}) \varphi(V), \quad (3.3)$$

for $\varphi \in \mathcal{V}(\mathcal{T})$, where $\mathcal{V}^N \subset \mathcal{V} \cap \Gamma_N$ is the subset of the manifold's vertices contained in the interior of Γ_N and $\tilde{\alpha}_V^N$ denotes the exterior angle measured by the edges of Γ_N at V . (If V is part of a smooth boundary, such an angle amounts to π , whereas at kinks of the boundary the angle has to be provided as input data.) The action of functional (3.3) on the finite-dimensional subspace $\mathcal{V}_h^k \subset \mathcal{V}(\mathcal{T})$ is computable if we are given the exact metric \bar{g} on and near Γ_N . For manifolds without boundary, there is no need to provide any boundary data.

Definition 3.1. Let $g \in \mathcal{R}^+(\mathcal{T})$ and $k \geq 0$ be an integer. The finite element curvature approximation $K_h(g)$ of degree $k+1$ is the unique function in \mathcal{V}_h^{k+1} determined by requiring that $K_h(g)|_{\Gamma_D} = K^D$ on Γ_D and for all $u_h \in \mathcal{V}_{h,\Gamma_D}^{k+1}$,

$$\int_{\mathcal{T}} K_h(g) u_h = \langle K_g, u_h \rangle_{\mathcal{V}(\mathcal{T})} - \langle \kappa^N, u_h \rangle_{\mathcal{V}(\mathcal{T})}. \quad (3.4)$$

3.2. Implementation issues

We now discuss how to numerically compute the quantities in (3.4) in the given computational coordinates x^i . Recall (from §2.4) that the tangent vector τ along the boundary ∂T is aligned with the boundary orientation of ∂T . Let \mathcal{V}_T denotes the set of three vertices of an element $T \in \mathcal{T}$. At any vertex $V \in \mathcal{V}_T$, the tangent τ undergoes a change in direction, between an incoming and an outgoing tangent vector, which we denote by τ_- and τ_+ , respectively. The angle at V with respect to the metric g is then computed by

$$\Delta_V^T g = \arccos \left(\frac{g(-\tau_-, \tau_+)}{\sqrt{g(\tau_-, \tau_-)} \sqrt{g(\tau_+, \tau_+)}} \right). \quad (3.5)$$

This is what we use to calculate the angle deficit functional $K_{V,g}^T$ (3.1).

Next, consider the interior source term K_g^T , defined using $K(g)$, and related to the Riemann curvature by (2.2). By (2.1), $R_{ijkl} = R(\partial_i, \partial_j, \partial_k, \partial_l)$ simplifies to

$$R_{ijkl} = (\partial_i \Gamma_{jk}^p + \Gamma_{jk}^q \Gamma_{iq}^p - \partial_j \Gamma_{ik}^p - \Gamma_{ik}^q \Gamma_{jq}^p) g_{pl} = \partial_i \Gamma_{jkl} - \partial_j \Gamma_{ikl} - \Gamma_{ilp} \Gamma_{jk}^p + \Gamma_{jlp} \Gamma_{ik}^p, \quad (3.6)$$

where Γ_{ij}^k and Γ_{ijk} are as in (2.5). For two-dimensional manifolds the Gauss curvature can be expressed [14] by $K(g) = R_{1221}/\det g$. Hence by (2.17),

$$\langle K_g^T, \varphi \rangle_{\mathcal{V}(\mathcal{T})} = \int_T K(g) \varphi \sqrt{\det g} dx^1 \wedge dx^2 = \int_{\tilde{T}} \frac{\Phi_*(R_{1221} \varphi)}{\sqrt{\det g} \det(D\Phi)} da. \quad (3.7)$$

It thus remains to discuss the computation of the edge sources $K_{E,g}^T$ using the definition of $\kappa(g)$ in (2.3). In finite element computations, we usually do not have ready access to the g -arclength parameter s used there. But $\kappa(g)$ can be computed using the readily accessible τ and $\tilde{\nu}$ of §2.4, as shown below. Let $\gamma(t)$ be an orientation-preserving parametrization that gives an oriented mesh edge $E \subset \partial T$ as $E = \{\gamma(t) : t_0 \leq t \leq t_1\}$. Parametrizing scalar functions a on E by t , we abbreviate da/dt to \dot{a} . Note that the components of $\tau = \tau^k \partial_k$ are given by $\tau^k = \dot{\gamma}^k$ and their derivatives by $d^2 \gamma^k / dt^2 = \ddot{\gamma}^k$. Let

$$\dot{\tau} = \dot{\tau}^k \partial_k, \quad G_{uv}^w = g(u^i v^j \Gamma_{ij}^k \partial_k, w), \quad (3.8)$$

where $u = u^i \partial_i, v = v^i \partial_i, w \in \mathfrak{X}(T)$ and recall that $\tilde{\nu}$ was defined in (2.6).

Lemma 3.2. *The geodesic curvature along each edge of an element boundary ∂T is given by*

$$\kappa(g) = \frac{\sqrt{\det g}}{g_{\tau\tau}^{3/2}} (g_{\hat{\tau}\tilde{\nu}} + G_{\tau\tau}^{\tilde{\nu}}). \quad (3.9)$$

Proof. By (2.3) and our definitions of $\hat{\tau}, \hat{\nu}$ in §2.4,

$$\kappa(g) = g(\nabla_{\hat{\tau}(s)} \hat{\tau}(s), \hat{\nu}(s)) \quad (3.10)$$

where s is the g -arclength parameter. Inverting $s(t) = \int_0^t g(\tau(\alpha), \tau(\alpha))^{1/2} d\alpha$ to write t as a function of s , applying the chain rule to $\mu(s) = \gamma(t(s))$, and using $dt/ds = g_{\tau\tau}^{-1/2}$,

$$\frac{d\hat{\tau}^k}{ds} = \frac{d^2\mu^k}{ds^2} = \frac{d^2\gamma^k}{dt^2} \left(\frac{dt}{ds} \right)^2 + \frac{d\gamma^k}{dt} \frac{d^2t}{ds^2} = \frac{\dot{\tau}^k}{g_{\tau\tau}} + \tau^k \frac{d^2t}{ds^2}.$$

Using the properties of the connection ∇ (see e.g. [32]),

$$\nabla_{\hat{\tau}} \hat{\tau} = \frac{d\hat{\tau}^k}{ds} \partial_k + \hat{\tau}^i \hat{\tau}^j \Gamma_{ij}^k \partial_k = \frac{\dot{\tau}}{g_{\tau\tau}} + \tau \frac{d^2t}{ds^2} + \hat{\tau}^i \hat{\tau}^j \Gamma_{ij}^k \partial_k. \quad (3.11)$$

Hence (3.10), (3.11), and the g -orthogonality of τ with $\hat{\nu}$, implies that at the point $\gamma(t)$,

$$\kappa(g) = \frac{g(\dot{\tau}, \hat{\nu})}{g_{\tau\tau}} + \frac{g(\tau^i \tau^j \Gamma_{ij}^k \partial_k, \hat{\nu})}{g_{\tau\tau}}. \quad (3.12)$$

Now, by (2.7) and (2.8), $\hat{\nu} = \tilde{\nu}(\det g/g_{\tau\tau})^{1/2}$, so (3.12) implies

$$\kappa(g) = \frac{(\det g)^{1/2}}{g_{\tau\tau}^{3/2}} [g(\dot{\tau}, \tilde{\nu}) + g(\tau^i \tau^j \Gamma_{ij}^k \partial_k, \tilde{\nu})] \quad (3.13)$$

which proves (3.9). ■

Returning to the edge source term, using Lemma 3.2 and (2.18),

$$K_{E,g}^T(\varphi, g) = \int_E \kappa(g) \varphi \sqrt{g_{\tau\tau}} = \int_{\Phi(E)} \Phi_* \left(\frac{\sqrt{\det g}}{g_{\tau\tau}} (g_{\hat{\tau}\tilde{\nu}} + G_{\tau\tau}^{\tilde{\nu}}) \varphi \right) \mathrm{d}l. \quad (3.14)$$

Thus, through (3.5), (3.7), and (3.14), we have shown it is possible to easily compute all the terms in the curvature approximation (3.4) using standard finite element tools.

3.3. A model case for further analysis

Having shown how curvature of general manifolds can be computed, we now focus our analysis on the following model case for the remainder of the paper. We assume that the manifold M , as a set, equals $\Omega \subset \mathbb{R}^2$, a bounded open connected domain, that $\Gamma_N = \emptyset$, and that \bar{g} has zero Gaussian curvature, $K(\bar{g}) = 0$, at the boundary (so zero Dirichlet boundary data is prescribed everywhere, cf. Section 3.1). The set Ω forms the full parameter domain of M for the single trivial chart $\Phi : M \rightarrow \Omega$ with Φ equaling the identity map. The triangulation \mathcal{T} of M is now a conforming finite element mesh in the planar domain Ω and its elements are (possibly curved) triangles.

In this setting, an element $T \in \mathcal{T}$ can be considered as either the Euclidean manifold (T, δ) , equipped with the identity metric δ , or the Riemannian manifold (T, g) . Let us reconsider the tangent vector τ on an element boundary ∂T with the orientation described in §2.4, previously left un-normalized. Henceforth, we assume that

$$1 = \delta(\tau, \tau). \quad (3.15)$$

We computed the normal vector $\tilde{\nu}$ from τ by (2.6) for the manifold (T, g) . For the manifold (T, δ) , a generally different Euclidean normal vector arises at any p in ∂T and we denote it by ν . It can be

computed by simply replacing g with δ in (2.6), i.e., $\nu \in T_p M$ satisfies

$$\delta(\nu, X) = dx^1 \wedge dx^2(\tau, X) \quad \text{for all } X \in T_p M. \quad (3.16)$$

Analogous to (2.10), we now have the accompanying coordinate expression,

$$\nu^k = -\delta^{kj} \varepsilon_{ji} \tau^i = -\varepsilon^k_i \tau^i. \quad (3.17)$$

Note that (3.15) implies that $\delta(\nu, \nu) = 1$. These identities, together with (2.8) guide us move between the δ -orthonormal tangent and normal vectors (τ and ν) and g -orthonormal tangent and normal vectors ($\hat{\tau}$ and $\hat{\nu}$), while preserving the orientation. Jumps of functions of ν and τ on the Euclidean element boundaries $(\partial T, \delta)$, $T \in \mathcal{T}$, are defined in analogy to (2.15b).

Recall the parameterization $\gamma(t)$ along an edge E and accompanying notation considered before (3.8). We now claim that

$$\dot{\nu} = -\delta(\nu, \dot{\tau})\tau, \quad \dot{\tau} = \delta(\nu, \dot{\tau})\nu. \quad (3.18)$$

This follows by differentiating the equation $\delta(\nu, \nu) = 1$ with respect to τ , yielding $\delta(\dot{\nu}, \nu) = 0$. Hence there must be a scalar α such that $\dot{\nu} = \alpha\tau$. Now differentiating $\delta(\nu, \tau) = 0$, we find that the α must satisfy $\delta(\alpha\tau, \tau) + \delta(\nu, \dot{\tau}) = 0$, so $\alpha = -\delta(\nu, \dot{\tau})$, thus proving the first identity in (3.18). A similar argument using $\delta(\tau, \tau) = 1$ proves the second identity in (3.18). Later, we will have occasion to consider variations of $\sigma_{\tau\nu} = \sigma(\tau, \nu)$ along an edge for some tensor $\sigma \in \mathcal{T}_0^2(M)$. By chain rule,

$$\frac{d}{dt}(\sigma_{\nu\tau}(\gamma(t))) = \dot{\nu}^i \tau^j \sigma_{ij}(\gamma(t)) + \nu^i \dot{\tau}^j \sigma_{ij}(\gamma(t)) + \nu^i \tau^j \frac{d}{dt}(\sigma_{ij}(\gamma(t))).$$

Hence (3.18), together with $\dot{\gamma} = \tau$, yields

$$\partial_\tau(\sigma_{\nu\tau}) = (\partial_\tau[\sigma])_{\nu\tau} + (\sigma_{\nu\nu} - \sigma_{\tau\tau}) \delta(\nu, \dot{\tau}), \quad (3.19)$$

on a curved edge, where $[\sigma]$ is the matrix whose (i, j) th entry is σ_{ij} .

We proceed to display the curvature approximation formula in coordinates for this model case using the Euclidean normal (ν) and tangent (τ).

Lemma 3.3. *The geodesic curvature along any mesh edge E is given by*

$$\kappa(g) = \frac{\sqrt{\det g}}{g_{\tau\tau}^{3/2}} (\dot{\tau}^\nu + \Gamma_{\tau\tau}^\nu)$$

where $\Gamma_{\tau\tau}^\nu = \tau^i \tau^j \Gamma_{ij}^k \delta_{kl} \nu^l$ and $\dot{\tau}^\nu = \delta(\dot{\tau}, \nu)$.

Proof. Comparing (3.16) with (2.6),

$$g(\tilde{\nu}, X) = \delta(\nu, X) \quad (3.20)$$

for any $X \in T_p M$. Using (3.20) in Lemma 3.2, the result follows. \blacksquare

In this model case of a single parameter domain, since the identity metric δ is well defined throughout, the angle deficit in (3.1) can be reformulated using δ as a sum of element contributions at each vertex. Define

$$\langle K_{V,g}^T, u_h \rangle_{\mathcal{V}(\mathcal{T})} = (\triangle_V^T \delta - \triangle_V^T g) u_h(V).$$

When summing $\triangle_V^T \delta$ over all $T \in \mathcal{T}_V$, we clearly obtain 2π for all interior vertices (boundary vertices are excluded as we assume homogeneous Dirichlet boundary conditions in this model case). Hence

$$\sum_{V \in \mathcal{V}} \langle K_{V,g}, u_h \rangle_{\mathcal{V}(\mathcal{T})} = \sum_{T \in \mathcal{T}} \sum_{V \in \mathcal{V}_T} \langle K_{V,g}^T, u_h \rangle_{\mathcal{V}(\mathcal{T})}. \quad (3.21)$$

Proposition 3.4. *In this model case, equation (3.4) implies that for all $u_h \in \mathring{\mathcal{V}}_h^k$,*

$$\begin{aligned} \int_{\mathcal{T}} K_h(g) u_h &= \sum_{T \in \mathcal{T}} \sum_{V \in \mathcal{V}_T} (\triangle_V^T \delta - \triangle_V^T g) u_h(V) \\ &\quad + \sum_{T \in \mathcal{T}} \left(\int_{\partial T} \frac{\sqrt{\det g}}{g_{\tau\tau}} (\dot{\tau}^\nu + \Gamma_{\tau\tau}^\nu) u_h \, dl + \int_T K(g) u_h \sqrt{\det g} \, da \right). \end{aligned} \quad (3.22)$$

If $g \in \mathcal{S}^+(M)$, then all terms vanish except the last.

Proof. Equation (3.22) follows from (3.21), (3.7), (3.14), and Lemma 3.3, once Φ is set to the identity. To prove the last statement, divide the set of mesh vertices \mathcal{V} into the set of boundary and interior vertices $\mathcal{V}^{\text{bnd}} = \mathcal{V} \cap \partial M$ and $\mathcal{V}^{\text{int}} = \mathcal{V} \setminus \mathcal{V}^{\text{bnd}}$. At every interior vertex $V \in \mathcal{V}^{\text{int}}$, a rearrangement gives

$$\sum_{T \in \mathcal{T}} \sum_{V \in \mathcal{V}_T^{\text{int}}} \langle K_{V,g}^T, u_h \rangle_{\mathcal{V}(\mathcal{T})} = \sum_{V \in \mathcal{V}^{\text{int}}} \sum_{T \in \mathcal{T}_V} (\triangle_V^T \delta - \triangle_V^T g) u_h(V),$$

which vanishes because the smoothness of g implies $\sum_{T \in \mathcal{T}_V} \triangle_V^T g = 2\pi = \sum_{T \in \mathcal{T}_V} \triangle_V^T \delta$. The element boundary integrals can be rewritten using the set of interior mesh edges \mathcal{E}^{int} , as

$$\sum_{T \in \mathcal{T}} \int_{\partial T} \frac{\sqrt{\det g}}{g_{\tau\tau}} (\dot{\tau}^\nu + \Gamma_{\tau\tau}^\nu) u_h \, dl = \sum_{E \in \mathcal{E}^{\text{int}}} \int_E \frac{\sqrt{\det g}}{g_{\tau\tau}} [\dot{\tau}^\nu + \Gamma_{\tau\tau}^\nu] u_h \, dl, \quad (3.23)$$

since $u_h = 0$ on Γ_D and that the trace of $\sqrt{\det g}/g_{\tau\tau}$ is well defined (single valued) on E due to the given smoothness of $g \in \mathcal{S}^+(M)$. It is easy to see that $\dot{\tau}$ has the same value from adjacent elements of E while τ and ν changes sign, so $[\dot{\tau}^\nu] = 0$ and $[\Gamma_{\tau\tau}^\nu] = 0$. Hence (3.23) vanishes. ■

4. Covariant derivatives using the nonsmooth metric

The objective of this section is to formulate a covariant incompatibility operator that can be applied to our situation with piecewise smooth metrics. To this end, we first define several covariant derivatives in the smooth case, restricting ourselves to a single element, i.e., the smooth Riemannian manifold $(T, g|_T)$. Then we proceed to consider the changes needed due to the jumps of the metric across element interfaces.

4.1. Covariant curl and incompatibility for smooth metric

For $\mu \in \Lambda^1(T)$, define

$$(F\mu)(X, Y) = (\nabla_X \mu)(Y) - (\nabla_Y \mu)(X) \quad (4.1)$$

for any $X, Y \in \mathfrak{X}(T)$. Next, for $\sigma \in \mathcal{T}_0^2(T)$ writing $\sigma_Z(Y) = \sigma(Z, Y)$ for any $Y, Z \in \mathfrak{X}(T)$, define an operation analogous to (4.1) by

$$(F\sigma_Z)(X, Y) = (\nabla_X \sigma)(Z, Y) - (\nabla_Y \sigma)(Z, X). \quad (4.2)$$

Since the expressions in (4.1) and (4.2)–holding Z fixed–are skew-symmetric in X and Y , they may be viewed as elements of $\Lambda^2(T)$. Then we may use the Hodge star \star operation to convert them to 0-forms, since T is two dimensional. Doing so, define

$$\text{curl}_g \mu = \star(F\mu), \quad \mu \in \mathcal{T}_0^1(T) = \Lambda^1(T), \quad (4.3a)$$

$$(\text{curl}_g \sigma)(Z) = \star(F\sigma_Z), \quad \sigma \in \mathcal{T}_0^2(T), Z \in \mathfrak{X}(T). \quad (4.3b)$$

The latter, $\text{curl}_g \sigma$, due to linearity in Z , is in $\Lambda^1(T)$, while the former, $\text{curl}_g \mu$, is in $\Lambda^0(T)$. Combining these operations in succession, we define the *covariant incompatibility*,

$$\text{inc}_g \sigma = \text{curl}_g \text{curl}_g \sigma, \quad \sigma \in \mathcal{T}_0^2(T), \quad (4.3c)$$

on two-dimensional manifolds. Clearly $\text{inc}_g \sigma$ is in $\Lambda^0(T)$.

Remark 4.1. For $\mu \in \Lambda^1(T)$, the exterior derivative, $d\mu \in \Lambda^2(T)$, can be expressed in terms of the connection by

$$(d\mu)(X, Y) = (\nabla_X \mu)(Y) - (\nabla_Y \mu)(X),$$

see, e.g., [38]. Hence, $F\mu = d\mu$, which explains why (4.1), is used to define the curl of a 1-form. Next, for any $\sigma \in \mathcal{T}_0^2(T)$, consider the unique linear operator $A_\sigma : \mathfrak{X}(T) \rightarrow \mathfrak{X}(T)$ given by $g(A_\sigma X, Y) = \sigma(X, Y)$ for all $X, Y \in \mathfrak{X}(T)$. Viewing A_σ as a 1-form taking values in $\mathfrak{X}(T)$, its *exterior covariant derivative* $d^\nabla A_\sigma$, is a 2-form taking values in $\mathfrak{X}(T)$. It satisfies, for any $X, Y, Z \in \mathfrak{X}(T)$,

$$g((d^\nabla A_\sigma)(X, Y), Z) = (\nabla_X \sigma)(Y, Z) - (\nabla_Y \sigma)(X, Z),$$

which coincides with the right hand side of (4.2). Thus our definition of the covariant curl of a tensor σ can be understood through the exterior covariant derivative.

We will now quickly write down coordinate expressions for the covariant inc and curl. Expanding the right hand side of (4.2) using the Leibniz rule $(\nabla_X \sigma)(Z, Y) = X\sigma(Z, Y) - \sigma(\nabla_X Z, Y) - \sigma(Z, \nabla_X Y)$ twice, substituting $Z = \partial_i, X = \partial_j, Y = \partial_k$, and simplifying using (2.5a),

$$(F\sigma_{\partial_i})(\partial_j, \partial_k) = (\partial_j \sigma_{ik} - \Gamma_{ji}^m \sigma_{mk}) - (\partial_k \sigma_{ij} - \Gamma_{ki}^m \sigma_{mj}) \quad (4.4)$$

for $\sigma = \sigma_{jk} dx^j \otimes dx^k \in \mathcal{T}_0^2(T)$. Note that equation (4.4) can be rewritten as $F\sigma_{\partial_i} = \varepsilon^{jk}(\partial_j \sigma_{ik} - \Gamma_{ji}^m \sigma_{mk}) dx^1 \wedge dx^2$. Next, since (4.3b) implies $\text{curl}_g \sigma = (\star F\sigma_{\partial_i}) dx^i$, recalling that $\star(f dx^1 \wedge dx^2) = f/\sqrt{\det g}$ for any scalar field $f \in \Lambda^0(T)$, we arrive at

$$\text{curl}_g(\sigma_{jk} dx^j \otimes dx^k) = \frac{1}{\sqrt{\det g}} \varepsilon^{jk} (\partial_j \sigma_{ik} - \Gamma_{ji}^m \sigma_{mk}) dx^i. \quad (4.5a)$$

Similarly, one obtains coordinate expressions for the remaining operators in (4.3), namely

$$\text{curl}_g(\mu_i dx^i) = \frac{1}{\sqrt{\det g}} \varepsilon^{ij} \partial_i \mu_j, \quad (4.5b)$$

$$\text{inc}_g(\sigma_{jk} dx^j \otimes dx^k) = \frac{1}{\det g} \left(\varepsilon^{qi} \varepsilon^{jk} \partial_{jq} \sigma_{ik} - \varepsilon^{qi} \varepsilon^{jk} \partial_q (\Gamma_{ji}^m \sigma_{mk}) - \Gamma_{lq}^l \varepsilon^{qi} \varepsilon^{jk} (\partial_j \sigma_{ik} - \Gamma_{ji}^m \sigma_{mk}) \right). \quad (4.5c)$$

In the derivation of (4.5c), we have employed the useful formula

$$\Gamma_{lq}^l = \frac{\partial_q(\det g)}{2 \det g}. \quad (4.6)$$

It is useful to contrast the expressions in (4.5) with the standard Euclidean curl and inc. To this end we use matrix and vector proxies, $[\sigma] \in \mathbb{R}^{2 \times 2}$ and $[\mu] \in \mathbb{R}^2$, of $\mu \in \Lambda^1(T)$ and $\sigma \in \mathcal{T}_0^2(T)$, respectively [3]. These proxies are made up of coefficients in the coordinate basis expansion, specifically $[\sigma]$ is the matrix whose (i, j) th entry is $\sigma_{ij} = \sigma(\partial_i, \partial_j)$, and $[\mu]$ is the Euclidean vector whose i th component, denoted by $[\mu]_i$, equals $\mu_i = \mu(\partial_i)$. Then the standard two-dimensional curl operator applied to the vector $[\mu]$ gives $\text{curl}[\mu] = \varepsilon^{ij} \partial_i \mu_j$. When this operator is repeated row-wise on a matrix, we get the standard row-wise matrix curl, namely $[\text{curl}[\sigma]]_i = \varepsilon^{jk} \partial_j \sigma_{ik}$. The standard Euclidean

incompatibility operator [1, 4, 19] in two dimensions is $\text{inc}[\sigma] = \varepsilon^{qi}\varepsilon^{jk}\partial_{jq}\sigma_{ik}$. Using these, we can rewrite the formulas in (4.5) as

$$[\text{curl}_g \mu] = \frac{1}{\sqrt{\det g}} \text{curl}[\mu], \quad (4.7a)$$

$$[\text{curl}_g \sigma]_i = \frac{1}{\sqrt{\det g}} ([\text{curl}[\sigma]]_i - \varepsilon^{jk}\Gamma_{ji}^m\sigma_{mk}), \quad (4.7b)$$

$$[\text{inc}_g \sigma] = \frac{1}{\det g} \left(\text{inc}[\sigma] - \varepsilon^{qi}\varepsilon^{jk}\partial_q(\Gamma_{ji}^m\sigma_{mk}) - \Gamma_{lq}^l\varepsilon^{qi}(\text{curl}[\sigma]_i - \varepsilon^{jk}\Gamma_{ji}^m\sigma_{mk}) \right). \quad (4.7c)$$

Note how the expressions for covariant curl and covariant inc contain, but differ from their Euclidean analogues.

Other useful covariant operators include

$$\text{rot}_g f = -(\star df)^\sharp, \quad f \in \Lambda^0(T), \quad (4.8a)$$

$$(\text{rot}_g X)(\mu, \eta) = \mu(\nabla_{(\star\eta)^\sharp} X), \quad \mu, \eta \in \Lambda^1(T), X \in \mathfrak{X}(T). \quad (4.8b)$$

Clearly, $\text{rot}_g f$ is in $\mathfrak{X}(T)$, while $\text{rot}_g X \in \mathcal{T}_2^0(T)$. Their coordinate expressions are

$$\text{rot}_g f = \frac{\varepsilon^{kp}\partial_p f}{\sqrt{\det g}}\partial_k = \frac{[\text{rot } f]^k}{\sqrt{\det g}}\partial_k, \quad (4.9a)$$

$$\text{rot}_g X = \frac{\varepsilon^{pi}(\partial_i X^m + \Gamma_{ik}^m X^k)}{\sqrt{\det g}}\partial_m \otimes \partial_p = \frac{[\text{rot } X]^{mp} + \varepsilon^{pi}\Gamma_{ik}^m X^k}{\sqrt{\det g}}\partial_m \otimes \partial_p, \quad (4.9b)$$

where, in the latter expressions, the proxy notation has been extended to $\mathfrak{X}(T)$ and $\mathcal{T}_2^0(T)$ in an obvious fashion to use the Euclidean matrix and vector rot.

It is easy to see that the following integration by parts formula

$$\int_{(T,g)} (\text{curl}_g \sigma)(Z) = \int_{(T,g)} \sigma(\text{rot}_g Z) + \int_{(\partial T,g)} \sigma(Z, \hat{\tau}) \quad (4.10)$$

holds for all $\sigma \in \mathcal{T}_0^2(T)$ and $Z \in \mathfrak{X}(T)$. (This can be seen, e.g., using the coordinate expressions (4.9b) and (4.7b) and standard integration by parts on the Euclidean parameter domain.) Here $\hat{\tau}$ is the unit tangent defined in (2.8), the integrals are computed as indicated in (2.17), and $\sigma(\text{rot}_g Z)$ denotes the result obtained by acting the $\mathcal{T}_0^2(T)$ -tensor σ on the $\mathcal{T}_2^0(T)$ -tensor $\text{rot}_g Z$. Equation (4.10) shows that rot_g can be interpreted as the adjoint of curl_g . A similar integration by parts formula for $\phi \in \Lambda^0(T)$ and $\mu \in \Lambda^1(T)$

$$\int_{(T,g)} \phi \text{curl}_g \mu = \int_{(T,g)} \mu(\text{rot}_g \phi) + \int_{(\partial T,g)} \phi \mu(\hat{\tau}) \quad (4.11)$$

connects the other curl_g and rot_g defined in (4.3a) and (4.8a).

4.2. Covariant curl in the Regge metric

We proceed to extend the definitions of the covariant operators to the case when the metric g is only *tt*-continuous (see (2.11)) across element interfaces. Let \check{M} denote the open set obtained from M by removing all the mesh vertices (after its triangulation by \mathcal{T}). The topological manifold \check{M} can be endowed with a natural *glued smooth structure* based on the *tt*-continuity of g , as alluded to in the literature [15, 20, 30, 31], [34, Theorem 3.3] and [49]. This glued smooth structure is different from that given by the coordinates x^i (see §3.3) in which we plan to conduct all computations. A striking difference is that while g is only *tt*-continuous in x^i , it is fully continuous in the natural glued smooth structure.

The glued smooth structure can be understood using the following coordinate construction around any interior mesh edge E . Let $z \in E$ and let U_z denote an open neighborhood of z not intersecting any other mesh edge or mesh vertex. Let $d_g(\cdot, \cdot)$ denote the distance function generated by g on the manifold \check{M} . For any $p \in U_z$, let $\pi(p) = \arg \min_{q \in E} d_g(q, p)$. We use $T_{\pm}, \hat{\nu}_{\pm}, \hat{\tau}_{\pm}$ introduced in (2.15). Let E_p denote the submanifold of E connecting z to $\pi(p)$ oriented in the $\hat{\tau}_{\pm}$ direction. Then for any $p \in U_z$, define new coordinates

$$\check{x}^1(p) = \pm d_g(\pi(p), p) \quad \text{if } p \in T_{\pm}, \quad \check{x}^2(p) = \int_{(E_p, g)} 1. \quad (4.12)$$

Denote the coordinate frame of \check{x}^i by $\check{\partial}_i$. It can be shown [30] that $\check{\partial}_1 = \hat{\nu}_{\pm}$ and $\check{\partial}_2 = \hat{\tau}_{\pm}$ at points in $U_z \cap E$, and that $g(\check{\partial}_i, \check{\partial}_j)$ is continuous across $U_z \cap E$ for all i, j . Augmenting the set \check{M} with the maximal atlas giving such coordinates, we obtain a manifold with the glued smooth structure, which we continue to denote by \check{M} . Moreover, (\check{M}, g) is a Riemannian manifold with piecewise smooth and *globally continuous metric* g .

For the next result, we need the subspace of smooth vector fields

$$\mathfrak{X}_c(\check{M}) = \{X \in \mathfrak{X}(\check{M}) : \text{support of } X \text{ is relatively compact in } \check{M}\}.$$

Because the transformations $\partial_i = (\partial \check{x}^j / \partial x^i) \check{\partial}_j$ and $dx^i = (\partial x^i / \partial \check{x}^j) d\check{x}^j$ are smooth within mesh elements, previously defined piecewise smooth spaces like $\mathcal{R}(\mathcal{T})$ carry over to the glued smooth structure.

Proposition 4.2. *For all $\sigma \in \mathcal{R}(\mathcal{T})$ and $\varphi \in \mathfrak{X}_c(\check{M})$, we have*

$$\int_{(\check{M}, g)} \sigma(\text{rot}_g \varphi) = \int_{\mathcal{T}} (\text{curl}_g \sigma)(\varphi) - \int_{\partial \mathcal{T}} g(\varphi, \hat{\nu}) \sigma(\hat{\nu}, \hat{\tau}). \quad (4.13)$$

Proof. The integral on the left hand side of (4.13) may equally well be written as $\int_{\mathcal{T}} \sigma(\text{rot}_g \varphi)$, since the set of vertices excluded in \check{M} is of measure zero. Then, integrating by parts, element by element, using (4.10),

$$\int_{\mathcal{T}} \sigma(\text{rot}_g \varphi) = \int_{\mathcal{T}} (\text{curl}_g \sigma)(\varphi) - \int_{\partial \mathcal{T}} \sigma(\varphi, \hat{\tau}).$$

Now, using the g -orthogonal decomposition $\varphi = g(\varphi, \hat{\tau})\hat{\tau} + g(\varphi, \hat{\nu})\hat{\nu}$, we have

$$\int_{\partial \mathcal{T}} \sigma(\varphi, \hat{\tau}) = \int_{\partial \mathcal{T}} g(\varphi, \hat{\nu}) \sigma(\hat{\nu}, \hat{\tau}) + \int_{\partial \mathcal{T}} g(\varphi, \hat{\tau}) \sigma(\hat{\tau}, \hat{\tau}).$$

Boundary mesh edges do not contribute to the last integral since φ is compactly supported. Across an interior mesh edge, since g is continuous in the glued smooth structure of \check{M} , and since σ is *tt-continuous*, the contributions to the last integral from adjacent elements cancel each other. Hence (4.13) follows. \blacksquare

We use (\check{M}, g) to extend the definition of covariant curl. Recall that the adjoint of curl_g is rot_g , as shown by (4.10). Hence, as in the theory of Schwartz distributions, a natural extension would be to consider $\text{curl}_g \sigma$, for $\sigma \in \mathcal{R}(\mathcal{T})$, as a linear functional on $\mathfrak{X}_c(\check{M})$ defined by

$$\langle \text{curl}_g \sigma, \varphi \rangle_{\mathfrak{X}_c(\check{M})} = \int_{(\check{M}, g)} \sigma(\text{rot}_g \varphi) = \int_{\mathcal{T}} (\text{curl}_g \sigma)(\varphi) - \int_{\partial \mathcal{T}} g(\varphi, \hat{\nu}) \sigma(\hat{\nu}, \hat{\tau}) \quad (4.14)$$

for all $\varphi \in \mathfrak{X}_c(\check{M})$, where we have used Proposition 4.2 in the second equality. The next key observation is that we may extend the above functional to act on a piecewise smooth vector field $W \in \mathfrak{X}(\mathcal{T})$ instead of the smooth φ , provided W is g -normal continuous (an intrinsically verifiable property on the manifold).

Definition 4.3. For any $\sigma \in \mathcal{R}(\mathcal{T})$, define $\operatorname{curl}_g \sigma$ as a linear functional on $\mathring{\mathcal{W}}_g(\mathcal{T})$, the space defined in (2.16), by

$$\langle \operatorname{curl}_g \sigma, W \rangle_{\mathring{\mathcal{W}}_g(\mathcal{T})} = \int_{\mathcal{T}} (\operatorname{curl}_g \sigma)(W) - \int_{\partial \mathcal{T}} g(W, \hat{\nu}) \sigma(\hat{\nu}, \hat{\tau}) \quad (4.15)$$

for all $W \in \mathring{\mathcal{W}}_g(\mathcal{T})$, where the first term on the right hand side is evaluated using the smooth case in (4.3b). The rationale for this definition is that there are functions φ in $\mathfrak{X}_c(\check{M})$ approaching $W \in \mathring{\mathcal{W}}_g(\mathcal{T})$ in such a way that the right hand side of (4.14) converges to that of (4.15): see Proposition A.1 in Appendix A. Furthermore, because of the g -normal continuity of W , the last term in (4.15) vanishes when σ is globally smooth, so (4.15) indeed extends curl_g on smooth functions.

4.3. Implementation issues in computing covariant curl

We now develop a formula for computing the extended covariant curl in the given computational coordinates x^i (not \check{x}^i). We use the Euclidean parameter domain (Ω, δ) and the Euclidean δ -orthonormal tangent and normal (τ and ν) on element boundaries (see §3.3). Abbreviating $\delta(w, X)$ to w^X , consider (2.16) for $g = \delta$, namely

$$\begin{aligned} \mathcal{W}(\Omega) &= \left\{ w \equiv [w^1, w^2] : \Omega \rightarrow \mathbb{R}^2 \mid w^i \in C^\infty(\mathcal{T}), \llbracket w^\nu \rrbracket = 0 \right\}, \\ \mathring{\mathcal{W}}(\Omega) &= \left\{ w \in \mathcal{W}(\Omega) \mid w^\nu|_{\partial\Omega} = 0 \right\}. \end{aligned}$$

Their finite element subspaces of interest are

$$\begin{aligned} \mathcal{W}_h^k &= \{w \in \mathcal{W}(\Omega) : \text{for all } T \in \mathcal{T}, w|_T = \Phi_T^* \hat{w} \text{ for some } \hat{w} \in \mathcal{P}^k(\hat{T}, \mathbb{R}^2)\}, \\ \mathring{\mathcal{W}}_h^k &= \{w \in \mathcal{W}_h^k : w^\nu|_{\partial\Omega} = 0\}, \end{aligned} \quad (4.16)$$

where the pull-back $\Phi_T^* \hat{w}$ is the Piola transformation. For $k > 0$, (4.16) coincides with the *Brezzi–Douglas–Marini finite element space (BDM)* [13] on the parameter domain. In practice, it is more convenient to work with the *BDM* space than (2.16). For any $w = [w^1, w^2] \in \mathring{\mathcal{W}}(\Omega)$, let

$$Q_g w = \frac{w^1(x^1, x^2) \partial_1 + w^2(x^1, x^2) \partial_2}{\sqrt{\det g}}. \quad (4.17)$$

Proposition 4.4 (Extended covariant curl in computational coordinates).

(1) A vector field w on Ω is in $\mathring{\mathcal{W}}(\Omega)$ if and only if $Q_g w$ is in $\mathring{\mathcal{W}}_g(\mathcal{T})$.

(2) For any $\sigma \in \mathcal{R}(\mathcal{T})$ and $w \in \mathring{\mathcal{W}}(\Omega)$,

$$\begin{aligned} &\langle \operatorname{curl}_g \sigma, Q_g w \rangle_{\mathring{\mathcal{W}}_g(\mathcal{T})} \\ &= \sum_{T \in \mathcal{T}} \left(\int_T \frac{[\operatorname{curl}[\sigma]]_i w^i - \sigma_{mk} \varepsilon^{jk} \Gamma_{ji}^m w^i}{\sqrt{\det g}} \, da - \int_{\partial T} \frac{g_{\tau\tau} \sigma_{\nu\tau} - g_{\nu\tau} \sigma_{\tau\tau}}{g_{\tau\tau} \sqrt{\det g}} w^\nu \, dl \right) \end{aligned} \quad (4.18a)$$

$$= \sum_{T \in \mathcal{T}} \left(\int_T \sigma_{mk} \frac{[\operatorname{rot}[w]]^{mk} - \varepsilon^{kj} (\Gamma_{lj}^l w^m - \Gamma_{ji}^m w^i)}{\sqrt{\det g}} \, da + \int_{\partial T} \frac{\sigma_{\tau\tau} g_{i\tau} w^i}{g_{\tau\tau} \sqrt{\det g}} \, dl \right). \quad (4.18b)$$

Proof. By (3.20) and (2.7),

$$w^\nu = \delta(w, \nu) = g(w, \hat{\nu}) = g(w, \hat{\nu} \sqrt{g_{\hat{\nu}\hat{\nu}}}) = g(w, \hat{\nu}) \frac{\sqrt{g_{\tau\tau}}}{\sqrt{\det g}} = g(Q_g w, \hat{\nu}) \sqrt{g_{\tau\tau}}. \quad (4.19)$$

Hence the continuity of $g_{\tau\tau}$ across element interfaces implies that

$$\llbracket g(Q_g w, \hat{\nu}) \rrbracket = 0 \quad \text{if and only if} \quad \llbracket w^\nu \rrbracket = 0.$$

Similarly $w^\nu|_{\partial\Omega} = 0$ if and only if $g(Q_g w, \hat{\nu}) = 0$ vanishes on the boundary. Hence $Q_g w \in \mathring{\mathcal{W}}_g(\mathcal{T})$ if and only if $w \in \mathring{\mathcal{W}}(\Omega)$.

To prove (4.18a), we write (4.15) in coordinates. Observe that the coordinate expression for covariant curl in (4.7b) and the integration formula (2.17) imply

$$\int_{\mathcal{T}} (\operatorname{curl}_g \sigma)(Q_g w) = \sum_{T \in \mathcal{T}} \int_T \frac{[\operatorname{curl}[\sigma]]_i [Q_g w]^i - \sigma_{mk} \varepsilon^{jk} \Gamma_{ji}^m [Q_g w]^i}{\sqrt{\det g}} \sqrt{\det g} \, da,$$

which coincides with the sum of integrals over elements T in (4.18a). For the element boundary integrals of $g(Q_g w, \hat{\nu}) \sigma(\hat{\nu}, \hat{\tau})$ contributing to $\langle \operatorname{curl}_g \sigma, Q_g w \rangle_{\mathring{\mathcal{W}}_g(\mathcal{T})}$, first note that (4.19) implies

$$g(Q_g w, \hat{\nu}) \sigma(\hat{\nu}, \hat{\tau}) = \frac{w^\nu}{\sqrt{g_{\tau\tau}}} \frac{\sigma(\delta(\hat{\nu}, \nu)\nu + \delta(\hat{\nu}, \tau)\tau, \tau)}{\sqrt{g_{\tau\tau}}}. \quad (4.20)$$

We simplify by chasing the definitions of $\hat{\nu}$ and τ . (We detail the argument this once and will not expand on later similar occasions.)

$$\begin{aligned} \delta(\hat{\nu}, \nu) &= g(\hat{\nu}, \tilde{\nu}) = g(\hat{\nu}, \hat{\nu} \sqrt{g_{\tilde{\nu}\tilde{\nu}}}) && \text{by (3.20) and (2.8)} \\ &= \frac{\sqrt{g_{\tau\tau}}}{\sqrt{\det g}} && \text{by (2.7),} \\ \delta(\hat{\nu}, \tau) &= \frac{\delta(\tilde{\nu}, \tau)}{\sqrt{g_{\tilde{\nu}\tilde{\nu}}}} = \frac{\sqrt{\det g}}{\sqrt{g_{\tau\tau}}} \delta(\tilde{\nu}, \tau) && \text{by (2.8) and (2.7),} \\ &= -\frac{\sqrt{\det g}}{\sqrt{g_{\tau\tau}}} g^{kj} \varepsilon_{ji} \tau^i \delta_{km} \tau^m && \text{by (2.10),} \\ &= \frac{-g(\nu, \tau)}{\sqrt{g_{\tau\tau}} \det g}, \end{aligned}$$

where, in the last step, we have simplified using the cofactor expansion of g^{kj} and (3.17). Hence (4.20) implies

$$g(Q_g w, \hat{\nu}) \sigma(\hat{\nu}, \hat{\tau}) = \frac{w^\nu}{g_{\tau\tau}} \left(\frac{\sqrt{g_{\tau\tau}}}{\sqrt{\det g}} \sigma_{\nu\tau} - \frac{g_{\nu\tau}}{\sqrt{g_{\tau\tau}} \det g} \sigma_{\tau\tau} \right) = \frac{w^\nu (\sigma_{\nu\tau} g_{\tau\tau} - g_{\nu\tau} \sigma_{\tau\tau})}{g_{\tau\tau} \sqrt{g_{\tau\tau}} \det g}.$$

Integrating this over each element boundary using the measure $\sqrt{g_{\tau\tau}} dl$ and summing over elements, the right hand sides of (4.15) and (4.18a) are seen to be the same.

To prove the second identity (4.18b), consider any $W \in \mathring{\mathcal{W}}_g(\mathcal{T})$. We start by applying the integration by parts formula (4.10) to the first term on the right hand side of the definition (4.15):

$$\begin{aligned} \langle \operatorname{curl}_g \sigma, W \rangle_{\mathring{\mathcal{W}}_g(\mathcal{T})} &= \int_{\mathcal{T}} \sigma(\operatorname{rot}_g W) + \int_{\partial T} \sigma(W, \hat{\tau}) - \int_{\partial T} g(W, \hat{\tau}) \sigma(\hat{\nu}, \hat{\tau}) \\ &= \int_{\mathcal{T}} \sigma(\operatorname{rot}_g W) + \int_{\partial \mathcal{T}} g(W, \hat{\tau}) \sigma_{\hat{\tau}\hat{\tau}} \end{aligned}$$

after simplifying using g -orthogonal decomposition $W = g(W, \hat{\tau})\hat{\tau} + g(W, \hat{\nu})\hat{\nu}$ on element boundaries. Substituting $W = Q_g w$, applying the quotient rule to compute $\operatorname{rot}_g(Q_g w)$ using (4.6), and expressing the result in x^i coordinates, (4.18b) follows. ■

In analogy with the finite element curvature approximation, we may now also lift the functional $\operatorname{curl}_g \sigma$ to a finite element space to get a computable representative of the covariant curl on the parameter domain Ω . Using the BDM space in (4.16), we define $\operatorname{curl}_{g,h} \sigma$, for any $\sigma \in \mathcal{R}(\mathcal{T})$, as the unique element in $\mathring{\mathcal{W}}_h^k$ satisfying

$$\int_{\Omega} \delta(\operatorname{curl}_{g,h} \sigma, w_h) da = \langle \operatorname{curl}_g \sigma, Q_g w_h \rangle_{\mathring{\mathcal{W}}_g(\mathcal{T})} \quad \text{for all } w_h \in \mathring{\mathcal{W}}_h^k, \quad (4.21)$$

where the right hand side can be evaluated using either of the formulas in (4.18).

4.4. Covariant incompatibility in the Regge metric

To extend the smooth covariant incompatibility defined in (4.3c), we use the space $\mathcal{V}(\mathcal{T})$ of piecewise smooth and globally continuous functions on M . For any $u \in \mathcal{V}(\mathcal{T})$, the vector field $\text{rot}_g u$, by definition (4.8a), satisfies $g(\text{rot}_g u, \hat{\nu}) = g(-(\star du)^\sharp, \hat{\nu}) = -(\star du)(\hat{\nu})$. Hence (2.9) implies

$$g(\operatorname{rot}_g u, \hat{\nu}) = -(du)(\hat{\tau}), \quad (4.22)$$

so in particular, $\|g(\operatorname{rot}_g u, \hat{\nu})\| = 0$ due to the continuity of u . Also note that in the formula (4.3c) for the smooth case, $\operatorname{inc}_g \sigma = \operatorname{curl}_g \operatorname{curl}_g \sigma$, the outer curl_g 's adjoint is the rot_g appearing in (4.11). These facts motivate us to use Definition 4.3 to extend inc_g to tt -continuous σ as follows.

Definition 4.5. For any $\sigma \in \mathcal{R}(\mathcal{T})$, extend $\text{inc}_g \sigma$ as a linear functional on $\mathring{\mathcal{V}}(\mathcal{T})$ by

$$\langle \text{inc}_g \sigma, u \rangle_{\dot{\mathcal{V}}(\mathcal{T})} = \langle \text{curl}_g \sigma, \text{rot}_g u \rangle_{\dot{\mathcal{W}}_g(\mathcal{T})} \quad (4.23)$$

for all $u \in \mathring{\mathcal{V}}(\mathcal{T})$. Note that $\text{rot}_g u$ is an allowable argument in the right hand side pairing since it is g -normal continuous (and hence in $\mathring{\mathcal{W}}_g(\mathcal{T})$) by (4.22). The next result shows that (4.23) indeed extends the smooth case.

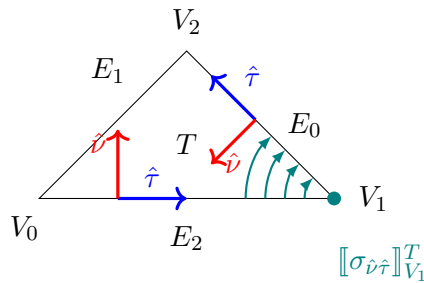


FIGURE 4.1. Illustration of the vertex jump defined in (4.24).

The “vertex jump” of σ at a vertex $V \in \mathcal{V}_T$ of an element $T \in \mathcal{T}$ (cf. [17, 28] and see Figure 4.1), denoted by $[\![\sigma_{\hat{\nu}\hat{\tau}}]\!]_V^T$, represents the jump in the value of $\sigma(\hat{\nu}, \hat{\tau})$ across the vertex V when traversing ∂T in the $\hat{\tau}$ -direction. Alternately, enumerating the vertices of \mathcal{V}_T as V_0, V_1, V_2 so that the indices increase while moving in the $\hat{\tau}$ -direction, naming the edge opposite to V_i as E_i , and calculating the indices mod 3, we put

$$\|\sigma_{\hat{\nu}\hat{\tau}}\|_{V_i}^T = (\sigma(\hat{\nu}, \hat{\tau})|_{E_{i-1}} - \sigma(\hat{\nu}, \hat{\tau})|_{E_{i+1}}) (V_i). \quad (4.24)$$

Proposition 4.6. *For any $\sigma \in \mathcal{R}(\mathcal{T})$ and $u \in \mathring{\mathcal{V}}(\mathcal{T})$,*

$$\langle \text{inc}_g \sigma, u \rangle_{\dot{\mathcal{V}}(\mathcal{T})} = \int_{\mathcal{T}} u \text{ inc}_g \sigma - \int_{\partial \mathcal{T}} u (\text{curl}_g \sigma + d\sigma_{\hat{\nu}\hat{\tau}})(\hat{\tau}) - \sum_{T \in \mathcal{T}} \sum_{V \in \mathcal{V}_T} [\![\sigma_{\hat{\nu}\hat{\tau}}]\!]_V^T u(V).$$

When σ is globally smooth, all terms on the right hand side vanish except the first.

Proof. By (4.23), (4.15), (4.11), and (4.22),

$$\begin{aligned} \langle \text{inc}_g \sigma, u \rangle_{\dot{\mathcal{V}}(\mathcal{T})} &= \int_{\mathcal{T}} (\text{curl}_g \sigma)(\text{rot}_g u) - \int_{\partial \mathcal{T}} \sigma_{\hat{\nu} \hat{\tau}} g(\text{rot}_g u, \hat{\nu}) \\ &= \int_{\mathcal{T}} u \cdot \text{inc}_g \sigma - \int_{\partial \mathcal{T}} u \cdot (\text{curl}_g \sigma)(\hat{\tau}) + \int_{\partial \mathcal{T}} \sigma_{\hat{\nu} \hat{\tau}} (du)(\hat{\tau}). \end{aligned}$$

Now, on the edge E_i oriented from end point V_{i-1} to V_i (indexed mod 3; see Figure 4.1), by the one-dimensional integration by parts formula

$$\int_{(E_i, g)} \sigma_{\hat{\nu}\hat{\tau}} (du)(\hat{\tau}) = \sigma_{\hat{\nu}\hat{\tau}}(V_i) u(V_i) - \sigma_{\hat{\nu}\hat{\tau}}(V_{i-1}) u(V_{i-1}) - \int_{(E_i, g)} (d\sigma_{\hat{\nu}\hat{\tau}})(\hat{\tau}) u.$$

When summing over the three edges $E_i \subset \partial T$, the above vertex values of $\sigma_{\hat{\nu}\hat{\tau}}$ yield vertex jumps. Hence the first statement follows by summing over all T in \mathcal{T} .

To prove the second statement, note that the edge integrals from adjacent triangles cancel each other. To show that the last term with vertex contributions also vanish, let \mathcal{E}_V denote the set of vertices connected to $V \in \mathcal{V}$ by an edge and let $\hat{\tau}_V$ denote the g -unit tangent vector along an $E \in \mathcal{E}_V$ pointing away from V . Then the jump $[\![\sigma(\hat{\nu}, \hat{\tau}_V)]\!]$ on any edge $E \in \mathcal{E}_V$ is defined as before, using (2.15). Its limit as we approach a vertex V along any edge $E \in \mathcal{E}_V$, is denoted by $[\![\sigma]\!]_{\hat{\nu}\hat{\tau}}^V$. Using it, the last sum can be rearranged to

$$\sum_{T \in \mathcal{T}} \sum_{V \in \mathcal{V}_T} [\![\sigma_{\hat{\nu}\hat{\tau}}]\!]_V^T u(V) = - \sum_{V \in \mathcal{V}^{\text{int}}} \sum_{E \in \mathcal{E}_V} [\![\sigma]\!]_{\hat{\nu}\hat{\tau}}^V u(V),$$

where $\mathcal{V}^{\text{int}} \subset \mathcal{V}$ is the subset of mesh vertices in the interior of the domain. Each summand on the right hand side vanishes when σ is smooth. \blacksquare

As before, one may now lift the incompatibility functional into a finite element space to get a computable representative. Namely, for any $\sigma \in \mathcal{R}(\mathcal{T})$ and $g \in \mathcal{R}^+(\mathcal{T})$, let $\text{inc}_{g,h} \sigma$ be the unique function in $\mathring{\mathcal{V}}_h^{k+1}$ satisfying

$$\int_{\Omega} (\text{inc}_{g,h} \sigma) u_h \, \text{da} = \langle \text{inc}_g \sigma, u_h \rangle_{\mathring{\mathcal{V}}(\mathcal{T})}, \quad \text{for all } u_h \in \mathring{\mathcal{V}}_h^{k+1}, \quad (4.25)$$

where the right hand side can be computed using the formula in Proposition 4.6.

4.5. Linearization of curvature

Linearization of curvature was discussed in various forms by many previous authors. For example, the linearization of our vertex curvature sources can be guessed from the three-dimensional case presented in [17], while that of the edge and interior curvature sources were derived in [27] (making use of [23]) in terms of the covariant divergence operator. Here we revisit the topic to derive the linearization of edge and interior curvature sources directly in terms of the covariant incompatibility and curl operators. While doing so, we also present different and elementary proofs.

The variational derivative of a scalar function $f : \mathcal{S}(T) \rightarrow \mathbb{R}$ in the direction of a $\sigma \in \mathcal{S}(T)$ is given by

$$D_\sigma(f(\rho)) = \lim_{t \rightarrow 0} \frac{f(\rho + t\sigma) - f(\rho)}{t}$$

when the limit exists. We use this exclusively for scalar functions of the metric g (i.e., with $\rho = g$ above). Note that the changes in $\rho(p)$ and $\sigma(p)$ as p varies in M are immaterial in the above definition. Hence, we may use Riemann normal coordinates [32] to prove the pointwise identities of tensorial quantities in the next result. Let \tilde{x}^i denote the Riemann normal coordinates given by a chart covering a point $p \in T$, $\tilde{\partial}_i$ denote the corresponding coordinate frame, $\tilde{\sigma}_{ij} = \sigma(\tilde{\partial}_i, \tilde{\partial}_j)$ for any $\sigma \in \mathcal{T}_0^2(T)$, $\tilde{R}_{ijkl} = R(\tilde{\partial}_i, \tilde{\partial}_j, \tilde{\partial}_k, \tilde{\partial}_l)$, and let $\tilde{\Gamma}_{ijk}, \tilde{\Gamma}_{ij}^k$ be defined by (2.5) with ∂_i replaced by $\tilde{\partial}_i$. Then, by [32, Proposition 5.11],

$$\tilde{g}_{ij}|_p = \delta_{ij}, \quad \tilde{\partial}_k \tilde{g}_{ij}|_p = 0, \quad \tilde{\Gamma}_{ijk}|_p = 0, \quad (4.26)$$

which greatly simplify calculations. As an example, consider the expression for covariant incompatibility of a $\sigma \in \mathcal{S}(T)$ given by (4.7c) in coordinate proxies. It simplifies in normal coordinates, by

virtue of (4.26), to $[\text{inc}_g \sigma] = \text{inc}[\tilde{\sigma}] - \varepsilon^{ij} \varepsilon^{kl} \tilde{\sigma}_{ml} \tilde{\partial}_i \tilde{\Gamma}_{jk}^m$. Expanding out the last term in terms of \tilde{g}_{ij} , using (2.5b), and simplifying,

$$[\text{inc}_g \sigma] = \text{inc}[\tilde{\sigma}] - \frac{1}{2} \text{tr}[\tilde{\sigma}] \text{ inc}[\tilde{g}]. \quad (4.27)$$

Lemma 4.7 (Variations of curvature terms). *Consider an element manifold (T, g) for $T \in \mathcal{T}$. Let p be an arbitrary point in T and let $X, Y \in T_p M$. Let q be any point in one of the edges E of ∂T and let $\tau \in T_q E$. Then*

$$D_\sigma(K(g) \text{vol}_{T,g}(X, Y)) = -\frac{1}{2} \text{vol}_{T,g}(X, Y) \text{ inc}_g \sigma, \quad \text{at the point } p \in T, \quad (4.28a)$$

$$D_\sigma(\kappa(g) \text{vol}_{E,g}) = \frac{1}{2} \text{vol}_{E,g}(\text{curl}_g \sigma + d\sigma_{\hat{\tau}\hat{\nu}})(\tau), \quad \text{at the point } q \in E, \quad (4.28b)$$

$$D_\sigma(\triangle_V^T g) = -\frac{1}{2} [\sigma_{\hat{\nu}\hat{\tau}}]_V^T, \quad \text{at every vertex } V \text{ of } T. \quad (4.28c)$$

Proof. We prove (4.28a), using the coordinate formula $K(g) = R_{1221}/\det g$ and the Jacobi formula, which implies $D_\sigma(\sqrt{\det g}) = \frac{1}{2}\sqrt{\det g} \text{ tr}(g^{-1}\sigma)$. Together they give

$$D_\sigma(K(g) \text{vol}_{T,g}(\partial_1, \partial_2)) = \frac{1}{\sqrt{\det g}} \left(D_\sigma(R_{1221}) - \frac{1}{2} \text{tr}(g^{-1}\sigma) R_{1221} \right)$$

in any coordinate frame. Specializing to Riemann normal coordinates, since (4.26) implies that the last two terms of (3.6) vanish, $\tilde{R}_{1221} = \tilde{\partial}_1 \tilde{\Gamma}_{221} - \tilde{\partial}_2 \tilde{\Gamma}_{211} = -\frac{1}{2} \text{inc}[\tilde{g}]$, so

$$D_\sigma(K(g) \text{vol}_{T,g}(\tilde{\partial}_1, \tilde{\partial}_2)) = -\frac{1}{2} \text{inc}[\tilde{\sigma}] + \frac{1}{4} \text{tr}[\tilde{\sigma}] \text{ inc}[\tilde{g}].$$

Hence (4.28a) follows from (4.27).

To prove (4.28b), we start with its right hand side. By (4.7b),

$$(\text{curl}_g \sigma + d\sigma_{\hat{\tau}\hat{\nu}})(\tau) = \frac{1}{\sqrt{\det g}} ([\text{curl}[\sigma]]_i - \varepsilon^{jk} \Gamma_{ji}^m \sigma_{mk}) \tau^i + \tau^i \partial_i \sigma_{\hat{\tau}\hat{\nu}}.$$

At any point on the edge E , without loss of generality, we may choose a Riemann normal coordinate system so that $\tilde{\partial}_1 = \tilde{\tau} = \hat{\tau}$ and $\tilde{\partial}_2 = \tilde{\nu} = \hat{\nu}$. Then, using (4.26), the above expression becomes

$$(\text{curl}_g \sigma + d\sigma_{\hat{\tau}\hat{\nu}})(\tilde{\tau}) = [\text{curl}[\tilde{\sigma}]]_i \tilde{\tau}^i + \partial_{\tilde{\tau}} \sigma_{\tilde{\tau}\tilde{\nu}} = [\text{curl}[\tilde{\sigma}]]_i \tilde{\tau}^i + (\tilde{\partial}_{\tilde{\tau}}[\tilde{\sigma}])_{\tilde{\nu}\tilde{\tau}} + (\sigma_{\tilde{\nu}\tilde{\nu}} - \sigma_{\tilde{\tau}\tilde{\tau}}) \dot{\tilde{\tau}}_{\tilde{\nu}}, \quad (4.29)$$

where we used (3.19) to get the last equality. Now we work on the left hand side of (4.28b). Differentiating the expression for geodesic curvature from Lemma 3.3, we get

$$\begin{aligned} D_\sigma(\kappa(g) \text{vol}_{E,g}) &= D_\sigma(g_{\tau\tau}^{-1} \sqrt{\det g} (\dot{\tau}_\nu + \Gamma_{\tau\tau}^\nu)) \\ &= \frac{\sqrt{\det g}}{g_{\tau\tau}} \left[\left(\frac{1}{2} \text{tr}(g^{-1}\sigma) - \frac{\sigma_{\tau\tau}}{g_{\tau\tau}} \right) (\Gamma_{\tau\tau}^\nu + \dot{\tau}^\nu) + \tau^i \tau^j \nu^l \delta_{kl} (g^{km} \Gamma_{ijm}(\sigma) - g^{ka} \sigma_{ab} g^{bm} \Gamma_{ijm}) \right] \end{aligned}$$

in general coordinates. Specializing to the previously used Riemann normal coordinates, applying (4.26) and simplifying $\Gamma_{ijm}(\sigma)$,

$$D_\sigma(\kappa(g) \text{vol}_{E,g}) = \left(\frac{1}{2} \text{tr}[\tilde{\sigma}] - [\tilde{\sigma}]_{\tau\tau} \right) \dot{\tilde{\tau}}^\nu + (\tilde{\partial}_{\tilde{\tau}}[\tilde{\sigma}])_{\tilde{\nu}\tilde{\tau}} - \frac{1}{2} (\tilde{\partial}_{\tilde{\nu}}[\tilde{\sigma}])_{\tilde{\tau}\tilde{\tau}}.$$

This coincides with the expression in (4.29), so (4.28b) is proved.

To prove (4.28c), let $\theta = \triangle_V^T g$ denote the angle in (3.5) and let $\hat{\tau}_\pm = \tau_\pm / \sqrt{g_{\tau_\pm\tau_\pm}}$ denote the g -normalized incoming and outgoing tangents at V . Since τ_\pm does not vary with g ,

$$\begin{aligned} -D_\sigma \cos \theta &= D_\sigma \left(\frac{g_{\tau_-\tau_+}}{\sqrt{g_{\tau_-\tau_-} g_{\tau_+\tau_+}}} \right) = \frac{D_\sigma g_{\tau_-\tau_+}}{\sqrt{g_{\tau_-\tau_-} g_{\tau_+\tau_+}}} + g_{\tau_-\tau_+} D_\sigma \frac{1}{\sqrt{g_{\tau_-\tau_-} g_{\tau_+\tau_+}}} \\ &= \sigma_{\hat{\tau}_-\hat{\tau}_+} - \frac{1}{2} g_{\hat{\tau}_-\hat{\tau}_+} (\sigma_{\hat{\tau}_-\hat{\tau}_-} + \sigma_{\hat{\tau}_+\hat{\tau}_+}). \end{aligned} \quad (4.30)$$

Let $\hat{\nu}_\pm$ be such that $\hat{\tau}_\pm, \hat{\nu}_\pm$ form an ordered orthonormal basis matching the orientation of T under consideration. Then $g_{\hat{\tau}_+ \hat{\nu}_-} = \sin \theta = -g_{\hat{\tau}_- \hat{\nu}_+}$. Substituting $\sigma_{\hat{\tau}_- \hat{\tau}_+} = \frac{1}{2}\sigma(\hat{\tau}_-, g_{\hat{\tau}_+ \hat{\tau}_-} \hat{\tau}_- + g_{\hat{\tau}_+ \hat{\nu}_-} \hat{\nu}_-) + \frac{1}{2}\sigma(g_{\hat{\tau}_- \hat{\tau}_+} \hat{\tau}_+ + g_{\hat{\tau}_- \hat{\nu}_+} \hat{\nu}_+, \hat{\tau}_+)$ into (4.30),

$$-D_\sigma \cos \theta = \frac{1}{2}(g_{\hat{\tau}_+ \hat{\nu}_-} \sigma_{\hat{\tau}_- \hat{\nu}_-} + g_{\hat{\tau}_- \hat{\nu}_+} \sigma_{\hat{\nu}_+ \hat{\tau}_+}) = \frac{\sin \theta}{2}(\sigma_{\hat{\tau}_- \hat{\nu}_-} - \sigma_{\hat{\nu}_+ \hat{\tau}_+}) = -\frac{\sin \theta}{2}[\![\sigma_{\hat{\nu}_+ \hat{\tau}_-}]\!]_V^T.$$

Since $D_\sigma \theta = -(D_\sigma \cos \theta) / \sin \theta$, the result is proved. \blacksquare

5. Connection approximation

In this section we approximate the Levi-Civita connection when only an approximation to the true metric is given, namely $g \in \mathcal{R}^+(\mathcal{T})$. To do so, we assume we are given a g -orthonormal frame (e_1, e_2) in each $T \in \mathcal{T}$. Then, the connection is fully determined by a single *connection form* $\varpi(g; \cdot) \equiv \varpi_g \in \wedge^1(T)$, within each element T , given by

$$\varpi_g(X) = g(e_1, \nabla_X e_2) = -g(\nabla_X e_1, e_2) \quad (5.1)$$

for any $X \in \mathfrak{X}(M)$. This section is largely based on [10] (so we will be brief), but we note that while they approximate the Hodge star of ϖ_g , we approximate ϖ_g directly (and also note that the orientation in their work is opposite to ours).

To extend the connection to accommodate the possible discontinuities of the frame (e_1, e_2) across element interfaces, let $\sphericalangle_g(a, b)$ denote the counterclockwise angle from b to a measured in the g -inner product, for any two vectors $a, b \in T_p M$. This angle is well defined even for points p on a mesh edge E (excluding the vertices) since we use the glued smooth structure (see (4.12)) in which g is continuous across the edge. On each interior mesh edge E , let $T_\pm, \hat{\nu}_\pm, \hat{\tau}_\pm$ be as in (2.15), orient the edge E by $\hat{\tau}^E = \hat{\tau}_+$, and put $\hat{\nu}^E = \hat{\nu}_+$, $e_{\pm, i} = e_i|_{T_\pm}$. Let $\Theta^E = \sphericalangle_g(e_{+, 1}, e_{-, 1})$; see Figure 5.1. (It is possible to compute this angle without resorting to the coordinates in (4.12), as we will explain later in Appendix B.) This is the angle by which a vector must be rotated while parallel transporting it across the edge E in the $\hat{\nu}^E$ direction. To account for this rotation, we extend ϖ_g as follows:

Definition 5.1. Given $g \in \mathcal{R}^+(\mathcal{T})$ and g -orthonormal piecewise smooth frame $e_1, e_2 \in \mathfrak{X}(\mathcal{T})$, define $\varpi_g \in \mathring{\mathcal{W}}_g(\mathcal{T})'$ by

$$\langle \varpi_g, W \rangle_{\mathring{\mathcal{W}}_g(\mathcal{T})} = \int_{\mathcal{T}} \varpi_g(W) + \sum_{E \in \mathcal{E}^{\text{int}}} \int_{(E, g)} \Theta^E g(W, \hat{\nu}^E) \quad (5.2)$$

for all $W \in \mathring{\mathcal{W}}_g(\mathcal{T})$.

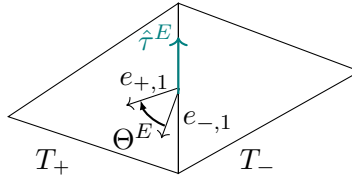


FIGURE 5.1. Angle between frames on different elements.

Within each element, the well-known identity $d\varpi_g = K(g)\text{vol}_{T, g}$ holds. Equivalently, using the curl in (4.3a), $\text{curl}_g(\varpi_g|_T) = K(g|_T)$ for each $T \in \mathcal{T}$. To speak of $\text{curl}_g \varpi_g$ for the functional ϖ_g in (5.2), we must extend curl_g . Motivated by (4.11), we define

$$\langle \text{curl}_g \mu, u \rangle_{\mathring{\mathcal{V}}(\mathcal{T})} = \langle \mu, \text{rot}_g u \rangle_{\mathring{\mathcal{W}}_g(\mathcal{T})}, \quad \text{for all } u \in \mathring{\mathcal{V}}(\mathcal{T}), \mu \in \mathring{\mathcal{W}}_g(\mathcal{T})'. \quad (5.3)$$

The right hand side is well defined for $\mu \in \mathring{\mathcal{W}}_g(\mathcal{T})'$ since $\text{rot}_g u \in \mathring{\mathcal{W}}_g(\mathcal{T})$ by (4.22). Next, for each $V \in \mathcal{V}$ and $E \in \mathcal{E}_V$, let s_{EV} equal $+1$ if $\hat{\tau}^E$ points towards V and -1 otherwise. Following [10], we assume that at each interior vertex V , the “consistency” condition

$$\sum_{E \in \mathcal{E}_V} s_{EV} \Theta^E(V) + \sum_{T \in \mathcal{T}_V} \triangle_V^T g = 2\pi \quad (5.4)$$

holds. It can be seen from the proof of [10, Proposition 5.4] that the left hand side above always equals $2\pi m$ for some integer m . The condition (5.4) requires that e_i be chosen so as to achieve $m = 1$. (We’ll give a recipe for doing this shortly: see (5.7) below.)

Proposition 5.2. *Let K_g be as in (3.2), ϖ_g be as (5.2) for a g -orthonormal frame e_i satisfying (5.4), and $\text{curl}_g \varpi_g$ be as given by (5.3). Then $\text{curl}_g \varpi_g = K_g$.*

Proof. This was proved in [10], so we will merely indicate how to apply their result to

$$\langle \text{curl}_g \varpi_g, u \rangle_{\mathring{\mathcal{V}}(\mathcal{T})} = \langle \varpi_g, \text{rot}_g u \rangle_{\mathring{\mathcal{W}}_g(\mathcal{T})} = \int_{\mathcal{T}} \varpi_g(\text{rot}_g u) + \sum_{E \in \mathcal{E}^{\text{int}}} \int_{(E,g)} \Theta^E g(\text{rot}_g u, \hat{\nu}^E).$$

Using $\alpha \wedge (\star \beta) = g^{-1}(\alpha, \beta) \text{vol}_{T,g}$ with $\alpha = \varpi_g$ and $\beta = du$ (considering u as a 0-form),

$$\int_{(T,g)} \varpi_g(\text{rot}_g u) = - \int_T g^{-1}(\varpi(g), \star du_h) \text{vol}_{T,g} = \int_T \varpi(g) \wedge du_h,$$

and using (2.9),

$$\int_{(E,g)} \Theta^E g(\text{rot}_g u, \hat{\nu}^E) = - \int_{(E,g)} \Theta^E du_h(\hat{\tau}^E).$$

Now invoking [10, Proposition 5.4], the result follows. ■

A computable representative of the connection form is obtained by lifting the ϖ_g into the BDM finite element space (defined in (4.16)) on the parameter domain, as follows.

Definition 5.3 (Connection 1-form approximation). Define $\varpi_h(g)$ as the unique function in $\mathring{\mathcal{W}}_h^k$ such that for all $v_h \in \mathring{\mathcal{W}}_h^k$

$$\int_{\Omega} \delta(\varpi_h(g), v_h) \, da = \langle \varpi_g, Q_g v_h \rangle_{\mathring{\mathcal{W}}_g(\mathcal{T})} \quad (5.5)$$

where Q_g is as Proposition 4.4 and the right hand side is evaluated using (5.2).

In the remainder, we assume that $\varpi_h(g)$ is computed using a specific g -orthonormal frame (e_1, e_2) satisfying (5.4), that we describe now. We start with a globally smooth δ -orthonormal Euclidean basis (E_1, E_2) on the parameter domain (e.g., the standard unit basis on \mathbb{R}^2). Then, this basis is continuously transformed to a g -orthonormal frame as in the next lemma. Let $G(t) = \delta + t(g - \delta)$. We consider the ordinary differential equation (ODE)

$$\dot{u}(t)u(t)^{-1} = -\frac{1}{2}G(t)^{-1}(g - \delta), \quad u(0) = I. \quad (5.6)$$

Lemma 5.4. *The solution of ODE (5.6) is given by $u(t) = G(t)^{-1/2}$. The frame $(u(t)E_1, u(t)E_2)$ is $G(t)$ -orthonormal, so at $t = 1$, it is g -orthonormal.*

Proof. Let $g = V\Lambda V^{-1}$ be a diagonalization of g with eigenvalues λ_i in $\Lambda = \text{diag}(\lambda_i)$ and eigenvectors in the orthogonal matrix V . Then $G(t) = V((1-t)\delta + t\Lambda)V^{-1}$ and $G(t)^{-1/2} = V \text{diag}(1 + t(\lambda_i - 1))^{-1/2}V^{-1}$. Using these expressions, the statements of the lemma can be easily verified. ■

We use the g -orthonormal frame

$$e_i = u(1)E_i = g^{-1/2}E_i \quad (5.7)$$

for computations. As stated in [10], since the frame E_i obviously satisfies (5.4) with $g = \delta$, the chosen e_i obtained by the continuous deformation of the metric and frame, satisfies (5.4). In Appendix B we present a stable algorithm for computing the right hand side of (5.5) using the discontinuous metric g in the computational coordinates.

6. Error analysis

In this section, we prove a priori estimates for the error in the previously defined approximations. We restrict ourselves to the model case (see §3.3) and work on the parameter domain Ω , where we shall use the Euclidean dot product $u \cdot v = \delta(u, v)$ and the standard Frobenius inner product $A : B$ between matrices A, B . We assume that the triangulation \mathcal{T} consists of affine-equivalent elements, is shape-regular, and is quasi-uniform of meshsize $h := \max_{T \in \mathcal{T}} \text{diam}(T)$.

6.1. Convergence results

All results here concern the canonical interpolant into the Regge space \mathcal{R}_h^k (defined in (2.13)) of degree $k \geq 0$. This well-known interpolant [34], denoted by $\mathcal{I}_k^{\mathcal{R}} : C^0(\Omega, \mathcal{S}) \rightarrow \mathcal{R}_h^k$, satisfies following equations

$$\int_E (\mathcal{I}_k^{\mathcal{R}} \sigma)_{\tau\tau} q \, dl = \int_E \sigma_{\tau\tau} q \, dl \quad \text{for all } q \in \mathcal{P}^k(E) \text{ and edges } E \text{ of } \partial T, \quad (6.1a)$$

$$\int_T \mathcal{I}_k^{\mathcal{R}} \sigma : \rho \, da = \int_T \sigma : \rho \, da \quad \text{for all } \rho \in \mathcal{P}^{k-1}(T, \mathbb{R}^{2 \times 2}). \quad (6.1b)$$

Note that when ρ is a skew-symmetric matrix, both sides of (6.1b) vanish, so (6.1b) is nontrivial only for symmetric ρ . Throughout, we use standard Sobolev spaces $W^{s,p}(\Omega)$ and their norms and seminorms for any $s \geq 0$ and $p \in [1, \infty]$. When the domain is Ω , we omit it from the norm notation if there is no chance of confusion. We also use the element-wise norms $\|u\|_{W_h^{s,p}}^p = \sum_{T \in \mathcal{T}} \|u\|_{W_h^{s,p}(T)}^p$, with the usual adaption for $p = \infty$. When $p = 2$, we put $\|\cdot\|_{H_h^s} = \|\cdot\|_{W_h^{s,2}}$. Let

$$\|\sigma\|_2 = \|\sigma\|_{L^2} + h\|\sigma\|_{H_h^1}, \quad \|\sigma\|_\infty = \|\sigma\|_{L^\infty} + h\|\sigma\|_{W_h^{1,\infty}}.$$

Most of our results assume that $k \geq 0$ is an integer, and the following regularity assumptions are fulfilled

$$\bar{g} \in W^{1,\infty}(\Omega, \mathcal{S}^+), \quad \bar{g}^{-1} \in L^\infty(\Omega, \mathcal{S}^+). \quad (6.2)$$

We use $a \lesssim b$ to indicate that there is an h -independent generic constant C , depending on Ω and the shape-regularity of the mesh \mathcal{T} , such that $a \leq Cb$. The C may additionally depend either on $\{\|\bar{g}\|_{W^{1,\infty}}, \|\bar{g}^{-1}\|_{L^\infty}, \varpi(\bar{g}), K(\bar{g})\}$, or on $\{\|g\|_{W_h^{1,\infty}}, \|\bar{g}^{-1}\|_{L^\infty}\}$, depending on whether we assume (6.2) or not, respectively. We use $(\cdot, \cdot)_D$ to denote the integral of the appropriate inner product (scalar, dot product, Frobenius product, etc.) of its arguments over a Euclidean measurable set D , e.g., $(\sigma_{\tau\tau}, q)_E$ and $(\sigma, \rho)_T$ equal the right hand sides of (6.1a) and (6.1b), respectively.

Theorem 6.1 (Approximation of covariant curl). *Suppose $g \in \mathcal{R}^+(\mathcal{T})$, $\sigma_h \in \mathcal{R}_h^k$, $v_h \in \mathring{\mathcal{W}}_h^k$ (the BDM space in (4.16)), $\sigma \in H^1(\Omega, \mathcal{S}) \cap C^0(\Omega, \mathcal{S})$, and let $\text{curl}_{g,h}$ be the lifted curl operator as defined in (4.21). Then, there exists an $h_0 > 0$ such that for all $h < h_0$,*

$$(\text{curl}_{g,h}(\sigma - \mathcal{I}_k^{\mathcal{R}} \sigma), v_h)_\Omega \lesssim \|\sigma - \mathcal{I}_k^{\mathcal{R}} \sigma\|_2 \|v_h\|_{L^2}, \quad (6.3)$$

and if $k \geq 0$, $g = \mathcal{I}_k^{\mathcal{R}} \bar{g}$ and the regularity assumptions (6.2) hold,

$$(\operatorname{curl}_{\bar{g},h} \sigma_h - \operatorname{curl}_{g,h} \sigma_h, v_h)_{\Omega} \lesssim \|\bar{g} - g\|_{\infty} \|\sigma_h\|_{H_h^1} \|v_h\|_{L^2}, \quad (6.4)$$

$$(\operatorname{curl}_{\bar{g},h} \sigma_h - \operatorname{curl}_{g,h} \sigma_h, v_h)_{\Omega} \lesssim \|\bar{g} - g\|_2 \|\sigma_h\|_{W_h^{1,\infty}} \|v_h\|_{L^2}. \quad (6.5)$$

Proofs of this and other theorems in this subsection are presented in later subsections. For now, let us note that on Euclidean manifolds with $\bar{g} = \delta$, the expressions of our distributional covariant curl (either (4.15) or (4.18a)) reduce to

$$(\operatorname{curl}_{\delta,h} \sigma, v_h)_{\Omega} = (\operatorname{curl}[\sigma], v_h)_{\Omega} - \sum_{T \in \mathcal{T}} (\sigma_{\tau\nu}, v_h \cdot \nu)_{\partial T}.$$

It is easy to see from (6.1) (and integrating the right hand side above by parts) that

$$(\operatorname{curl}_{\delta,h}(\sigma - \mathcal{I}_k^{\mathcal{R}} \sigma), v_h)_{\Omega} = 0 \quad (6.6)$$

for all $v_h \in \mathcal{W}_h^k$. This equality has the flavor of typical FEEC identities (also known as commuting diagram properties). On general manifolds however, it appears that we must trade this equality for the inequality (6.3). The remaining inequalities (6.4)–(6.5) bound the nonlinear changes in the covariant operator arising due to the perturbations in the metric. Theorem 6.1 directly implies error bounds in L^2 norm, while error bounds in stronger norms follow from it:

Corollary 6.2. *Under the assumptions of Theorem 6.1, for all $1 \leq l \leq k$,*

$$\begin{aligned} \|\operatorname{curl}_{g,h}(\sigma - \mathcal{I}_k^{\mathcal{R}} \sigma)\|_{H_h^l} &\lesssim h^{-l} (\|\sigma - \mathcal{I}_k^{\mathcal{R}} \sigma\|_2 + h^{k+1} |\operatorname{curl}_{g,h}(\sigma)|_{H^{k+1}}), \\ \|\operatorname{curl}_{\bar{g},h} \sigma_h - \operatorname{curl}_{g,h} \sigma_h\|_{H_h^l} &\lesssim h^{-l} (\|\bar{g} - g\|_{\infty} \|\sigma_h\|_{H_h^1} + h^{k+1} |\operatorname{curl}_{\bar{g},h} \sigma_h|_{H_h^{k+1}}), \\ \|\operatorname{curl}_{\bar{g},h} \sigma_h - \operatorname{curl}_{g,h} \sigma_h\|_{H_h^l} &\lesssim h^{-l} (\|\bar{g} - g\|_2 \|\sigma_h\|_{W_h^{1,\infty}} + h^{k+1} |\operatorname{curl}_{\bar{g},h} \sigma_h|_{H_h^{k+1}}). \end{aligned}$$

Similar results can be proved for the incompatibility operator.

Theorem 6.3 (Approximation of covariant incompatibility operator). *Suppose $g \in \mathcal{R}^+(\mathcal{T})$, $\sigma_h \in \mathcal{R}_h^k$, $u_h \in \mathcal{V}_h^{k+1}$ (the Lagrange space in (2.14)), $\sigma \in H^1(\Omega, \mathcal{S}) \cap C^0(\Omega, \mathcal{S})$, and let $\operatorname{inc}_{g,h}$ be the lifted inc operator as defined in (4.25). Then, there exists an $h_0 > 0$ such that for all $h < h_0$,*

$$(\operatorname{inc}_{g,h}(\sigma - \mathcal{I}_k^{\mathcal{R}} \sigma), u_h)_{\Omega} \lesssim \|\sigma - \mathcal{I}_k^{\mathcal{R}} \sigma\|_2 |u_h|_{H^1}, \quad (6.8)$$

and if $k \geq 0$, $g = \mathcal{I}_k^{\mathcal{R}} \bar{g}$ and the regularity assumptions (6.2) hold,

$$(\operatorname{inc}_{\bar{g},h} \sigma_h - \operatorname{inc}_{g,h} \sigma_h, u_h)_{\Omega} \lesssim \|\bar{g} - g\|_{\infty} \|\sigma_h\|_{H_h^1} |u_h|_{H^1}, \quad (6.9)$$

$$(\operatorname{inc}_{\bar{g},h} \sigma_h - \operatorname{inc}_{g,h} \sigma_h, u_h)_{\Omega} \lesssim \|\bar{g} - g\|_2 \|\sigma_h\|_{W_h^{1,\infty}} |u_h|_{H^1}. \quad (6.10)$$

Here again, as in the case of covariant curl, comparison with the Euclidean case is illuminating. On Euclidean manifolds, instead of (6.8), the stronger result

$$(\operatorname{inc}_{\delta,h}(\sigma - \mathcal{I}_k^{\mathcal{R}} \sigma), u_h)_{\Omega} = 0 \quad (6.11)$$

holds for the distributional incompatibility (which has element, edge, and vertex contributions: see Proposition 4.6). Indeed, (6.11) follows immediately from (6.6) and (4.23). The theorem also implies error bounds in stronger norms.

Corollary 6.4. *Under the assumptions of Theorem 6.3, for all $0 \leq l \leq k$,*

$$\|\operatorname{inc}_{g,h}(\sigma - \mathcal{I}_k^{\mathcal{R}} \sigma)\|_{H_h^l} \lesssim h^{-l-1} (\|\sigma - \mathcal{I}_k^{\mathcal{R}} \sigma\|_2 + h^{k+1} |\operatorname{inc}_{g,h}(\sigma)|_{H^k}),$$

$$\|\operatorname{inc}_{\bar{g},h} \sigma_h - \operatorname{inc}_{g,h} \sigma_h\|_{H_h^l} \lesssim h^{-l-1} (\|\bar{g} - g\|_{\infty} \|\sigma_h\|_{H_h^1} + h^{k+1} |\operatorname{inc}_{\bar{g},h} \sigma_h|_{H_h^k}),$$

$$\|\operatorname{inc}_{\bar{g},h} \sigma_h - \operatorname{inc}_{g,h} \sigma_h\|_{H_h^l} \lesssim h^{-l-1} (\|\bar{g} - g\|_2 \|\sigma_h\|_{W_h^{1,\infty}} + h^{k+1} |\operatorname{inc}_{\bar{g},h} \sigma_h|_{H_h^k}).$$

Our remaining results are for the approximations of connection and curvature. Let I denote the identity operator (on some space that will be obvious from context) and let $\Pi_k^{\mathcal{W}}$ and $\Pi_{k+1}^{\mathcal{V}}$ denote the L^2 -orthogonal projection into $\mathring{\mathcal{W}}_h^k$ and $\mathring{\mathcal{V}}_h^{k+1}$, respectively.

Theorem 6.5 (Approximation of Gauss curvature). *Suppose regularity assumptions (6.2) hold, $k \geq 0$, $g = \mathcal{I}_k^{\mathcal{R}} \bar{g}$, $K(\bar{g}) \in H^k(\Omega)$, and $K_h(g) \in \mathring{\mathcal{V}}_h^{k+1}$ be the lifted Gaussian curvature as in (3.4). Then, there exists an $h_0 > 0$ such that for all $h < h_0$,*

$$\begin{aligned} \|K_h(g) - K(\bar{g})\|_{H^{-1}} &\lesssim \|\bar{g} - g\|_{\infty} + h \left\| (I - \Pi_{k+1}^{\mathcal{V}}) K(\bar{g}) \right\|_{L^2} \\ &\lesssim h^{k+1} (\|\bar{g}\|_{W^{k+1,\infty}} + |K(\bar{g})|_{H^k}). \end{aligned}$$

Corollary 6.6. *Under the assumptions of Theorem 6.5, for all $0 \leq l \leq k$,*

$$|K_h(g) - K(\bar{g})|_{H_h^l} \lesssim h^{-l} (h^{-1} \|\bar{g} - g\|_{\infty} + \|(I - \Pi_{k+1}^{\mathcal{V}}) K(\bar{g})\|_{L^2} + h^k |K(\bar{g})|_{H^k}).$$

Theorem 6.7 (Approximation of Levi-Civita connection). *Suppose regularity assumptions (6.2) hold, $k \geq 0$, $g = \mathcal{I}_k^{\mathcal{R}} \bar{g}$, $\bar{g} \in H^{k+1}(\Omega)$, $\varpi(\bar{g}) \in H^{k+1}(\Omega)$, and let $\varpi_h(g) \in \mathring{\mathcal{W}}_h^k$ be the lifted connection 1-form as in (5.5). Then, there exists an $h_0 > 0$ such that for all $h < h_0$,*

$$\|\varpi_h(g) - \varpi(\bar{g})\|_{L^2} \lesssim \|\bar{g} - g\|_2 + \left\| (I - \Pi_k^{\mathcal{W}}) \varpi(\bar{g}) \right\|_{L^2}, \quad (6.12)$$

and when $k \geq 1$,

$$\|\varpi_h(g) - \varpi(\bar{g})\|_{L^2} \lesssim h^{k+1} (\|\bar{g}\|_{H^{k+1}} + |\varpi(\bar{g})|_{H^{k+1}}). \quad (6.13)$$

Corollary 6.8. *Under the assumptions of Theorem 6.7, for all $1 \leq l \leq k$,*

$$\|\varpi_h(g) - \varpi(\bar{g})\|_{H_h^l} \lesssim h^{-l} (\|\bar{g} - g\|_2 + \|(I - \Pi_k^{\mathcal{W}}) \varpi(\bar{g})\|_{L^2} + h^{k+1} |\varpi(\bar{g})|_{H^{k+1}}).$$

Since the curvature $K(\bar{g})$ has second order derivatives of the metric \bar{g} , at first glance it may seem surprising that Theorem 6.5 gives H^{-1} -convergence of curvature approximations at the same rate as $\|\bar{g} - g\|_{\infty}$. Even for the lowest order case $k = 0$ (while using piecewise constant metric approximations), where one might only expect convergence in the H^{-2} -norm, the theorem gives first order convergence of the curvature in the H^{-1} -norm. The convergence rates of Theorems 6.7 and 6.5 are both higher than those proved in [10, 27]. As we shall see, the reason behind these higher rates is a property of the Regge interpolant proved in Lemma 6.10 in the next subsection.

6.2. Distributional Christoffel symbols of the first kind

In a neighborhood where the metric g is smooth, the Christoffel symbols of the first kind, $\Gamma_{lmn}(g)$, are given by (2.5b). To see what further terms must be supplied to obtain their distributional version when the metric g is only tt -continuous across an element interface, consider a ψ^{lmn} in the Schwartz test space $\mathcal{D}(\Omega)$ of smooth compactly supported functions. Since $\Gamma_{lmn}(\cdot)$ is a linear first order differential operator applied to a smooth metric argument, its distributional definition is standard:

$$\langle \Gamma_{lmn}(g), \psi^{lmn} \rangle_{\mathcal{D}(\Omega)} = -\frac{1}{2} \int_{\Omega} \left(g_{mn} \partial_l \psi^{lmn} + g_{nl} \partial_m \psi^{lmn} - g_{lm} \partial_n \psi^{lmn} \right) \mathrm{d}a. \quad (6.14)$$

Let $\psi^{l\nu n} = \psi^{lqn} \delta_{jq} \nu^q$ and define $\psi^{\nu mn}$, $\psi^{\nu\nu n}$, $\psi^{\nu\nu\tau}$ etc. similarly. For any $T \in \mathcal{T}$ and any smooth ψ on \bar{T} , let

$$\Gamma_T(g, \psi) := (\Gamma_{lmn}(g), \psi^{lmn})_T + \frac{1}{2} (g_{\nu\nu}, \psi^{\nu\nu\nu})_{\partial T} + (g_{\nu\tau}, \psi^{\nu\nu\tau})_{\partial T}. \quad (6.15)$$

Proposition 6.9. *For all $\psi \in \mathcal{D}(\Omega)$, the distributional Christoffel symbols satisfy*

$$\langle \Gamma_{lmn}(g), \psi^{lmn} \rangle_{\mathcal{D}(\Omega)} = \sum_{T \in \mathcal{T}} \Gamma_T(g, \psi).$$

Proof. Integrating (6.14) by parts, element by element,

$$\begin{aligned} \langle \Gamma_{lmn}(g), \psi^{lmn} \rangle_{\mathcal{D}(\Omega)} &= - \sum_{T \in \mathcal{T}} \int_T \frac{1}{2} g_{lm} (\partial_n \psi^{nlm} + \partial_n \psi^{lnm} - \partial_n \psi^{lmn}) \, da \\ &= \sum_{T \in \mathcal{T}} \left(\int_T \Gamma_{lmn}(g) \psi^{lmn} \, da + \int_{\partial T} g_{lm} \frac{1}{2} (\psi^{\nu lm} + \psi^{\nu lm} - \psi^{\nu lm}) \, dl \right). \end{aligned}$$

We can split the integrand over ∂T into $\nu\nu$, $\tau\nu$, $\nu\tau$, and $\tau\tau$ components. When summing over ∂T for all $T \in \mathcal{T}$, the tt -continuity of g implies that the $\tau\tau$ -terms cancel out. The remaining terms give the boundary contribution as $\sum_{T \in \mathcal{T}} \frac{1}{2} \int_{\partial T} (g_{\nu\nu} \psi^{\nu\nu\nu} + 2g_{\nu\tau} \psi^{\nu\nu\tau}) \, dl$, so the result follows. \blacksquare

Proposition 6.9 serves to motivate the introduction of

$$\Gamma(g, \Sigma) := \sum_{T \in \mathcal{T}} \Gamma_T(g, \Sigma), \quad (6.16)$$

for piecewise smooth $g \in \mathcal{R}^+(\mathcal{T})$ and $\Sigma \in C^\infty(\mathcal{T}, \mathbb{R}^{2 \times 2 \times 2})$. As we proceed to analyze distributional covariant operators, it is perhaps not a surprise that this quantity will reappear in our analysis with various arguments Σ , including those in $\mathcal{P}^k(\mathcal{T}, \mathbb{R}^{2 \times 2 \times 2}) = \{\Sigma : \Sigma|_T \in \mathcal{P}^k(T, \mathbb{R}^{2 \times 2 \times 2}) \text{ for all } T \in \mathcal{T}\}$. The next result gives a property of $\Gamma(\cdot, \cdot)$ in connection with the Regge interpolation error.

Lemma 6.10 (Christoffel orthogonality). *If $k \geq 0$, $g = \mathcal{I}_k^{\mathcal{R}} \bar{g}$ with $\bar{g} \in W^{1,\infty}(\Omega, \mathcal{S}^+)$, $\bar{g}^{-1} \in L^\infty(\Omega, \mathcal{S}^+)$, then for any $\Sigma_h \in \mathcal{P}^k(\mathcal{T}, \mathbb{R}^{2 \times 2 \times 2})$,*

$$\Gamma(\bar{g} - g, \Sigma_h) = 0. \quad (6.17)$$

Proof. We start with (6.15) on $T \in \mathcal{T}$ and integrate by parts

$$\begin{aligned} \Gamma_T(\bar{g} - g, \Sigma_h) &= (\Gamma_{ijl}(\bar{g} - g), \Sigma_h^{ijl})_T + (\Sigma_h^{\nu\nu i}, (\bar{g} - g)_{\nu\tau} \tau_i + \frac{1}{2} (\bar{g} - g)_{\nu\nu} \nu_i)_{\partial T} \\ &= -\frac{1}{2} ((\bar{g} - g)_{ij}, \partial_l (\Sigma_h^{lij} + \Sigma_h^{ilj} - \Sigma_h^{ijl}))_T - \frac{1}{2} ((\bar{g} - g)_{\tau\tau}, \Sigma_h^{\nu\tau\tau} + \Sigma_h^{\tau\nu\tau} - \Sigma_h^{\tau\tau\nu})_{\partial T}. \end{aligned}$$

The first and second inner products above vanish by (6.1b) and (6.1a), respectively. \blacksquare

6.3. Basic estimates

We need a number of preliminary estimates to proceed with the analysis. The approximation properties of the Regge elements are well understood. By the Bramble–Hilbert lemma, on any $T \in \mathcal{T}$,

$$\|(I - \mathcal{I}_0^{\mathcal{R}}) \bar{g}\|_{L^p(T)} \lesssim h |\bar{g}|_{W^{1,p}(T)} \quad (6.18a)$$

for $\bar{g} \in W^{1,p}(T, \mathcal{S})$ and $p \in [1, \infty]$, for the lowest order case (and certainly for the higher $k \geq 1$). A similar estimate holds for the element-wise $L^2(T)$ -projection into the space of constants, which we denote by Π_0 :

$$\|(I - \Pi_0) f\|_{L^p(T)} \leq h C |f|_{W^{1,p}(T)} \quad (6.18b)$$

for $f \in W^{1,p}(T)$. Since $g = \mathcal{I}_k^{\mathcal{R}} \bar{g}$ approaches \bar{g} as $h \rightarrow 0$, we will tacitly assume throughout that h has become sufficiently small to guarantee that the approximated metric g is positive definite throughout.

Let $E \subset \partial T$ be an edge of T . We also need the following well-known estimates that follow from scaling arguments: for all $u \in H^1(T)$

$$\|u\|_{L^2(E)}^2 \lesssim h^{-1} \|u\|_{L^2(T)}^2 + h \|\nabla u\|_{L^2(T)}^2 \quad (6.19)$$

and for all $u \in \mathcal{P}^k(T)$,

$$\|u\|_{L^2(E)} \lesssim h^{-1/2} \|u\|_{L^2(T)}, \quad \|\nabla u\|_{L^2(T)} \lesssim h^{-1} \|u\|_{L^2(T)}. \quad (6.20)$$

Staying in the setting of (6.2), the following estimates are a consequence of [27, Lemma 4.5 and Lemma 4.6]: for $p \in [1, \infty]$,

$$\|g^{-1} - \bar{g}^{-1}\|_{L^p} \lesssim \|g - \bar{g}\|_{L^p}, \quad (6.21)$$

$$\|g\|_{W_h^{1,\infty}} + \|g^{-1}\|_{L^\infty} \lesssim 1, \quad (6.22)$$

$$\|\sqrt{\det g}\|_{L^\infty} + \|\sqrt{\det g^{-1}}\|_{L^\infty} \lesssim 1, \quad (6.23)$$

and for all x in the interior of any element $T \in \mathcal{T}$ and for all $u \in \mathbb{R}^2$,

$$u'u \lesssim u'g(x)u \lesssim u'u.$$

Moreover,

$$\|\sqrt{\det \bar{g}} - \sqrt{\det g}\|_{W_h^{l,p}(\Omega)} \lesssim \|g - \bar{g}\|_{W_h^{l,p}}, \quad l = 0, 1. \quad (6.24)$$

Better control of differences of some functions of the metric is possible through the next lemma. Let

$$\begin{aligned} \beta_1(g) &= \frac{1}{\sqrt{\det g}}, & \beta_2(g) &= \frac{g_{\nu\tau}}{g_{\tau\tau}} \beta_1(g), \\ \eta_1(\bar{g}, g) &= \frac{2g_{\nu\tau}(\bar{g} - g)_{\nu\tau} - g_{\tau\tau}(\bar{g} - g)_{\nu\nu}}{2\sqrt{\det g}^3}, & \eta_2(\bar{g}, g) &= \frac{2g_{\nu\nu}(\bar{g} - g)_{\nu\tau} - g_{\nu\tau}(\bar{g} - g)_{\nu\nu}}{2\sqrt{\det g}^3}. \end{aligned} \quad (6.25)$$

Lemma 6.11. *In the setting of (6.2), for sufficiently small h , there exist smooth functions $f_1, f_2 \in C^\infty(\mathcal{S}^+, \mathbb{R})$ such that at each point on ∂T ,*

$$\begin{aligned} \beta_1(\bar{g}) - \beta_1(g) &= (\bar{g} - g)_{\tau\tau} f_1(g) + \eta_1(\bar{g}, g) + \epsilon_1^2, \\ \beta_2(\bar{g}) - \beta_2(g) &= (\bar{g} - g)_{\tau\tau} f_2(g) + \eta_2(\bar{g}, g) + \epsilon_2^2, \end{aligned}$$

where $\max(\epsilon_1, \epsilon_2) = O(\|\bar{g} - g\|)$ for some Euclidean norm $\|\cdot\|$ at the point.

Proof. By Taylor expansion and (6.22),

$$\begin{aligned} \beta_1(\bar{g}) - \beta_1(g) &= -\frac{1}{2\sqrt{\det g}^3} \text{cof}(g) : (\bar{g} - g) + O(\epsilon^2) \\ &= -\frac{g_{\nu\nu}(\bar{g} - g)_{\tau\tau} - 2g_{\nu\tau}(\bar{g} - g)_{\nu\tau} + g_{\tau\tau}(\bar{g} - g)_{\nu\nu}}{2\sqrt{\det g}^3} + O(\epsilon^2) \\ &= (\bar{g} - g)_{\tau\tau} \frac{-g_{\nu\nu}}{2\sqrt{\det g}^3} + \frac{2g_{\nu\tau}(\bar{g} - g)_{\nu\tau} - g_{\tau\tau}(\bar{g} - g)_{\nu\nu}}{2\sqrt{\det g}^3} + O(\epsilon^2), \end{aligned}$$

where $\text{cof}(\cdot)$ denotes the cofactor matrix. Putting $f_1(g) := -\frac{1}{2}g_{\nu\nu}/\sqrt{\det g}^3 \in C^\infty(\mathcal{S}^+)$, the first identity is proved.

For the second identity, again starting with Taylor expansion and (6.22),

$$\beta_2(\bar{g}) - \beta_2(g) = \frac{-(\bar{g} - g)_{\tau\tau}}{\sqrt{\det g} g_{\tau\tau}^2} + \frac{2\det g(\bar{g} - g)_{\nu\tau} - g_{\nu\tau} \text{cof}(g) : (\bar{g} - g)}{2\sqrt{\det g}^3 g_{\tau\tau}} + O(\epsilon^2).$$

A simple calculation reveals

$$2 \det g(\bar{g} - g)_{\nu\tau} - g_{\nu\tau} \operatorname{cof}(g) : (\bar{g} - g) = g_{\tau\tau} (2g_{\nu\nu}(\bar{g} - g)_{\nu\tau} - g_{\nu\tau}(\bar{g} - g)_{\nu\nu}) - g_{\nu\tau}g_{\nu\nu}(\bar{g} - g)_{\tau\tau},$$

Thus the second identity follows after making an obvious choice of f_2 . \blacksquare

Lemma 6.12. *Let $g = \mathcal{I}_k^{\mathcal{R}} \bar{g}$ for some $k \geq 0$, $T \in \mathcal{T}$, $q \in \mathcal{P}^k(T)$, and let $E \subset \partial T$ be an edge of T . If $\bar{g} \in H^1(T, \mathcal{S}) \cap C^0(T, \mathcal{S})$ and $\Psi \in W^{1,\infty}(T)$,*

$$((g - \bar{g})_{\tau\tau}, \Psi q)_E \lesssim (\|g - \bar{g}\|_{L^2(T)} + h|g - \bar{g}|_{H^1(T)}) \|\Psi\|_{W^{1,\infty}(T)} \|q\|_{L^2(T)}. \quad (6.26)$$

If instead, $\bar{g} \in C^0(T, \mathcal{S})$ and $\Psi \in H^2(T)$, then

$$((g - \bar{g})_{\tau\tau}, \Psi q)_E \lesssim \|g - \bar{g}\|_{L^\infty(T)} (\|\Psi\|_{H^1(T)} + h|\Psi|_{H^2(T)}) \|q\|_{L^2(T)}. \quad (6.27)$$

Proof. Using (6.1a) with $q \Pi_0 \Psi \in \mathcal{P}^k(E)$,

$$((g - \bar{g})_{\tau\tau}, q\Psi)_E = ((g - \bar{g})_{\tau\tau}, q(I - \Pi_0)\Psi)_E.$$

Now, by Hölder inequality, the trace inequality (6.19), triangle inequality, and (6.18b),

$$\begin{aligned} ((g - \bar{g})_{\tau\tau}, q\Psi)_E &\lesssim \| (g - \bar{g})_{\tau\tau} \|_{L^2(E)} \|q\|_{L^2(E)} \| (I - \Pi_0)\Psi \|_{L^\infty(E)} \\ &\lesssim h^{-1} (\|g - \bar{g}\|_{L^2(T)}^2 + h^2 |g - \bar{g}|_{H^1(T)}^2)^{1/2} \|q\|_{L^2(T)} \| (I - \Pi_0)\Psi \|_{L^\infty(T)} \\ &\lesssim (\|g - \bar{g}\|_{L^2(T)} + h|g - \bar{g}|_{H^1(T)}) \|q\|_{L^2(T)} \|\Psi\|_{W^{1,\infty}(T)}. \end{aligned}$$

The proof of (6.27) is similar. \blacksquare

6.4. Analysis of the covariant curl approximation

This subsection is devoted to proving Theorem 6.1. We will start with the first estimate of the theorem, which is easier to prove. The remaining inequalities will be proved using Lemma 6.10 afterward.

Lemma 6.13. *Suppose $g \in \mathcal{R}^+(\mathcal{T})$, $\sigma \in H^1(\Omega, \mathcal{S}) \cap C^0(\Omega, \mathcal{S})$, $\sigma_h = \mathcal{I}_k^{\mathcal{R}} \sigma$, and $v_h \in \mathring{\mathcal{W}}_h^k$. Then,*

$$(\operatorname{curl}_{g,h}(\sigma - \sigma_h), v_h)_\Omega \lesssim \|\sigma - \sigma_h\|_2 \|v_h\|_{L^2}.$$

Proof. Using (4.21) and (4.18b),

$$\begin{aligned} (\operatorname{curl}_{g,h}(\sigma - \sigma_h), v_h)_\Omega &= \sum_{T \in \mathcal{T}} \left[\left((\sigma - \sigma_h)_{ij}, [\operatorname{rot}[v_h]]^{ij} \beta_1(g) \right)_T \right. \\ &\quad - \left. \left((\sigma - \sigma_h)_{ij}, \varepsilon^{jk} (\Gamma_{lk}^l v_h^i - \Gamma_{lk}^i v_h^l) \beta_1(g) \right)_T \right. \\ &\quad \left. - \left((\sigma - \sigma_h)_{\tau\tau}, v_h^i g_{i\tau} \beta_1(g) / g_{\tau\tau} \right)_{\partial T} \right] \end{aligned} \quad (6.28)$$

where β_1 is as in (6.25). The first term on the right is zero when $k = 0$. When $k \geq 1$, we use (6.1b) to insert a projection to constants:

$$\begin{aligned} \left((\sigma - \sigma_h)_{ij}, [\operatorname{rot}[v_h]]^{ij} \beta_1(g) \right)_T &= \left((\sigma - \sigma_h)_{ij}, (I - \Pi_0)([\operatorname{rot}[v_h]]^{ij} \beta_1(g)) \right)_T \\ &\lesssim \|\sigma - \sigma_h\|_{L^2(T)} h \|\operatorname{rot}[v_h]\|_{H^1(T)} \\ &\lesssim \|\sigma - \sigma_h\|_{L^2(T)} \|v_h\|_{L^2(T)}, \end{aligned}$$

where we also used (6.18b) and the inverse estimate (6.20). The second term in (6.28) is easily bounded by absorbing the maximum of g -dependent Γ_{ij}^k into a generic constant:

$$\left((\sigma - \sigma_h)_{ij}, \varepsilon^{jk} (\Gamma_{lk}^l v_h^i - \Gamma_{lk}^i v_h^l) \beta_1(g) \right)_T \lesssim \|\sigma - \sigma_h\|_{L^2(T)} \|v_h\|_{L^2(T)}.$$

Finally, for the last (boundary) term in (6.28), we use (6.26) of Lemma 6.12 for each edge $E \subset \partial T$, setting $\Psi = \beta_1(g)g_{i\tau}/g_{\tau\tau} \in W^{1,\infty}(T)$, after extending the constant tangent vector τ from E into the element T . Then

$$((\sigma - \sigma_h)_{\tau\tau}, v_h^i g_{i\tau} \beta_1(g)/g_{\tau\tau})_{\partial T} \lesssim (\|\sigma - \sigma_h\|_{L^2(T)} + h|\sigma - \sigma_h|_{H_h^1(T)})\|v_h\|_{L^2(T)},$$

where we have absorbed the norm $\|\Psi\|_{W^{1,\infty}(T)}$ from the lemma into the generic g -dependent constant in the inequality. Thus

$$(\operatorname{curl}_{g,h}(\sigma - \sigma_h), v_h)_{\Omega} \lesssim \sum_{T \in \mathcal{T}} (\|\sigma - \sigma_h\|_{L^2(T)} + h|\sigma - \sigma_h|_{H_h^1(T)})\|v_h\|_{L^2(T)}$$

and the result follows by applying Cauchy-Schwarz and Young inequalities. \blacksquare

Lemma 6.14. *Suppose (6.2) holds, $\sigma \in \mathcal{R}_h^k$, $v \in \mathring{\mathcal{W}}_h^k$, and $\sigma \in H^1(\Omega, \mathcal{S}) \cap C^0(\Omega, \mathcal{S})$. Then for sufficiently small h ,*

$$(\operatorname{curl}_{\bar{g},h} \sigma - \operatorname{curl}_{g,h} \sigma, v)_{\Omega} - \Gamma(\bar{g} - g, \Sigma) \lesssim \|\bar{g} - g\|_{\infty} \|\sigma\|_{H_h^1} \|v\|_{L^2}, \quad (6.29)$$

$$(\operatorname{curl}_{\bar{g},h} \sigma - \operatorname{curl}_{g,h} \sigma, v)_{\Omega} - \Gamma(\bar{g} - g, \Sigma) \lesssim \|\bar{g} - g\|_2 \|\sigma\|_{W_h^{1,\infty}} \|v\|_{L^2}. \quad (6.30)$$

where $\Sigma^{ijl} = \sigma_{mn} \varepsilon^{jm} g^{nl} v^i / \sqrt{\det g}$.

Proof. By (4.21) and (4.18a), putting $\alpha(g) = [\operatorname{curl}[\sigma]]_l v^l - \sigma_{ij} \varepsilon^{mi} \Gamma_{lm}^j(g) v^l$,

$$(\operatorname{curl}_{\bar{g},h} \sigma - \operatorname{curl}_{g,h} \sigma, v)_{\Omega} = \sum_{T \in \mathcal{T}} \int_T \frac{\alpha(\bar{g})}{\sqrt{\det \bar{g}}} - \frac{\alpha(g)}{\sqrt{\det g}} \, \mathrm{d}a - \int_{\partial T} \beta(\bar{g}) - \beta(g) \, \mathrm{d}l,$$

where $\beta(g) = \sigma_{\nu\tau} \beta_1(g) v^{\nu} - \sigma_{\tau\tau} \beta_2(g) v^{\nu}$ and β_i are as in (6.25). The first integrand, which we denote by A_T , can be simplified to

$$\begin{aligned} A_T &= \frac{\alpha(\bar{g})}{\sqrt{\det \bar{g}}} - \frac{\alpha(g)}{\sqrt{\det g}} \\ &= \alpha(\bar{g}) \left(\frac{1}{\sqrt{\det \bar{g}}} - \frac{1}{\sqrt{\det g}} \right) - \frac{\sigma_{ij} \varepsilon^{mi}}{\sqrt{\det g}} [\Gamma_{lm}^j(\bar{g}) - \Gamma_{lm}^j(g)] v^l. \end{aligned}$$

Using $\Gamma_{ij}^m(g) = g^{ml} \Gamma_{jl}(g)$ and the linearity of the Christoffel symbols of the first kind, $\Gamma_{lm}^j(\bar{g}) - \Gamma_{lm}^j(g) = g^{jq} \Gamma_{lmq}(\bar{g} - g) + (\bar{g}^{jq} - g^{jq}) \Gamma_{lmq}(\bar{g})$. Hence

$$A_T = \alpha(\bar{g}) [\beta_1(\bar{g}) - \beta_1(g)] - \frac{\sigma_{ij} \varepsilon^{mi}}{\sqrt{\det g}} (\bar{g} - g)^{jq} \Gamma_{lmq}(\bar{g}) v^l + \Sigma^{lmq} \Gamma_{lmq}(\bar{g} - g)$$

with $\Sigma^{lmq} = \sigma_{ij} \varepsilon^{mi} g^{jq} v^l / \sqrt{\det g}$.

Next, we focus on the boundary integrand $B_T = \beta(\bar{g}) - \beta(g)$. By Lemma 6.11,

$$\begin{aligned} B_T &= [\beta_1(\bar{g}) - \beta_1(g)] \sigma_{\nu\tau} v^{\nu} - [\beta_2(\bar{g}) - \beta_2(g)] \sigma_{\tau\tau} v^{\nu} \\ &= (\bar{g} - g)_{\tau\tau} [f_1(g) \sigma_{\nu\tau} + f_2(g) \sigma_{\tau\tau}] v^{\nu} + (\eta_1(\bar{g}, g) \sigma_{\nu\tau} - \eta_2(\bar{g}, g) \sigma_{\tau\tau}) v^{\nu} + (\sigma_{\nu\tau} \epsilon_1^2 - \sigma_{\tau\tau} \epsilon_2^2) v^{\nu}, \end{aligned}$$

with the η_i , f_i , and ϵ_i provided there. We claim that

$$(\eta_1(\bar{g}, g) \sigma_{\nu\tau} - \eta_2(\bar{g}, g) \sigma_{\tau\tau}) v^{\nu} = \Sigma^{\nu\tau} (\bar{g} - g)_{\nu\tau} + \frac{1}{2} \Sigma^{\nu\nu} (\bar{g} - g)_{\nu\nu}. \quad (6.31)$$

Indeed, by (3.17), $\sqrt{\det g} \Sigma^{\nu\nu q} = -\sigma_{ij} \tau^i g^{jq} v^{\nu}$. In this expression, we substitute the orthogonal decomposition $\sigma_{ij} \tau^i = \sigma_{\tau\tau} \delta_{jm} \tau^m + \sigma_{\tau\nu} \delta_{jm} \nu^m$, together with the cofactor expansion of g^{-1} , to get

$$\Sigma^{\nu\nu q} = (\det g)^{-3/2} (\sigma_{\tau\nu} g_{\tau m} - \sigma_{\tau\tau} g_{\nu m}) v^{\nu} \varepsilon^{qm}.$$

This yields expressions for both $\Sigma^{\nu\nu\tau}$ and $\Sigma^{\nu\nu\nu}$ on the right hand side of (6.31), which can again be simplified using (3.17) to verify (6.31). Gathering these observations together, we have proved that

$$\begin{aligned} (\operatorname{curl}_{\bar{g},h} \sigma - \operatorname{curl}_{g,h} \sigma, v)_\Omega &= \sum_{T \in \mathcal{T}} \int_T A_T \, da + \int_{\partial T} B_T \, dl \\ &= \sum_{T \in \mathcal{T}} \left[(\alpha(\bar{g}), \beta_1(\bar{g}) - \beta_1(g))_T + ((\bar{g} - g)^{jq}, \sigma_{ij} \varepsilon^{mi} v^l \beta_1(g) \Gamma_{lmq}(\bar{g}))_T \right. \\ &\quad + ((\bar{g} - g)_{\tau\tau}, [f_1(g) \sigma_{\nu\tau} + f_2(g) \sigma_{\tau\tau}] v^\nu)_{\partial T} \\ &\quad \left. + ((\sigma_{\nu\tau} \epsilon_1^2 - \sigma_{\tau\tau} \epsilon_2^2), v^\nu)_{\partial T} + \Gamma_T(\bar{g} - g, \Sigma) \right], \end{aligned} \quad (6.32)$$

where Γ_T is as defined in (6.15). Moving $\Gamma(\bar{g} - g, \Sigma)$ to the left hand side, we proceed to estimate the terms on the right one by one.

By Hölder inequality and (6.24)

$$\begin{aligned} (\alpha(\bar{g}), \beta_1(\bar{g}) - \beta_1(g))_T &\lesssim \|\beta_1(\bar{g}) - \beta_1(g)\|_{L^\infty(T)} \|\sigma\|_{H_h^1(T)} \|v\|_{L^2(T)} \\ &\lesssim \|\bar{g} - g\|_{L^\infty(T)} \|\sigma\|_{H_h^1(T)} \|v\|_{L^2(T)}. \end{aligned}$$

For the next term, we again use Hölder inequality, followed by (6.21), and (6.23):

$$((\bar{g} - g)^{jq}, \sigma_{ij} \varepsilon^{mi} v^l \beta_1(g) \Gamma_{lmq}(\bar{g}))_T \lesssim \|\bar{g} - g\|_{L^\infty(T)} \|\sigma\|_{L^2(T)} \|v\|_{L^2(T)}.$$

Next, to bound the boundary term over ∂T , we extend the constant vectors ν and τ from an edge E of ∂T to T , let $\Psi = f_1(g) \sigma_{\nu\tau} + f_2(g) \sigma_{\tau\tau} \in W^{1,\infty}(T)$ and $q = v^\nu \in \mathcal{P}^k(T)$ and apply (6.27) to get

$$\begin{aligned} ((\bar{g} - g)_{\tau\tau}, [f_1(g) \sigma_{\nu\tau} + f_2(g) \sigma_{\tau\tau}] v^\nu)_E &\lesssim \|\bar{g} - g\|_{L^\infty(T)} \|v_h\|_{L^2(T)} (\|\Psi\|_{H_h^1(T)} + h|\Psi|_{H_h^2(T)}) \\ &\lesssim \|\bar{g} - g\|_{L^\infty(T)} \|v_h\|_{L^2(T)} (\|\sigma\|_{H_h^1(T)} + h|\sigma|_{H_h^2(T)}) \\ &\lesssim \|\bar{g} - g\|_{L^\infty(T)} \|v_h\|_{L^2(T)} \|\sigma\|_{H_h^1(T)}, \end{aligned}$$

where we used (6.22) and (6.20). Finally, for the ϵ_i -terms in (6.32), noting that $\epsilon_i \lesssim \|\bar{g} - g\|_{L^\infty(\partial T)}^2 \lesssim h \|\bar{g} - g\|_{L^\infty(\partial T)}$, by a trace inequality,

$$\begin{aligned} ((\sigma_{\nu\tau} \epsilon_1^2 - \sigma_{\tau\tau} \epsilon_2^2), v^\nu)_{\partial T} &\lesssim h \|\bar{g} - g\|_{L^\infty(\partial T)} \|\sigma_h\|_{L^2(\partial T)} \|v_h\|_{L^2(\partial T)} \\ &\lesssim \|\bar{g} - g\|_{L^\infty(T)} \|\sigma_h\|_{L^2(T)} \|v_h\|_{L^2(T)}. \end{aligned}$$

Using these estimates in (6.32), we finish the proof of (6.29).

The proof of (6.30) is similar. ■

Lemma 6.15. *Adopt the assumptions of Lemma 6.14 and let Σ be as defined there. Then for sufficiently small h ,*

$$\Gamma(\bar{g} - g, \Sigma) \lesssim \|\bar{g} - g\|_\infty \|\sigma_h\|_{H_h^1} \|v\|_{L^2}, \quad (6.33)$$

$$\Gamma(\bar{g} - g, \Sigma) \lesssim \|\bar{g} - g\|_2 \|\sigma_h\|_{W_h^{1,\infty}} \|v\|_{L^2}. \quad (6.34)$$

Proof. First observe that in the case $k = 0$, the function Σ is constant on each $T \in \mathcal{T}$, so by the Christoffel orthogonality Lemma 6.10, $\Gamma(\bar{g} - g, \Sigma) = 0$. In the $k \geq 1$ case, define $g_0 := \mathcal{I}_0^R \bar{g}$, $\sigma^0 := \mathcal{I}_0^R \sigma$, and $\Sigma_0^{ijl} = \sigma_{mn}^0 \beta_1(g_0) \varepsilon^{jm} g_0^{nl} v^i$. Splitting

$$\begin{aligned} \Sigma^{ijl} - \Sigma_0^{ijl} &= \sigma_{mn} \beta_1(g) \varepsilon^{jm} g^{nl} v^i - \sigma_{mn}^0 \beta_1(g_0) \varepsilon^{jm} g_0^{nl} v^i \\ &= (\sigma_{mn} - \sigma_{mn}^0) \beta_1(g) g^{nl} \varepsilon^{jm} v^i + (\beta_1(g) g^{nl} - \beta_1(g_0) g_0^{nl}) \sigma_{mn}^0 \varepsilon^{jm} v^i \end{aligned}$$

it is easy to see from Hölder inequality, (6.21), and (6.18a) that

$$\|\Sigma - \Sigma_0\|_{L^1(T)} + h \|\Sigma - \Sigma_0\|_{L^1(\partial T)} \lesssim h \|\sigma\|_{H^1(T)} \|v\|_{L^2(T)}. \quad (6.35)$$

Since $\Sigma_0 \in \mathcal{P}^0(\mathcal{T}, \mathbb{R}^{2 \times 2 \times 2})$, Lemma 6.10 implies $\Gamma(\bar{g} - g, \Sigma) = \Gamma(\bar{g} - g, \Sigma - \Sigma_0)$,

$$\begin{aligned} \Gamma(\bar{g} - g, \Sigma) &= \sum_{T \in \mathcal{T}} \left[(\Gamma_{lmn}(\bar{g} - g), (\Sigma - \Sigma_0)^{lmn})_T \right. \\ &\quad \left. + \frac{1}{2} ((\bar{g} - g)_{\nu\nu}, (\Sigma - \Sigma_0)^{\nu\nu\nu})_{\partial T} + ((\bar{g} - g)_{\nu\tau}, (\Sigma - \Sigma_0)^{\nu\nu\tau})_{\partial T} \right] \\ &\lesssim \sum_{T \in \mathcal{T}} \left[\|\bar{g} - g\|_{W^{1,\infty}(T)} h \|\sigma\|_{H^1(T)} \|v\|_{L^2(T)} + \|\bar{g} - g\|_{L^\infty(\partial T)} \|\sigma\|_{H^1(T)} \|v\|_{L^2(T)} \right], \end{aligned}$$

where we have also used $\|\Gamma_{lmn}(\bar{g} - g)\|_{L^\infty(T)} \lesssim \|\bar{g} - g\|_{W^{1,\infty}(T)}$, Hölder inequality, and (6.35). By Cauchy-Schwarz inequality, (6.33) follows. The proof of (6.34) is similar. \blacksquare

Proof of Theorem 6.1. Error estimate (6.3) directly follows from Lemma 6.13. Using the estimates of Lemma 6.15 to bound the Γ -terms in the inequalities of Lemma 6.14, the remaining error estimates of the theorem follow. \blacksquare

Proof of Corollary 6.2. The proof follows along the lines of [27, p. 1818], where the error is compared to the weaker L^2 -norm using the Scott–Zhang interpolant, inverse estimates, and the triangle inequality. \blacksquare

6.5. Analysis of the covariant incompatibility

The error analysis here can now be given by a simple argument using Theorem 6.1.

Proof of Theorem 6.3. To prove (6.8), we note that by the definitions (4.23) and (4.25),

$$(\text{inc}_{g,h}(\sigma - \mathcal{I}_k^R \sigma), u_h)_\Omega = (\text{curl}_{g,h}(\sigma - \mathcal{I}_k^R \sigma), \text{rot } u_h)_\Omega$$

for all $u_h \in \mathring{\mathcal{V}}^{k+1}$. Since $\|\text{rot } u_h\|_{L^2} = |u_h|_{H^1}$, the estimate (6.8) follows from (6.3). The remaining estimates similarly follow from (6.4) and (6.5). \blacksquare

Proof of Corollary 6.4. This proof follows along the lines in [27, p. 1818]. \blacksquare

We conclude this short subsection with a few remarks on our analysis so far. To compare our analysis with [27], the easily spotted difference is that we use our operator inc_g instead of the operator $\text{div}_g \text{div}_g$ in [27]. These two operators are closely related in two dimensions (see Appendix C). A more substantial difference is that while [27] separately estimates certain element terms and inter-element jumps (by applying a triangle inequality first), we do not. Instead, we kept such terms together, gathered terms of good convergence rates, and identified the remainder as a collection of terms that look like those arising from the formula for distributional Christoffel symbols of first kind (6.16). The next key insight was the Christoffel orthogonality Lemma 6.10, which zeroed out the latter collection. Also notable from our analysis so far is the idea of splitting the error terms into a high-order ones and ones that might be sub-optimal in general, but vanishes in specific cases. Such an idea was also used in [48], where the convergence of a surface div div operator on an approximated triangulation is proven (in an extrinsic manner) to converge.

6.6. Analysis of the curvature approximation

Now we turn to the proof of Theorem 6.5. The key extra ingredient here is a technique pioneered in [27] to represent the curvature approximation using an integral of its first variation, as stated in

the next lemma. For any $g \in \mathcal{R}^+(\mathcal{T})$ and $\sigma \in \mathcal{R}(\mathcal{T})$, using inc_g of Definition 4.5, let

$$b_h(g, \sigma, u) = -\langle \text{inc}_g \sigma, u \rangle_{\mathcal{V}(\mathcal{T})}, \quad G(t) = \delta + t(g - \delta), \quad \bar{G}(t) = \delta + t(\bar{g} - \delta).$$

Lemma 6.16. *Let $g \in \mathcal{R}^+(\mathcal{T})$, $K_h(g) \in \mathring{\mathcal{V}}_h^{k+1}$ be as in Definition 3.1 for some $k \geq 0$. Also let \bar{g} be a smooth metric and let $K(\bar{g})$ denote its smooth Gauss curvature. Then*

$$\int_{\mathcal{T}} K_h(g) u_h = \frac{1}{2} \int_0^1 b_h(G(t), g - \delta, u_h) dt, \quad \text{for all } u_h \in \mathring{\mathcal{V}}_h^{k+1}, \quad (6.36)$$

$$\int_{\mathcal{T}} K(\bar{g}) u = \frac{1}{2} \int_0^1 b_h(\bar{G}(t), \bar{g} - \delta, u) dt, \quad \text{for all } u \in \mathring{\mathcal{V}}(\mathcal{T}). \quad (6.37)$$

Proof. Since $K_h(\delta) = 0$,

$$\int_{\mathcal{T}} K_h(g) u_h = \int_0^1 \frac{d}{dt} \int_{\mathcal{T}} K_h(G(t)) u_h.$$

Now, expand the inner integral using (3.4) and differentiate each term in the direction $\sigma = G'(t) = g - \delta$, using each of the three identities of Lemma 4.7. Comparing the result, term by term, to the expression in Proposition 4.6, equation (6.36) is proved. The proof of (6.37) is similar, after noting that the global smoothness of $\bar{g} - \delta$ implies that the jump terms in $b_h(\bar{G}(t), \bar{g} - \delta, u)$ vanish (by the last statement of Proposition 4.6). \blacksquare

To state a simple lemma before the error analysis, for any $u, v, f \in L^2(\Omega)$, let

$$(u, v)_g = \int_{\Omega} u v \sqrt{\det g} da, \quad \|u\|_g = (u, u)_g^{1/2},$$

and let $P_{k+1}^g : L^2(\Omega) \rightarrow \mathring{\mathcal{V}}_h^{k+1}$ denote the $(\cdot, \cdot)_g$ -orthogonal projector into $\mathring{\mathcal{V}}_h^{k+1}$.

Lemma 6.17. *For any $u \in H_0^1(\Omega)$ and any $g \in \mathcal{R}_h^k$,*

$$(K_h(g) - K(\bar{g}), u - P_{k+1}^g u)_{\bar{g}} \lesssim h \|u\|_{H^1} \|(I - \Pi_{k+1}^{\mathcal{V}}) K(\bar{g})\|_{L^2},$$

Proof. Since

$$\begin{aligned} (K_h(g) - K(\bar{g}), u - P_{k+1}^{\bar{g}} u)_{\bar{g}} &= (K(\bar{g}), u - P_{k+1}^{\bar{g}} u)_{\bar{g}} \\ &= ((I - P_{k+1}^{\bar{g}}) K(\bar{g}), (I - P_{k+1}^{\bar{g}}) u)_{\bar{g}} \\ &\lesssim h \|u\|_{H^1(\Omega)} \inf_{v_h \in \mathring{\mathcal{V}}_h^{k+1}} \|K(\bar{g}) - v_h\|_{L^2(\Omega)}, \end{aligned}$$

where we have used the equivalence of $L^2(\Omega)$ -norm and $\|\cdot\|_{\bar{g}}$ -norm. \blacksquare

Proof of Theorem 6.5. The general structure of the proof follows [27]. Let $u \in H_0^1(\Omega)$ and let $u_h \in \mathring{\mathcal{V}}_h^{k+1}$. Then

$$(K_h(g) - K(\bar{g}), u)_{\bar{g}} = (K_h(g) - K(\bar{g}), u - u_h + u_h)_{\bar{g}} = s_1 + s_2 + s_3$$

where $s_1 = (K_h(g), u_h)_g - (K(\bar{g}), u_h)_{\bar{g}}$, $s_2 = (K_h(g), u_h)_{\bar{g}} - (K_h(g), u_h)_g$, and $s_3 = (K_h(g) - K(\bar{g}), u - u_h)_{\bar{g}}$. We proceed to estimate each s_i .

By Lemma 6.16 and (4.25) we rewrite s_1 as follows:

$$\begin{aligned} s_1 &= \frac{1}{2} \int_0^1 b_h(G(t), g - \delta, u_h) - b_h(\bar{G}(t), \bar{g} - \delta, u_h) dt \\ &= \frac{1}{2} \int_0^1 b_h(G(t), g - \delta, u_h) - b_h(\bar{G}(t), g - \delta, u_h) dt + \frac{1}{2} \int_0^1 b_h(\bar{G}(t), g - \bar{g}, u_h) dt \\ &= \frac{1}{2} (\text{inc}_{\bar{G}(t), h}(g - \delta) - \text{inc}_{G(t), h}(g - \delta), u_h)_{\Omega} - \frac{1}{2} (\text{inc}_{\bar{G}(t), h}(g - \bar{g}), u_h)_{\Omega}. \end{aligned}$$

Now we can use Theorem 6.3. Applying (6.9) with $g = \bar{G}(t)$ and $\sigma_h = g - \delta \in \mathcal{R}_h^k$ and applying (6.8) with $g = \bar{G}(t)$ and $\sigma = \bar{g}$,

$$s_1 = (K_h(g), u_h)_g - (K(\bar{g}), u_h)_{\bar{g}} \lesssim \|\bar{g} - g\|_{\infty} \|\nabla u_h\|_{L^2}. \quad (6.38)$$

for any $u_h \in \mathring{\mathcal{V}}_h^{k+1}$, where we have also used $\|\cdot\|_2 \lesssim \|\cdot\|_{\infty}$ and (6.22).

For the next term s_2 , we use Hölder inequality and (6.24) to get

$$\begin{aligned} s_2 &= (K_h(g), u_h)_{\bar{g}} - (K_h(g), u_h)_g \\ &= (K_h(g)u_h, \sqrt{\det \bar{g}} - \sqrt{\det g})_{\Omega} \\ &\leq \|K_h(g)\|_{L^2} \|u_h\|_{L^2} \|\sqrt{\det(\bar{g})} - \sqrt{\det(g)}\|_{L^{\infty}} \\ &\lesssim \|\bar{g} - g\|_{L^{\infty}} \|K_h(g)\|_{L^2} \|u_h\|_{L^2}. \end{aligned}$$

Next, setting $u_h = K_h(g)$ in (6.38), we obtain

$$\|K_h(g)\|_{L^2}^2 \lesssim h^{-1} \|\bar{g} - g\|_{\infty} \|K_h(g)\|_{L^2} + \|K(\bar{g})\|_{L^2} \|K_h(g)\|_{L^2}$$

using the inverse inequality (6.20). Since standard estimates imply

$h^{-1} \|\bar{g} - g\|_{\infty} \lesssim 1$, we conclude that $\|K_h(g)\|_{L^2} \lesssim 1$, so

$$s_2 \lesssim \|\bar{g} - g\|_{L^{\infty}} \|u_h\|_{L^2}. \quad (6.39)$$

Finally, to estimate s_3 , let us now fix $u_h = P_{k+1}^{\bar{g}} u \in \mathring{\mathcal{V}}_h^{k+1}$. Then by Lemma 6.17:

$$s_3 \lesssim h \|u\|_{H^1} \left\| (I - \Pi_{k+1}^{\mathcal{V}}) K(\bar{g}) \right\|_{L^2}. \quad (6.40)$$

For this choice of u_h , we also have $|u_h - \Pi_{k+1}^{\mathcal{V}} u|_{H^1} \lesssim h^{-1} \|u_h - \Pi_{k+1}^{\mathcal{V}} u\|_{L^2} \lesssim \|u\|_{H^1}$, so by the stability [22] of the L^2 projection $\Pi_{k+1}^{\mathcal{V}}$ in H^1 , we conclude that $\|u_h\|_{H^1} \lesssim \|u\|_{H^1}$. This allowing us to replace u_h by u in the bounds for s_1 and s_2 . All together, (6.38), (6.39), and (6.40), imply

$$(K_h(g) - K(\bar{g}), u)_{\bar{g}} \lesssim (\|\bar{g} - g\|_{\infty} + h \left\| (I - \Pi_{k+1}^{\mathcal{V}}) K(\bar{g}) \right\|_{L^2}) \|u\|_{H^1}.$$

Thus, since $\|u/\sqrt{\det \bar{g}}\|_{H^1} \lesssim \|u\|_{H^1}$,

$$\begin{aligned} \|K_h(g) - K(\bar{g})\|_{H^{-1}} &= \sup_{u \in H_0^1} \frac{(K_h(g) - K(\bar{g}), u)_{\Omega}}{\|u\|_{H^1}} \\ &= \sup_{u \in H_0^1} \frac{(K_h(g) - K(\bar{g}), u/\sqrt{\det \bar{g}})_{\bar{g}}}{\|u\|_{H^1}} \\ &\lesssim \|\bar{g} - g\|_{\infty} + h \left\| (I - \Pi_{k+1}^{\mathcal{V}}) K(\bar{g}) \right\|_{L^2}, \end{aligned}$$

which proves the first estimate of the theorem. The second follows from standard interpolation error estimates. \blacksquare

Proof of Corollary 6.6. One can prove this following [27, p. 1818] using the improved estimate of Theorem 6.5] in place of the estimate used there. \blacksquare

6.7. Analysis of the connection approximation

The integral representation of the connection 1-form can be given analogously to the curvature case once we know the variation of the connection with respect to the metric. Recall that we compute the connection using the canonical g -orthonormal frame $e_i(t) = G(t)^{-1/2} E_i$ (see (5.7)) obtained using the flow (5.6) evaluated at $t = 1$. We only discuss the variation of ϖ_g with respect to g along this flow (i.e., unlike Lemma 4.7, the following is valid only for a specific direction σ).

Lemma 6.18. *Let $\sigma = dG/dt = g - \delta$. Then for all $X \in \mathfrak{X}(M)$,*

$$\frac{d}{dt} \varpi_{G(t)}(X) = -\frac{1}{2}(\operatorname{curl}_{G(t)} \sigma)(X), \quad (6.41a)$$

$$\frac{d}{dt} \Theta^E = \frac{1}{2} \llbracket \sigma_{\hat{\nu} \hat{\tau}} \rrbracket. \quad (6.41b)$$

Proof. Both identities follow from [10], e.g., with $e_i(t) = G(t)^{-1/2} E_i$,

$$\begin{aligned} 2 \frac{d}{dt} \varpi_{G(t)}(X) &= -(\nabla_{e_1} \sigma)(e_2, X) + (\nabla_{e_2} \sigma)(e_1, X) && \text{by [10, Eq. (7)],} \\ &= -(\nabla_{e_1} \sigma)(X, e_2) + (\nabla_{e_2} \sigma)(X, e_1) && \text{by symmetry of } \sigma, \\ &= -F \sigma_X(e_1, e_2) && \text{by (4.2),} \end{aligned}$$

which equals $-(\operatorname{curl}_{G(t)} \sigma)(X)$, thus proving (6.41a). For a proof of (6.41b), see [10, Prop. 2.20]. ■

Let $c_h(g, \sigma, v) = -\langle \operatorname{curl}_g \sigma, Q_g v \rangle_{\dot{\mathcal{W}}_g(\mathcal{T})}$ for $v \in \dot{\mathcal{W}}(\Omega)$, where Q_g is as in (4.17) and the distributional covariant curl is as defined in (4.18).

Lemma 6.19. *Let $g \in \mathcal{R}^+(\mathcal{T})$, $k \in \mathbb{N}_0$. There holds for $\varpi_h(g) \in \dot{\mathcal{W}}_h^k$ from Definition 5.3, the exact metric \bar{g} and its connection 1-form $\varpi(\bar{g})$*

$$\int_{\mathcal{T}} \varpi_h(g) Q_g v_h = \frac{1}{2} \int_0^1 c_h(G(t), g - \delta, v_h) dt, \quad \text{for all } v_h \in \dot{\mathcal{W}}_h^k, \quad (6.42)$$

$$\int_{\mathcal{T}} \varpi(\bar{g}) Q_g v = \frac{1}{2} \int_0^1 c_h(\bar{G}(t), \bar{g} - \delta, v) dt, \quad \text{for all } v \in \dot{\mathcal{W}}(\Omega). \quad (6.43)$$

Proof. The proof is similar to proof of Lemma 6.16: (6.42) follows from Lemma 6.18 and the fundamental theorem of calculus, and for (6.43), we note that the jump terms in $c_h(\bar{G}(t), \bar{g} - \delta, v)$ vanish due to the global smoothness of $\bar{g} - \delta$. ■

Proof of Theorem 6.7. For $v \in L^2(\Omega, \mathbb{R}^2)$ we add and subtract the L^2 -orthogonal projector $v_h = \Pi_k^{\mathcal{W}} v \in \dot{\mathcal{W}}_h^k$ and write

$$(\varpi_h(g) - \varpi(\bar{g}), v)_{\Omega} = s_1 + s_2$$

where $s_1 = (\varpi_h(g) - \varpi(\bar{g}), v - v_h)_{\Omega}$ and $s_2 = (\varpi_h(g) - \varpi(\bar{g}), v_h)_{\Omega}$. Due to the properties of the L^2 -orthogonal projector we obtain

$$s_1 = (\Pi_k^{\mathcal{W}} \varpi(\bar{g}) - \varpi(\bar{g}), v - v_h)_{\Omega} \lesssim \|v\|_{L^2} \left\| (I - \Pi_k^{\mathcal{W}}) \varpi(\bar{g}) \right\|_{L^2}.$$

For s_2 , we use Lemma 6.19 and (4.21) to get

$$\begin{aligned} s_2 &= \frac{1}{2} \int_0^1 c_h(G(t), g - \delta, v_h) - c_h(\bar{G}(t), g - \delta, v_h) + c_h(\bar{G}(t), g - \bar{g}, v_h) dt \\ &= \frac{1}{2} (\operatorname{curl}_{\bar{G}(t), h}(g - \delta) - \operatorname{curl}_{G(t), h}(g - \delta), v_h)_{\Omega} - \frac{1}{2} (\operatorname{curl}_{\bar{G}(t), h}(g - \bar{g}), v_h)_{\Omega}. \end{aligned}$$

Estimating using (6.3) and (6.5) of Theorem 6.1 and (6.22),

$$(\varpi_h(g) - \varpi(\bar{g}), v_h)_{\Omega} \lesssim \|\bar{g} - g\|_2 \|v_h\|_{L^2}.$$

Thus, we obtain

$$\begin{aligned} \|\varpi_h(g) - \varpi(\bar{g})\|_{L^2} &= \sup_{v \in L^2(\Omega, \mathbb{R}^2)} \frac{(\varpi_h(g) - \varpi(\bar{g}), v + v_h - v_h)_{\Omega}}{\|v\|_{L^2}} \\ &\lesssim \|\bar{g} - g\|_2 + \left\| (I - \Pi_k^{\mathcal{W}}) \varpi(\bar{g}) \right\|_{L^2}. \end{aligned}$$

proving (6.12). Inequality (6.13) follows by interpolation error estimates. ■

■

Proof of Corollary 6.8. This is analogous to proof of Corollary 6.2. ■

Remark 6.20 (Case $k = 0$ for connection approximation). In the case $k = 0$, the space $\mathring{\mathcal{W}}_h^0$ consists of piecewise constant vector fields with normal continuity. Thus every function in $\mathring{\mathcal{W}}_h^0$ is exactly divergence-free. If the exact connection 1-form $\varpi_{\bar{g}}$ is not divergence-free, then it cannot generally be approximated by functions in $\mathring{\mathcal{W}}_h^0$. Thus, no convergence for the connection approximation in the lowest order case $k = 0$ should be expected. This is confirmed by numerical experiments in the next section.

7. Numerical examples

In this section we confirm, by numerical examples, that the theoretical convergence rates from Theorem 6.5 and Theorem 6.7 are sharp. All experiments were performed in the open source finite element software NGSolve¹ [42, 43], where the Regge elements are available.

7.1. Curvature approximation

We consider the numerical example proposed in [27], where on the square $\Omega = (-1, 1) \times (-1, 1)$ the smooth Riemannian metric tensor

$$\bar{g}(x, y) := \begin{pmatrix} 1 + (\partial_x f)^2 & \partial_x f \partial_y f \\ \partial_x f \partial_y f & 1 + (\partial_y f)^2 \end{pmatrix}$$

with $f(x, y) := \frac{1}{2}(x^2 + y^2) - \frac{1}{12}(x^4 + y^4)$ is defined. This metric corresponds to the surface induced by the embedding $(x, y) \mapsto (x, y, f(x, y))$ and its exact Gauss curvature is given by

$$K(\bar{g})(x, y) = \frac{81(1 - x^2)(1 - y^2)}{(9 + x^2(x^2 - 3)^2 + y^2(y^2 - 3)^2)^2}.$$

The embedded surface and Gauss curvature are depicted in Figure 7.1.

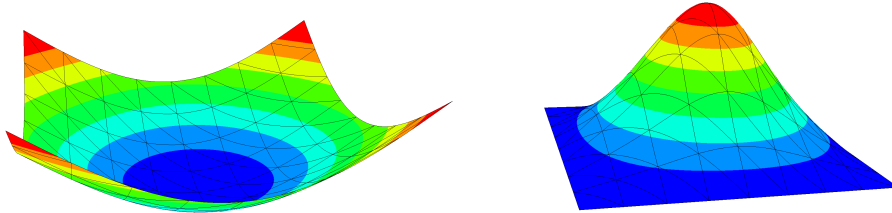


FIGURE 7.1. Left: Embedded surface, color indicates to z -component. Right: Exact Gauss curvature as graph over the domain Ω .

To test also the case of non-homogeneous Dirichlet and Neumann boundary conditions we consider only one quarter $\Omega = (0, 1) \times (0, 1)$ and define the right and bottom boundaries as Dirichlet and the remaining parts as Neumann boundary. To avoid possible super-convergence properties due to a structured grid, we perturb all internal points of the triangular mesh by a uniform distribution in

¹www.ngsolve.org

the range $[-\frac{h}{4}, \frac{h}{4}]$, h denoting the maximal mesh-size of the originally generate mesh. The geodesic curvature on the left boundary is exactly zero, whereas on the top boundary we compute

$$\kappa_g(\bar{g})|_{\Gamma_{\text{left}}} = 0, \quad \kappa_g(\bar{g})|_{\Gamma_{\text{top}}} = \frac{-27(x^2 - 1)y(y^2 - 3)}{(x^2(x^2 - 3)^2 + 9)^{3/2}\sqrt{x^2(x^2 - 3)^2 + y^2(y^2 - 3)^2 + 9}}.$$

The vertex expressions K_V at the vertices of the Neumann boundary can directly be computed by measuring the angle $\arccos(\frac{\bar{g}(\tau_1, \tau_2)}{\|\tau_1\|_{\bar{g}}\|\tau_2\|_{\bar{g}}})$.

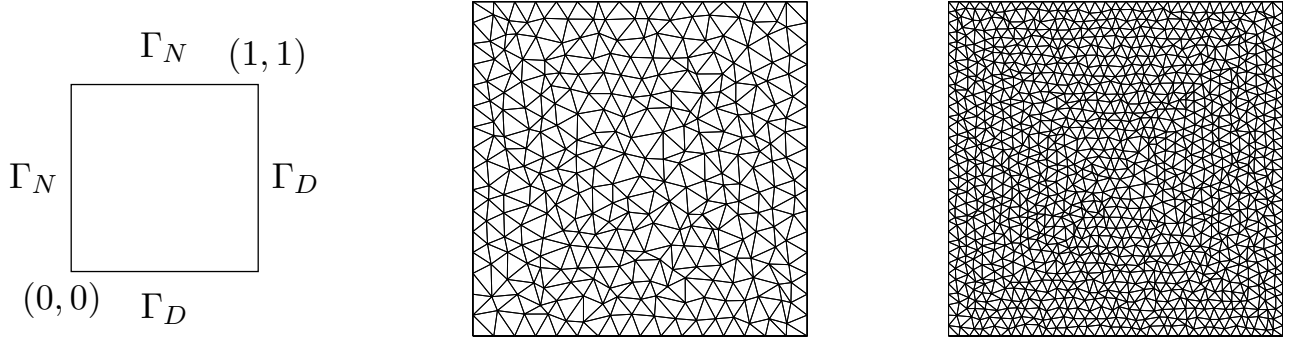


FIGURE 7.2. Left: Domain with Dirichlet and Neumann boundaries. Middle and right: perturbed unstructured triangular mesh grids.

To illustrate our theorems, we must use $g = \mathcal{I}_k^R \bar{g}$. In implementing the Regge interpolant, the moments on the edges have to coincide exactly: see (6.1). To this end, we use a high enough integration rule for interpolating \bar{g} for minimizing the numerical integration errors.

We compute and report the curvature error in the L^2 -norm, namely $\|K(\bar{g}) - K_h(g)\|_{L^2}$. We also report the H^{-1} -norm of the error. It can be computed by solving for $w \in H_0^1(\Omega)$ such that $-\Delta w = K(\bar{g}) - K_h(g)$ and observing that

$$\|K(\bar{g}) - K_h(g)\|_{H^{-1}} = \|w\|_{H^1}.$$

Of course the right hand side can generally be computed only approximately. To avoid extraneous errors, we approximate w using Lagrange finite elements of two degrees more, i.e., $w_h \in \mathcal{V}_h^{k+3}$ when $K_h(g) \in \mathcal{V}_h^{k+1}$.

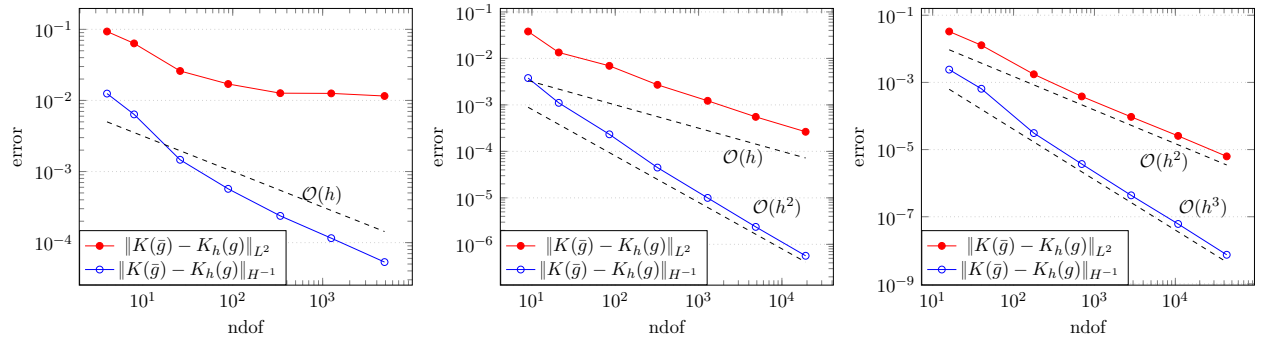


FIGURE 7.3. Convergence of Gauss curvature with respect to number of degrees of freedom (ndof) in different norms for Regge elements $g \in \mathcal{R}_h^k$ of order $k = 0, 1, 2$.

We start by approximating \bar{g} by the lowest order piecewise constant Regge elements $g \in \mathcal{R}_h^0$. As shown in Figure 7.3 (left), we do not obtain convergence in the L^2 -norm, but do obtain linear convergence in the weaker H^{-1} -norm, in agreement with Theorem 6.5. When increasing the approximation

order of Regge elements to linear and quadratic polynomials we observe the appropriate increase of the convergence rates: see Figure 7.3 (middle and right), confirming that the results stated in Theorem 6.5 and Corollary 6.6 are practically sharp. In Figure 7.4 snap-shots of the approximated Gauss curvature are shown.

Remark 7.1. Attempting to increase the polynomial order for the curvature approximation, say by placing $K_h(g)$ in \mathcal{V}_h^{k+2} , while the metric g remains in \mathcal{R}_h^k , may not generally produce additional orders of convergence. This is because the orthogonality properties of the canonical Regge interpolant, (6.1a)–(6.1b), and for the distributional Christoffel symbols, Lemma 6.10, may not be fulfilled in such cases. Indeed, we observed loss of one order of convergence when $K_h(g)$ is placed in \mathcal{V}_h^{k+2} in various examples.

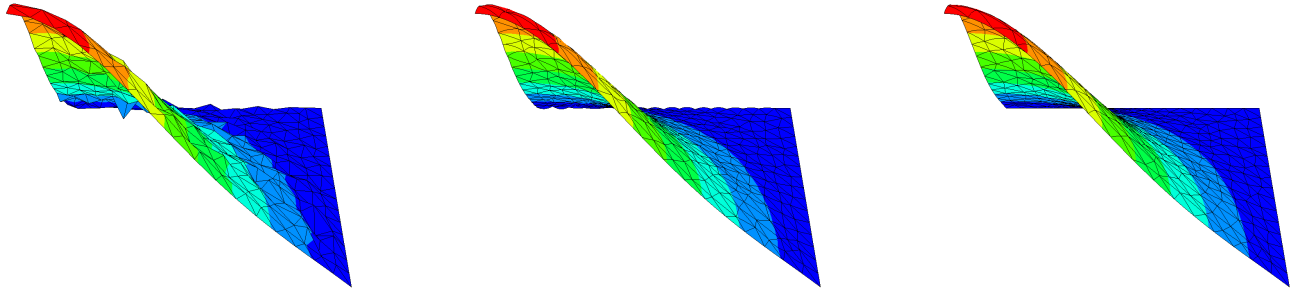


FIGURE 7.4. From left to right: Approximated Gauss curvature (top right quarter of the full curvature in Figure 7.1) with Lagrangian elements of order $k = 1, 2, 3$ and corresponding metric approximations $g = \mathcal{I}_{k-1}^{\mathcal{R}} \bar{g}$, respectively.

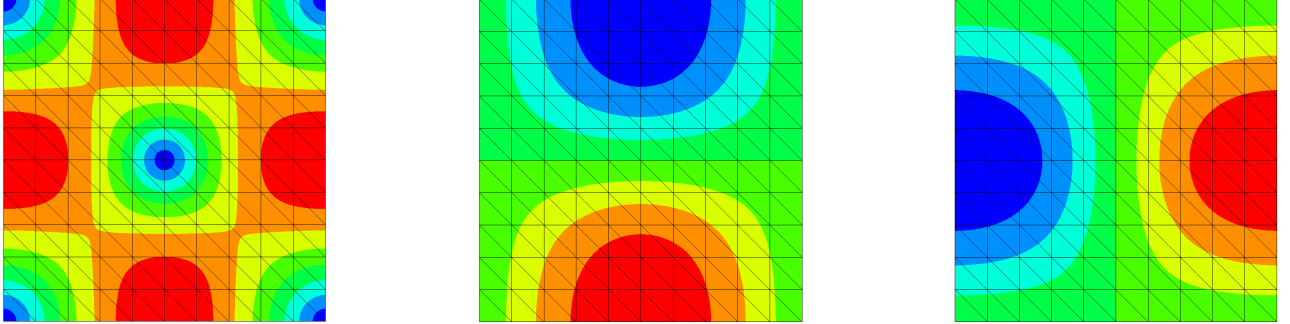
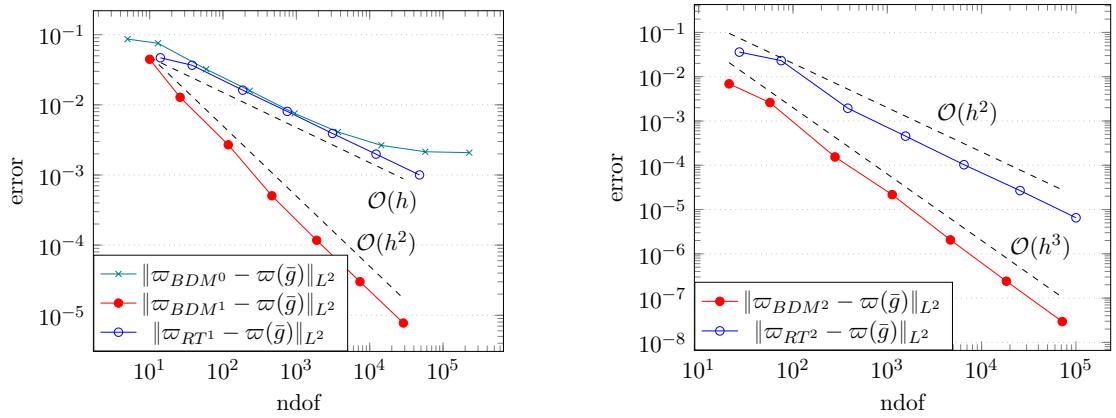
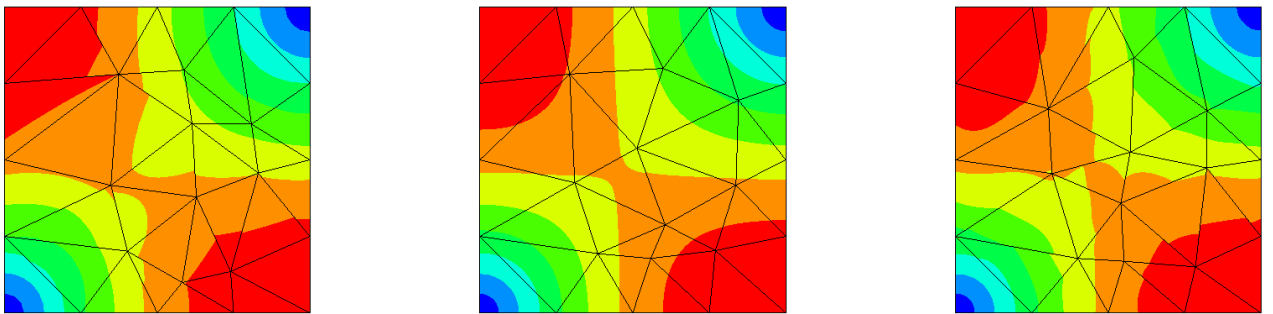
7.2. Connection 1-form approximation

For testing the convergence of the connection 1-form we consider the same metric tensor \bar{g} , same domain, and the same type of boundary conditions as before. The exact connection 1-form ϖ depicted in Figure 7.5 is given by

$$\varpi(\bar{g}) = -\frac{1}{2} \begin{pmatrix} (e_2)' \bar{g} \bar{\nabla}_{E_1} e_1 - (e_1)' \bar{g} \bar{\nabla}_{E_1} e_2 \\ (e_2)' \bar{g} \bar{\nabla}_{E_2} e_1 - (e_1)' \bar{g} \bar{\nabla}_{E_2} e_2 \end{pmatrix} = \begin{pmatrix} -\frac{3y(y^2-3)(x^2-1)(9+3\sqrt{A}+y^2(y^2-3)^2+x^2(x^2-3)^2)}{\sqrt{A}((A+9)\sqrt{A}+6A)} \\ \frac{3x(x^2-3)(y^2-1)(9+3\sqrt{A}+x^2(x^2-3)^2+y^2(y^2-3)^2)}{\sqrt{A}((A+9)\sqrt{A}+6A)} \end{pmatrix},$$

where $A = y^6 - 6y^4 + 9 + x^6 - 6x^4 + 9x^2$, $E_i \in \mathbb{R}^2$ are the Euclidean basis vectors, $e_i = \bar{g}^{-\frac{1}{2}} E_i$ in accordance with (5.7), and the covariant derivative $(\bar{\nabla}_X Y)^i = ((\bar{\nabla} X)Y)^i + \bar{\Gamma}_{jk}^i X^j Y^k$ with $\bar{\Gamma}_{ij}^k$ denoting the Christoffel symbol of second kind with respect to \bar{g} .

For the results shown in Figure 7.6 we use BDM and also Raviart–Thomas [39] RT elements. The optimal L^2 -convergence rates stated in Theorem 6.7 are confirmed for $k > 0$ to be sharp when using BDM^k elements for $k > 0$. If we increase the test-space, however, to RT^k elements, which additionally include specific polynomials of one order higher than BDM^k , one order of convergence is lost, compare also Figure 7.6 (If BDM^{k+1} elements are used in combination with $g \in \mathcal{R}_h^k$ the same behavior can be observed). Note, that to construct the finite element space $\mathcal{W}_h^0 = BDM^0$, we consider the lowest order Raviart–Thomas elements RT^0 and lock the linear part by enforcing that $\text{div}(RT^0) = 0$. As depicted in Figure 7.6 (left) the discrete solution converges linearly at the beginning, however, after some refinements the error stagnates. This is in accordance with the explanation provided in Remark 6.20. Solution snap-shots are displayed in Figure 7.7.


 FIGURE 7.5. Exact connection 1-form ω . Left: $\|\omega\|_2$, middle: x -component, right: y -component.

 FIGURE 7.6. L^2 -convergence of connection 1-form error with BDM and RT elements. Optimal convergence rates are observed for BDM^1 with $g = \mathcal{I}_1^R \bar{g}$ and BDM^2 with $g = \mathcal{I}_2^R \bar{g}$, whereas a deterioration of the rate is obtained when increasing the approximation space to RT^k with $g = \mathcal{I}_k^R \bar{g}$. Remark 6.20 explains why BDM^0 approximations with $g = \mathcal{I}_0^R \bar{g}$ do not generally converge.

 FIGURE 7.7. Norm of approximated connection 1-form. Optimal quadratic and cubic convergence for BDM^1 with $g = \mathcal{I}_1^R \bar{g}$ (left) and BDM^2 with $g = \mathcal{I}_2^R \bar{g}$ (middle) and expected reduced convergence for RT^2 with $g = \mathcal{I}_2^R \bar{g}$ (right).

Appendix A. Rationale for the g -normal continuity

This section briefly presents a justification for the usage of g -normal continuous vector fields in Definition 4.3. We show that there are smooth functions φ in $\mathfrak{X}_c(\check{M})$ approaching a g -normal continuous $W \in \mathring{\mathcal{W}}_g(\mathcal{T})$ in such a way that the right hand side of (4.14) converges to that of (4.15). For any mesh vertex $V \in \mathcal{V}$, let $B_\varepsilon(V) = \{q \in M : d_g(q, V) \leq \varepsilon\}$. Then put $D_\varepsilon = \cup_{V \in \mathcal{V}} B_\varepsilon(V)$ and $\check{M}_\varepsilon = M \setminus D_\varepsilon$. Let $U_i, \check{\Phi}_i : U_i \rightarrow \mathbb{R}^2$ denote a chart of the glued smooth structure. In the parameter domain $\check{\Phi}_i(U_i)$, using the Euclidean divergence operator, define $W^p(\text{div}, \check{\Phi}_i(U_i)) = \{w \in L^p(\check{\Phi}_i(U_i)), \text{div}(w) \in L^p(\check{\Phi}_i(U_i))\}$ for any $1 \leq p < \infty$ with its natural Euclidean norm. This norm and the duality pairings defined in (4.14) and (4.15) feature in the next result.

Proposition A.1. *Let $\sigma \in \mathcal{R}(\mathcal{T})$ and $W \in \mathring{\mathcal{W}}_g(\mathcal{T})$. For any given $\varepsilon_1 > 0$, there exists a $p > 2$, an $\varepsilon_2 > 0$, finitely many charts $\{(U_i, \check{\Phi}_i) : i \in I\}$ covering $\check{M}_{\varepsilon_2}$ in the glued smooth structure, a partition of unity ψ_i subordinate to U_i , and a smooth $\varphi \in \mathfrak{X}_c(\check{M})$ such that $\varphi = \sum_{i \in I} \varphi_i$ with support of φ_i contained in U_i , satisfies*

$$|\langle \text{curl}_g \sigma, \varphi \rangle_{\mathfrak{X}_c(\check{M})} - \langle \text{curl}_g \sigma, W \rangle_{\mathring{\mathcal{W}}_g(\mathcal{T})}| \leq \varepsilon_1, \quad \text{and} \quad (\text{A.1})$$

$$\|(\check{\Phi}_i)_*(\varphi_i - \psi_i W)\|_{W^p(\text{div}, \check{\Phi}_i(U_i \cap \check{M}_{\varepsilon_2}))} \leq \varepsilon_1, \quad \text{for all } i \in I. \quad (\text{A.2})$$

Proof. As a first step, we zero out the vector field W near vertices. For any $\varepsilon > 0$, let $0 \leq \chi_\varepsilon \leq 1$ be a smooth cutoff function satisfying $\chi_\varepsilon \equiv 1$ in \check{M}_ε and $\chi_\varepsilon \equiv 0$ in $D_{\varepsilon/2}$, and let

$$r_\varepsilon(W) = \sum_{T \in \mathcal{T}} \int_{(T \cap D_\varepsilon, g)} g(W, W)^{1/2} + \int_{(\partial T \cap D_\varepsilon, g)} g(W, W)^{1/2}.$$

Since σ is piecewise smooth, there is a constant C_σ depending only on σ (independent of ε) such that $|\langle \text{curl}_g \sigma, W - \chi_\varepsilon W \rangle_{\mathring{\mathcal{W}}_g(\mathcal{T})}| \leq C_\sigma r_\varepsilon(W)$. Since W is piecewise smooth, $r_\varepsilon(W)$ approaches zero as $\varepsilon \rightarrow 0$. Hence for the given ε_1 , there is a $\varepsilon_2 > 0$ such that

$$|\langle \text{curl}_g \sigma, W - \chi_\varepsilon W \rangle_{\mathring{\mathcal{W}}_g(\mathcal{T})}| \leq C_\sigma r_\varepsilon(W) \leq \frac{\varepsilon_1}{2} \quad \text{for all } \varepsilon \leq \varepsilon_2. \quad (\text{A.3})$$

Next, to approximate $\chi_{\varepsilon_2} W$ by a smooth vector field, we use the precompactness of $\check{M}_{\varepsilon_2/2}$ to extract a finite subcover from the maximal atlas of \check{M} . Denoting the resulting finitely many charts by $U_i, \check{\Phi}_i$, let ψ_i be a partition of unity subordinate to the cover U_i . We focus on a U_i that intersects an edge E (since the other cases are easier) and use the accompanying notation in (2.15). By the previous discussion of the coordinate construction (4.12), $\check{\partial}^1 = \hat{\nu}_+$ and $\check{\partial}^2 = \hat{\tau}_+$ along E , so the expansion $W = W^i \check{\partial}_i$ is g -orthonormal and

$$g(W|_{T_\pm}, \hat{\nu}_\pm) = \pm W^1|_{T_\pm} \text{ on } E \cap U_i. \quad (\text{A.4})$$

The g -normal continuity $\|g(W, \hat{\nu})\| = 0$ implies that $W_i = \psi_i \chi_{\varepsilon_2} W$ pushed forward to the parameter domain, namely $(\check{\Phi}_i)_* W_i$, has continuous normal component across $\check{\Phi}_i(E)$, a subset of the axis $\check{Y} = \{(\check{x}^1, \check{x}^2) \in \mathbb{R}^2 : \check{x}^1 = 0\}$. Hence $(\check{\Phi}_i)_* W_i$ is in $\check{W}^p(\text{div}, \check{\Phi}_i(U_i))$, the subspace of $W^p(\text{div}, \check{\Phi}_i(U_i))$ with zero normal traces on the boundary of $\check{\Phi}_i(U_i)$. By a well known density result in the Euclidean domain, there exists an infinitely smooth compactly supported vector field $\check{\varphi}_i$ on $\check{\Phi}_i(U_i)$ that is arbitrarily close to $(\check{\Phi}_i)_* W_i$, so letting $\varphi_i = (\check{\Phi}_i^{-1})_* \check{\varphi}_i$, we have

$$\|(\check{\Phi}_i)_*(\varphi_i - W_i)\|_{W^p(\text{div}, \check{\Phi}_i(U_i))} = \|\check{\varphi}_i - (\check{\Phi}_i)_* W_i\|_{W^p(\text{div}, \check{\Phi}_i(U_i))} \leq \varepsilon_1. \quad (\text{A.5})$$

Moreover, since $\chi_{\varepsilon_2} \equiv 1$ in $U_i \cap \check{M}_{\varepsilon_2}$, the functions W_i and $\psi_i W$ coincide there, so (A.2) follows. Constructing such φ_i on every U_i , put $\varphi = \sum_{i \in I} \varphi_i$.

To prove (A.1), in view of (A.3), it suffices to show that

$$|\langle \text{curl}_g \sigma, \chi_{\varepsilon_2} W \rangle_{\mathring{\mathcal{W}}_g(\mathcal{T})} - \langle \text{curl}_g \sigma, \varphi \rangle_{\mathfrak{X}_c(\check{M})}| \leq \frac{\varepsilon_1}{2}. \quad (\text{A.6})$$

Obviously, the element contributions in the difference above, $\int_{\mathcal{T}} (\operatorname{curl}_g \sigma)(\chi_{\varepsilon_2} W - \varphi)$, can be made arbitrarily small by (A.5), revising the choice of φ_i if needed. For the element boundary terms,

$$\int_{\partial\mathcal{T}} g(\chi_{\varepsilon_2} W - \varphi, \hat{\nu}) \sigma(\hat{\nu}, \hat{\tau}) = \sum_{i \in I} \int_{\partial\mathcal{T}} g(W_i - \varphi_i, \hat{\nu}) \sigma(\hat{\nu}, \hat{\tau}), \quad (\text{A.7})$$

we focus, as before, on a neighborhood U_i intersecting an edge $E = \partial T_- \cap \partial T_+$. On ∂T_+ , by (A.4), $g(W_i - \varphi_i, \hat{\nu}) = W_i^1 - \varphi_i^1$ yields the normal component of the pushforward $(\check{\Phi}_i)_*(W_i - \varphi_i)$ on \check{Y} -axis in the parameter domain. Since the latter converges to zero in $W^{p,p}(\operatorname{div}, \check{\Phi}_i(U_i))$ by (A.5), its normal trace converges to zero in $W^{-1/p,p}(\check{\Phi}_i(E \cap U_i))$. Choose $p > 2$ and q such that $1/p + 1/q = 1$. When $\sigma(\hat{\nu}, \hat{\tau})$ is mapped to $\check{\Phi}_i(E \cap U_i)$ and extended to \check{Y} -axis by zero, is in $W^{1-1/q,q}(\check{Y})$ since $1 - 1/q < 1/2$. Hence the contribution from $U_i \cap E$ to the right hand side of (A.7) vanishes. Repeating this argument on other charts, (A.6) is proved. \blacksquare

Appendix B. Angle computation for connection approximation

In this section we discuss and present a stable angle computation used in the connection 1-form approximation. Since g_{ij} is in general discontinuous across an edge E (in the computational coordinates x^i), we cannot use it to directly compute the angle between frame vectors on two different triangles. Instead, we compute angles the frame makes with an intermediate vector element by element and then use it to compute Θ^E as explained below.

Before going into details we make the following observation: if the metric g approximates a smooth metric \bar{g} , we expect that the frame e_i fixed by (5.7) will be such that their restrictions to adjacent elements, $(e_{+,1}, e_{+,2})$ and $(e_{-,1}, e_{-,2})$, will differ by a small angle, say less than π . This is the case in Figure B.1 (left), where the angle difference Θ^E is negative and $|\Theta^E| < \pi$.

On each interior mesh edge E , let $T_{\pm}, \hat{\nu}_{\pm}, \hat{\tau}_{\pm}$ be as in (2.15), orient the edge E by $\hat{\tau}^E = \hat{\tau}_+$, and put $\hat{\nu}^E = \hat{\nu}_+$, $e_{\pm,i} = e_i|_{T_{\pm}}$. Let $\Theta_{\pm}^E = \sphericalangle_g(e_{\pm,1}, \pm \hat{\nu}_{\pm})$. Clearly, Θ_{\pm}^E can be computed using $g|_{T_{\pm}}$, specifically using its components g_{ij} in the computational coordinates x^i on either triangle. Then $\Theta^E = \Theta_+^E - \Theta_-^E$ in most cases (and certainly in the case illustrated in left drawing of Figure B.1). In some cases however, such as that in the middle drawing of Figure B.1, although Θ^E is negative and $|\Theta^E| < \pi$, the number $\Theta_+^E - \Theta_-^E$ is positive and larger than π . Thus setting $\Theta^E = \Theta_+^E - \Theta_-^E$ would be incorrect and would lead to a bad numerical approximation of the connection 1-form. To cure this problem we change the choice of the starting angle on the fly. First, we compute $\Theta_{\pm}^E = \sphericalangle_g(e_{\pm,1}, \pm \hat{\nu}_{\pm})$ on every edge as a pre-processing step. On each edge, set

$$s_E = \begin{cases} +1, & \text{if } |\Theta_+^E - \Theta_-^E| < \pi, \\ -1, & \text{otherwise.} \end{cases} \quad (\text{B.1})$$

Then set $\tilde{\Theta}_{\pm}^E = \sphericalangle_g(e_{\pm,1}, \pm s_E \hat{\nu}_{\pm})$ and $\Theta^E = \tilde{\Theta}_+^E - \tilde{\Theta}_-^E$. In other words, we compute after reversing the sign of the artificially introduced g -normal vector $\hat{\nu}_{\pm}$ on both the adjacent elements of an edge if the modulus of the pre-computed angle is larger than π . This is illustrated in Figure B.1 (right), where the sign change of the normal vector is depicted in red. The following computational formula is easy to prove.

Proposition B.1. *Let $[\varpi]_i = \frac{1}{2}g_{jk}(\partial_i e_2^j + \Gamma_{li}^j e_2^l e_1^k - \partial_i e_1^j - \Gamma_{li}^j e_1^l e_2^k)$ where e_i is chosen as in (5.7). Then the connection 1-form $\varpi_h(g)$ of Definition 5.3 satisfies*

$$\int_{\Omega} \delta(\varpi_h(g), v) \, da = \sum_{T \in \mathcal{T}} \left(\int_T [\varpi]_i v^i \, da - \int_{\partial T} \sphericalangle_g(e_1, s_E g(\hat{\tau}_E, \hat{\tau}) \hat{\nu}) v^\nu \, dl \right),$$

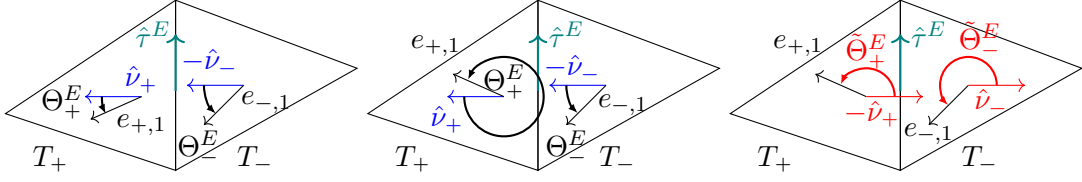


FIGURE B.1. Computation of angle difference. Left: $|\Theta_+^E - \Theta_-^E| < \pi$. Middle: $|\Theta_+^E - \Theta_-^E| > \pi$. Right: g -normal vector sign is swapped according to (B.1).

for all $v \in \mathring{\mathcal{W}}_h^k$.

Proof. By noting that $\pm \hat{\nu}_\pm^E = g(\hat{\tau}^E, \hat{\tau}_\pm) \hat{\nu}_\pm^E$ we obtain

$$\sum_{E \in \mathcal{E}^{\text{int}}} \int_{E,g} \Theta^E g(Q_g v, \hat{\nu}^E) = \sum_{E \in \mathcal{E}^{\text{int}}} \int_E (\tilde{\Theta}_+^E - \tilde{\Theta}_-^E) v^{\nu^E} \, \text{d}l = \sum_{T \in \mathcal{T}} \int_{\partial T} \triangle_g(e_1, s_E g(\hat{\tau}_E, \hat{\tau}) \hat{\nu}) v^\nu \, \text{d}l.$$

By symmetrization of (5.1) we have $\varpi(g; e_i) = \frac{1}{2} g_{jk} (\partial_i e_2^j + \Gamma_{li}^j e_2^l e_1^k - \partial_i e_1^j - \Gamma_{li}^j e_1^l e_2^k)$ and the claim follows. \blacksquare

Appendix C. Relation between distributional covariant inc and divdiv

In this section we show that the distributional covariant inc from Proposition 4.6 and the covariant distributional divdiv operator of a rotated sigma used in [10] coincide in the sense

$$\langle \text{div}_g \text{div}_g S_g \sigma, u \rangle_{\dot{\mathcal{V}}(\mathcal{T})} = -\langle \text{inc}_g \sigma, u \rangle_{\dot{\mathcal{V}}(\mathcal{T})} \quad \text{for all } u \in \dot{\mathcal{V}}(\mathcal{T}), \quad (\text{C.1})$$

where the covariant divergence is defined below. This is in common with the Euclidean identity $\text{divdiv} S \sigma = \text{divdiv} g - \Delta \text{tr}(\sigma) = -\text{inc} \sigma$, $\text{tr}(\cdot)$ denoting the trace of a matrix. The distributional covariant divdiv reads

$$\begin{aligned} \langle \text{div}_g \text{div}_g S_g \sigma, u \rangle_{\dot{\mathcal{V}}(\mathcal{T})} &= \int_{\mathcal{T}} u \, \text{div}_g \text{div}_g S_g \sigma + \int_{\partial \mathcal{T}} u ((\text{div}_g S_g \sigma)^\flat(\hat{\nu}) + (d\sigma_{\hat{\nu}}\hat{\tau})(\hat{\tau})) \\ &\quad + \sum_{T \in \mathcal{T}} \sum_{V \in \mathcal{V}_T} [\![\sigma_{\hat{\nu}}\hat{\tau}]\!]_V^T u(V), \end{aligned} \quad (\text{C.2})$$

where $S_g \sigma = \sigma - \text{tr}_g(\sigma)g$ with $\text{tr}_g(\sigma) = \sigma_{ij} g^{ij}$. (Note that the authors in [10] used $(\hat{\nu}, \hat{\tau})$ as positively oriented frame, whereas we use $(\hat{\tau}, \hat{\nu})$ such that the signs in the boundary and vertex terms differ. Also, a different orientation in the vertex jump is used.)

The covariant divergence is defined as the L^2 -adjoint of the covariant gradient. For $f \in \wedge^0(\Omega)$ its covariant gradient is given by the equation

$$g(\text{grad}_g f, v) = df(v) \quad \text{for all } v \in \mathfrak{X}(\Omega)$$

and $\text{div}_g : \mathfrak{X}(\Omega) \rightarrow \wedge^0(\Omega)$ by

$$\int_{\Omega} g(\text{grad}_g f, v) = \int_{\Omega} f \, \text{div}_g v, \quad \text{for all } v \in \mathring{\mathcal{W}}_g(\Omega), f \in \wedge^0(\Omega),$$

in coordinates

$$\text{div}_g v = \frac{1}{\sqrt{\det g}} \partial_i (\sqrt{\det g} v^i), \quad v \in \mathfrak{X}(\Omega).$$

The usual extension to tensor fields, see e.g. [27], $\operatorname{div}_g : \mathcal{T}_0^2(\Omega) \rightarrow \mathfrak{X}(\Omega)$ reads in coordinates

$$\operatorname{div}_g \sigma = (\partial_j \sigma^{ij} + \Gamma_{lj}^i \sigma^{lj} + \Gamma_{jl}^i \sigma^{il}) \partial_i, \quad \sigma \in \mathcal{T}_0^2(\Omega),$$

where $\sigma^{ij} = g^{ik} \sigma_{kl} g^{lj}$ for $\sigma \in \mathcal{T}_0^0(\Omega)$.

Lemma C.1. *There holds for $g \in \mathcal{R}^+(\mathcal{T})$ and $\sigma \in \mathcal{R}(\mathcal{T})$*

$$(1) \star(\operatorname{div}_g S_g \sigma)^\flat = -\operatorname{curl}_g \sigma \text{ and } (\operatorname{div}_g S_g \sigma)^\flat(\hat{\nu}) = (\operatorname{curl}_g \sigma)(\hat{\tau}) \text{ on } \partial \mathcal{T},$$

$$(2) \operatorname{div}_g \operatorname{div}_g S_g \sigma = \operatorname{div}_g \operatorname{div}_g \sigma - \Delta_g \operatorname{tr}_g(\sigma) = -\operatorname{inc}_g \sigma \text{ on } \mathcal{T},$$

where $\Delta_g f := \operatorname{div}_g \operatorname{grad}_g f$, $f \in \Lambda^0(\Omega)$ denotes the Laplace–Beltrami operator.

Proof. In the first identity only first order derivatives of g are involved. Thus, in normal coordinates, \tilde{x}^i (see §4.5), $(\operatorname{div}_g S_g \sigma)^\flat$ becomes the Euclidean version $\operatorname{div}(\sigma - \operatorname{tr}(\sigma)\delta)$, which reads in components

$$(\operatorname{div}_g S_g \sigma)^\flat = \begin{pmatrix} \tilde{\partial}_2 \tilde{\sigma}_{12} - \tilde{\partial}_1 \tilde{\sigma}_{22} \\ \tilde{\partial}_1 \tilde{\sigma}_{12} - \tilde{\partial}_2 \tilde{\sigma}_{11} \end{pmatrix}.$$

The Hodge star operator performs a counterclockwise 90-degree rotation, $\tilde{\star} = -\varepsilon^{ij}$, so that

$$\star(\operatorname{div}_g S_g \sigma)^\flat = -\begin{pmatrix} \tilde{\partial}_1 \tilde{\sigma}_{12} - \tilde{\partial}_2 \tilde{\sigma}_{11} \\ \tilde{\partial}_1 \tilde{\sigma}_{22} - \tilde{\partial}_2 \tilde{\sigma}_{12} \end{pmatrix} = -\operatorname{curl} \tilde{\sigma},$$

which coincides with $-\operatorname{curl}_g \sigma$ in normal coordinates. The identity $(\operatorname{div}_g S_g \sigma)^\flat(\hat{\nu}) = (\operatorname{curl}_g \sigma)(\hat{\tau})$ follows now by (2.9).

The identity $\operatorname{div}_g \operatorname{div}_g S_g \sigma = \operatorname{div}_g \operatorname{div}_g \sigma - \Delta_g \operatorname{tr}_g(\sigma)$ is well known [27], so we focus on proving its relationship with inc , by means of normal coordinates. The Laplace–Beltrami operator becomes

$$[\Delta_g \operatorname{tr}_g(\sigma)] = [\operatorname{div}_g \nabla_g \operatorname{tr}_g(\sigma)] = [\operatorname{div}_g(g^{ij} \partial_j \operatorname{tr}_g(\sigma))] = \tilde{\partial}_i^2 \operatorname{tr}(\tilde{\sigma} \tilde{g}^{-1}) = \Delta \operatorname{tr}(\tilde{\sigma}) - \operatorname{tr}(\tilde{\sigma} \Delta \tilde{g})$$

and the $\operatorname{div}\operatorname{div}$ part becomes

$$[\operatorname{div}_g \operatorname{div}_g \sigma] = \operatorname{div}\operatorname{div}[\tilde{\sigma}] - 2\tilde{\partial}_{ij}^2 \tilde{g}_{ik} \tilde{\sigma}_{kj} + \tilde{\partial}_i \tilde{\Gamma}_{lji} \tilde{\sigma}_{lj} - \tilde{\partial}_i \tilde{\Gamma}_{jlj} \tilde{\sigma}_{il}.$$

Note that we abused notation and summed over repeated indices all of which are subscripts (forgivable while using normal coordinates). Furthermore, by inserting the definition of Christoffel symbols of the first kind, a lengthy but elementary computation gives

$$\begin{aligned} -2\tilde{\partial}_{ij}^2 \tilde{g}_{ik} \tilde{\sigma}_{kj} + \tilde{\partial}_i \tilde{\Gamma}_{lji} \tilde{\sigma}_{lj} - \tilde{\partial}_i \tilde{\Gamma}_{jlj} \tilde{\sigma}_{il} &= \tilde{\sigma}_{11} \left(\frac{1}{2} \tilde{\partial}_1^2 \tilde{g}_{22} - \tilde{\partial}_1^2 \tilde{g}_{11} - \frac{1}{2} \tilde{\partial}_2^2 \tilde{g}_{11} - \tilde{\partial}_1 \tilde{\partial}_2 \tilde{g}_{12} \right) \\ &\quad - 2\tilde{\sigma}_{12} (\tilde{\partial}_1^2 \tilde{g}_{12} + \tilde{\partial}_2^2 \tilde{g}_{12}) - \tilde{\sigma}_{22} \left(\tilde{\partial}_2^2 \tilde{g}_{22} + \frac{1}{2} \tilde{\partial}_1^2 \tilde{g}_{22} + \tilde{\partial}_1 \tilde{\partial}_2 \tilde{g}_{12} - \frac{1}{2} \tilde{\partial}_2^2 \tilde{g}_{11} \right). \end{aligned}$$

Combining these,

$$[\operatorname{div}_g \operatorname{div}_g S_g \sigma] = -\operatorname{inc}[\tilde{\sigma}] + \frac{1}{2} \operatorname{tr}[\tilde{\sigma}] \operatorname{inc}[\tilde{g}],$$

which finishes the proof by comparing with (4.27). \blacksquare

Using the results of Lemma C.1 and comparing the terms of (C.2) with Proposition 4.6 the proof of the (C.1) is finished.

References

- [1] Samuel Amstutz and Nicolas Van Goethem. Analysis of the Incompatibility Operator and Application in Intrinsic Elasticity with Dislocations. *SIAM J. Math. Anal.*, 48(1):320–348, 2016.
- [2] Samuel Amstutz and Nicolas Van Goethem. Existence and asymptotic results for an intrinsic model of small-strain incompatible elasticity. *Discrete Contin. Dyn. Syst., Ser. B*, 25(10):3769–3805, 2020.

- [3] Douglas N. Arnold. *Finite element exterior calculus*. Society for Industrial and Applied Mathematics, 2018.
- [4] Douglas N. Arnold, Gerard Awanou, and Ragnar Winther. Finite elements for symmetric tensors in three dimensions. *Math. Comput.*, 77(263):1229–1251, 2008.
- [5] Douglas N. Arnold, Richard S. Falk, and Ragnar Winther. Finite element exterior calculus, homological techniques, and applications. *Acta Numer.*, 15:1–155, 2006.
- [6] Douglas N. Arnold, Richard S. Falk, and Ragnar Winther. Finite element exterior calculus: from Hodge theory to numerical stability. *Bull. Am. Math. Soc.*, 47(2):281–354, 2010.
- [7] Douglas N. Arnold and Kaibo Hu. Complexes from Complexes. *Found. Comput. Math.*, 21(6):1739–1774, 2021.
- [8] Douglas N. Arnold and Shawn W. Walker. The Hellan–Herrmann–Johnson Method with Curved Elements. *SIAM J. Numer. Anal.*, 58(5):2829–2855, 2020.
- [9] John W. Barrett, Daniele Oriti, and Ruth M. Williams. Tullio Regge’s legacy: Regge calculus and discrete gravity. <https://arxiv.org/abs/1812.06193>, 2018.
- [10] Yakov Berchenko-Kogan and Evan S. Gawlik. Finite element approximation of the Levi-Civita connection and its curvature in two dimensions. *Found. Comput. Math.*, 2022.
- [11] Daniele Boffi, Franco Brezzi, and Michel Fortin. *Mixed finite element methods and applications*, volume 44. Springer, 2013.
- [12] Vincent Borrelli, Frederic Cazals, and Jean-Marie Morvan. On the angular defect of triangulations and the pointwise approximation of curvatures. *Comput. Aided Geom. Des.*, 20(6):319–341, 2003.
- [13] Franco Brezzi, Jim Douglas, and Luisa D. Marini. Two families of mixed finite elements for second order elliptic problems. *Numer. Math.*, 47(2):217–235, 1985.
- [14] Manfredo P. do Carmo. *Riemannian Geometry*. Birkhäuser, 1992.
- [15] Jeff Cheeger, Werner Müller, and Robert Schrader. On the curvature of piecewise flat spaces. *Commun. Math. Phys.*, 92(3):405–454, 1984.
- [16] Snorre H. Christiansen. A characterization of second-order differential operators on finite element spaces. *Math. Models Methods Appl. Sci.*, 14(12):1881–1892, 2004.
- [17] Snorre H. Christiansen. On the linearization of Regge calculus. *Numer. Math.*, 119(4):613–640, 2011.
- [18] Snorre H. Christiansen. Exact formulas for the approximation of connections and curvature. <https://arxiv.org/abs/1307.3376>, 2015.
- [19] Snorre H. Christiansen, Jay Gopalakrishnan, Johnny Guzmán, and Kaibo Hu. A discrete elasticity complex on three-dimensional Alfeld splits. <https://arxiv.org/abs/2009.07744>, 2020.
- [20] C. J. S. Clarke and Tevian Dray. Junction conditions for null hypersurfaces. *Class. Quant. Grav.*, 4(2):265–275, 1987.
- [21] Maria I. Comodi. The Hellan–Herrmann–Johnson Method: Some New Error Estimates and Postprocessing. *Math. Comput.*, 52(185):17–29, 1989.
- [22] Michel Crouzeix and Vidar Thomée. The Stability in L_p and W_p^1 of the L_2 -projection onto Finite Element Function Spaces. *Math. Comput.*, 48(178):521–532, 1987.
- [23] Arthur E. Fischer and Jerrold E. Marsden. Deformations of the scalar curvature. *Duke Math. J.*, 1975.
- [24] Hans Fritz. Isoparametric finite element approximation of Ricci curvature. *IMA J. Numer. Anal.*, 33(4):1265–1290, 2013.

- [25] Hans Fritz. Numerical Ricci–DeTurck flow. *Numer. Math.*, 131(2):241–271, 2015.
- [26] Evan S. Gawlik. Finite Element Methods for Geometric Evolution Equations. In Frank Nielsen and Frédéric Barbaresco, editors, *Geometric Science of Information*, pages 532–540. Springer, 2019.
- [27] Evan S. Gawlik. High-Order Approximation of Gaussian Curvature with Regge Finite Elements. *SIAM J. Numer. Anal.*, 58(3):1801–1821, 2020.
- [28] Patrice Hauret and Frédéric Hecht. A Discrete Differential Sequence for Elasticity Based upon Continuous Displacements. *SIAM J. Sci. Comput.*, 35(1):B291–B314, 2013.
- [29] W. Israel. Singular hypersurfaces and thin shells in general relativity. *Il Nuovo Cimento B Series*, 44(1):1–14, 1966.
- [30] Nikolaï N. Kosovskii. Gluing of Riemannian manifolds of curvature $\geq \kappa$. *Algebra Anal.*, 14(3):140–157, 2002.
- [31] Nikolaï N. Kosovskii. Gluing with branching of Riemannian manifolds of curvature $\leq \kappa$. *Algebra Anal.*, 16(4):132–145, 2004.
- [32] John M. Lee. *Riemannian manifolds: an introduction to curvature*. Springer, 1997.
- [33] John M. Lee. *Introduction to Smooth Manifolds*. Springer, 2012.
- [34] Lizao Li. *Regge Finite Elements with Applications in Solid Mechanics and Relativity*. PhD thesis, University of Minnesota, 2018.
- [35] Dan Liu and Guoliang Xu. Angle deficit approximation of Gaussian curvature and its convergence over quadrilateral meshes. *Comput.-Aided Des.*, 39(6):506–517, 2007.
- [36] Michael Neunteufel. *Mixed Finite Element Methods for Nonlinear Continuum Mechanics and Shells*. PhD thesis, TU Wien, 2021.
- [37] Michael Neunteufel and Joachim Schöberl. Avoiding Membrane Locking with Regge Interpolation. *Comput. Methods Appl. Mech. Eng.*, 373: article no. 113524, 2021.
- [38] Peter Petersen. *Riemannian Geometry*. Springer, 2016.
- [39] Pierre-Arnaud Raviart and Jean-Marie Thomas. A mixed finite element method for 2-nd order elliptic problems. In *Mathematical Aspects of Finite Element Methods*, volume 66, pages 292–315. Springer, 1977.
- [40] Tullio Regge. General relativity without coordinates. *Il Nuovo Cimento (1955–1965)*, 19(3):558–571, 1961.
- [41] Tullio Regge and Ruth M. Williams. Discrete structures in gravity. *J. Math. Phys.*, 41(6):3964–3984, 2000.
- [42] Joachim Schöberl. NETGEN An advancing front 2D/3D-mesh generator based on abstract rules. *Comput. Vis. Sci.*, 1(1):41–52, 1997.
- [43] Joachim Schöberl. C++ 11 implementation of finite elements in NGSolve, 2014. Institute for Analysis and Scientific Computing, Vienna University of Technology.
- [44] Rafael Sorkin. Time-evolution problem in Regge calculus. *Phys. Rev. D*, 12:385–396, 1975.
- [45] Robert S. Strichartz. Defining Curvature as a Measure via Gauss–Bonnet on Certain Singular Surfaces. *J. Geom. Anal.*, 30(1):153–160, 2020.
- [46] John M. Sullivan. *Curvatures of Smooth and Discrete Surfaces*, pages 175–188. Birkhäuser, 2008.
- [47] Loring W. Tu. *Differential Geometry: Connections, Curvature, Characteristic Classes*. Springer, 2017.
- [48] Shawn W. Walker. The Kirchhoff plate equation on surfaces: the surface Hellan–Herrmann–Johnson method. *IMA J. Numer. Anal.*, 42:3094–3134, 2022.

ANALYSIS OF CURVATURE APPROXIMATIONS FOR REGGE METRICS

- [49] Max Wardetzky. *Discrete differential operators on polyhedral surfaces—convergence and approximation*. PhD thesis, Freie Universität Berlin, 2006.
- [50] Hassler Whitney. *Geometric integration theory*. Princeton University Press, 1957.
- [51] Ruth M. Williams and Philip A. Tuckey. Regge calculus: a brief review and bibliography. *Class. Quant. Grav.*, 9(5):1409–1422, 1992.
- [52] Guoliang Xu. Convergence analysis of a discretization scheme for Gaussian curvature over triangular surfaces. *Comput. Aided Geom. Des.*, 23(2):193–207, 2006.
- [53] Zhiqiang Xu and Guoliang Xu. Discrete schemes for Gaussian curvature and their convergence. *Comput. Math. Appl.*, 57(7):1187–1195, 2009.